^{15}N NUCLEAR MAGNETIC RESONANCE STUDIES OF THE ACTIVE SITES OF ENZYMES AND *IN VIVO* NITROGEN METABOLISM

Thesis by

Keiko Kanamori

In Partial Fulfillment of the Requirements

for the Degree of

Doctor of Philosophy

California Institute of Technology

Pasadena, California

1981

(Submitted August 14, 1980)

To Hiroo, Atty and Teddy

ACKNOWLEDGMENTS

I would like to express my deep gratitude to my research advisor, Professor John D. Roberts, for his guidance, encouragement and patience during the course of this study. His insight, knowledge and attitude towards science have made it a truly rewarding experience to work for him. I am grateful to all members of his group, past and present, for their support and numerous assistance along the way.

I would like to express my sincere thanks to Professor John H. Richards and his group for their kindness and generosity in permitting me to use many of their facilities over the years; the work described in Part I would not have been possible without their generous assistance.

I would like to thank Professor William W. Bachovchin for many helpful suggestions and collaboration in the work described in Part I and for teaching me many useful techniques during my first year. The contribution of Professor Bert L. Vallee to the project is also gratefully acknowledged. I would also like to thank Timothy L. Legerton and Professor Richard L. Weiss for their valuable contributions to the work described in Part IV.

I am grateful to Mrs. Rose Meldrum for skillful illustrations and typing, and Ms Vere Snell for her excellent typing of most of this thesis.

Support was received from the Institute in the form of Graduate Research Assistantship from 1977 to 80; this support is greatly appreciated.

Finally, I would like to thank the members of my family for their patience and companionship during the busy years.

ABSTRACT

PART I

A ^{15}N Nuclear Magnetic Resonance Study of the Active-site Conformation of Arsanilazo-carboxypeptidase A

To determine whether the catalytic zinc of carboxypeptidase A (CPA) is complexed to the active-site tyrosine (Tyr-248) in solution, a ^{15}N probe, an arsanilazo group enriched in ^{15}N at both azo nitrogens, has been selectively coupled to Tyr-248 with retention of full catalytic activity, and the resulting arsanilazotyrosyl-248 carboxypeptidase A (Zn.Azo-CPA) studied by ^{15}N NMR spectroscopy over pH range from 7.0 to 10.3. Its azo nitrogen resonances, N_α (proximal to Tyr-248) and N_β (distal), show 8.3 ppm and 23.5 ppm shielding respectively relative to the corresponding resonances of apoarsanilazotyrosyl-248 carboxypeptidase A at pH 8.8. By comparison with the ^{15}N shifts of a model azotyrosine and its zinc complex, these shift differences indicate substantial complexation of the azotyrosyl-248 with the catalytic zinc at pH 8.8. Consistent with such complexation is the fact that the azo nitrogen resonances of Zn.Azo-CPA show large deshieldings on addition of a slowly hydrolyzing substrate glycyl-L-tyrosine or an inhibitor β-phenylpropionate, each of which binds to the catalytic zinc and therefore is expected to break any azotyrosine-Zn complex. The results demonstrate unequivocally that the molecular basis for the properties of Zn.Azo-CPA observed by other spec-

tral techniques is a Zn-azotyrosyl-248 complex, with the N_β nitrogen (and presumably the phenolic oxygen) as ligand to zinc. Furthermore, the high sensitivity of ^{15}N shifts to coordination with zinc permits at least a semi-quantitative estimate of the degree of azotyrosine-Zn complexation and indicates that the major conformation of Zn.Azo-CPA, and by implication, of CPA in solution could be the one in which the active-site tyrosine is complexed to zinc, in contrast to the major conformation in the crystalline enzyme in which the Tyr-248 hydroxyl is 17 Å from the zinc.

The binding of the quasi-substrate, glycyl-L-tyrosine, or the inhibitor, β-phenylpropionate, to Zn.Azo-CPA causes a greater deshielding of the N_β resonance than can be accounted for solely by the disruption of azotyrosyl-Zn complex. The N_β shift is also a sensitive probe of intramolecular hydrogen bonding of this nitrogen with Tyr-248 hydroxyl whose postulated catalytic function is to donate a proton to the leaving amine group of the substrate. The N_β resonance of Zn.Azo-CPA-Gly-Tyr complex is deshielded by 8.9 ppm relative to that of Apo.Azo-CPA at pH 8.8, a result consistent with a partial hydrogen bonding of Tyr-248 hydroxyl with the amide nitrogen of the scissile peptide bond of the substrate. In the Zn.Azo-CPA-β-phenylpropionate complex, a 28.2 ppm deshielding of the N_β resonance relative to that of the apoenzyme indicates disruption of the hydrogen bond between N_β and Tyr-248 hydroxyl; the most reasonable explanation is that the tyrosine hydroxyl hydrogen-bonds to the carboxylate group of the inhibitor.

PART II

Benzoate Catalysis in the Hydrolysis of endo-5-[4'(5')imidazolyl]-bicyclo[2.2.1] hept-endo-2-yl trans-cinnamate: Implications for the Charge-transfer Mechanism of Catalysis by Serine Proteases

The acceleration, by a factor of 2500, of the hydrolysis of endo-5-[4'(5') imidazolyl]bicyclo[2.2.1]hept-endo-2-yl trans-cinnamate by 0.5 M sodium benzoate in 42 mol % dioxane in water can be explained without resort to operation of a "charge-relay" mechanism similar to that often postulated to account for the enzymatic activity of serine proteases. The degree of ionization of 4-methylimidazole and of sodium benzoate in 42 mol % dioxane in water at 60°C have been measured by NMR spectroscopy.

PART III

Studies of pH and Anion Complexation Effects on L-Arginine by Natural Abundance ^{15}N Nuclear Magnetic Resonance Spectroscopy

Natural-abundance nitrogen-15 nuclear magnetic resonance (NMR) spectroscopy has been used to investigate (1) the effect of pH on the ^{15}N chemical shifts of L-arginine and (2) the possible effects on ^{15}N chemical shifts and T_1 values of the complexation of L-arginine with chloride ions, phosphate ions, and adenosine triphosphate (ATP) in aqueous solutions. Guanidine carbonate solutions and protamine sulfate solutions containing some of these ions have also been examined. On protonation of the guanidinium group of L-arginine, the guanidino nitrogens and the -NH-nitrogen show upfield shifts of 15 and 3 ppm, respectively, as a result of change in the second-order paramagnetic effect, while the α-amino nitrogen shows an 8-ppm downfield shift on protonation as a result of decreased shielding. Complexation with equimolar phosphate ions produces a small downfield shift of approximately 0.8 ppm in the chemical shift of the guanidino nitrogens of L-arginine. No significant changes in ^{15}N shifts or T_1 values were observed on complexation with chloride ions or adenosine triphosphate.

PART IV

A ^{15}N nuclear magnetic resonance study of amino acid metabolism in Neurospora crassa

^{15}N nuclear magnetic resonance spectra of suspensions of intact Neurospora crassa mycelia, cultured in $^{15}NH_4Cl$-containing medium, have been obtained at 18.25 MHz. Well-resolved ^{15}N resonances of free metabolites that play crucial roles in intermediary nitrogen metabolism, such as the amide nitrogen of glutamine, the α-amino nitrogens of glutamate and other amino acids, the guanidino nitrogens of arginine and the ureido nitrogens of citrulline are observed, as well as those of cellular components such as chitin and uridine diphosphates. The guanidino nitrogens of intracellular arginine are found to have a spin-lattice relaxation time of 1.06 sec and nuclear Overhauser enhancement of -3.6, indicating that these nuclei have a correlation time of the order of 10^{-10} sec in the intracellular environment. This suggests that a pulsing rate of a few seconds with proton decoupling is favorable for the observation of protonated nitrogens of small metabolites in intact microorganisms.

The time course of the assimilation of $^{15}NH_4^+$ into glutamine and glutamate was followed in vivo in two N. crassa strains, one capable of synthesizing glutamate directly from NH_4^+ and α-keto-glutarate, and the other incapable of this synthesis. Preliminary

results demonstrate that an alternative pathway of NH_4^+ assimilation into glutamate exists in N. crassa, and suggests that this takes place via the amide nitrogen of glutamine.

Potential utility of ^{15}N NMR spectroscopy for study of the in vivo turnover rates of nitrogenous metabolites, for elucidation of previously unknown pathways and for cellular regulation of nitrogen metabolism in intact microorganisms is discussed.

ABSTRACTS OF THE PROPOSITIONS

PROPOSITION I

A ^{15}N NMR study of the ionization state of the coenzyme pyridoxal phosphate at the active site of aspartate aminotransferase is proposed.

PROPOSITION II

A ^{15}N NMR study of the mode of binding of the inhibitor sulfanilamide to the catalytic zinc of carbonic anhydrase is proposed.

PROPOSITION III

Chromosomal localization of the gene for the ζ chain of human embryonic hemoglobin is proposed, with a view to obtaining clues to the evolutionary relationship of the ζ chain to the α globin chain.

PROPOSITION IV

A resonance Raman study of electron polarization in a chromophoric substrate 4-dimethylaminocinnamaldehyde bound to alcohol dehydrogenase is proposed.

PROPOSITION V

A study of the mechanism of action of an anticancer drug, streptozotocin, by radiochromatography is proposed.

TABLE OF CONTENTS

PART I

A ^{15}N Nuclear Magnetic Resonance Study of the Active-site Conformation of Arsanilazo-carboxypeptidase A

	Page
Abstract	v
Introduction	2
Experimental	8
Results and Discussion	11
^{15}N shifts of arsanilazo-N-acetyltyrosine (DAT)	11
^{15}N shifts of tetrazolylazo-N-acetyltyrosine (TAT) and its zinc complex	16
^{15}N shifts of arsanilazotyrosyl-248 CPA (Zn.Azo-CPA)	18
^{15}N shifts of apoarsanilazotyrosyl-248 CPA (Apo.Azo-CPA)	25
^{15}N shifts of Gly-Tyr and β-phenylpropionate complexes of Zn.Azo-CPA	27
Conclusion	36
References	39

PART II

Benzoate Catalysis in the Hydrolysis of endo-5-[4'(5')imidazolyl]-bicyclo[2.2.1] hept-endo-2-yl trans-cinnamate: Implications for the Charge-transfer Mechanism of Catalysis by Serine Proteases

Abstract	vii
Introduction	43

Page

Experimental 46

Results and Discussion 46

References 52

PART III

Studies of pH and Anion Complexation Effects on L-Arginine by Natural Abundance ^{15}N Nuclear Magnetic Resonance Spectroscopy

Abstract viii

Introduction 54

Experimental 55

Results and Discussion 56

References 65

PART IV

A ^{15}N Nuclear Magnetic Resonance Study of Amino Acid Metabolism in Neurospora crassa

Abstract ix

Introduction 68

Experimental 72

Page

Results and Discussion 74

1. The ^{15}N shift, the spin-lattice relaxation time and the nuclear Overhauser enhancement of intracellular arginine ($^{15}N_{\omega,\omega'}$) in N. crassa 74
2. ^{15}N spectra of intact N. crassa mycelia cultured in $^{15}NH_4^+$-containing medium 86
3. The time course of assimilation of $^{15}NH_4^+$ into glutamine and glutamate in two N. crassa strains 101

References 117

PROPOSITIONS

Abstracts xi

Proposition I 122

Proposition II 138

Proposition III 148

Proposition IV 158

Proposition V 164

LIST OF TABLES

Part	Table	Title	Page
I	I	^{15}N shifts of arsanilazotyrosyl-248 carboxypeptidase A (Zn.Azo-CPA), its Gly-Tyr and β-phenylpropionate complexes, Apo.Azo-CPA and model compounds	32
II	I	^{15}N and ^{13}C shifts of 4-methylimidazole and benzoic acid in 42 mol % dioxane in water	48
III	I	^{15}N NMR shifts of guanidine carbonate, L-arginine and protamine sulfate in presence of anions	60
	II	T_1 values for L-arginine nitrogens in the presence of anions.....	63
IV	I	T_1 values of intracellular and extracellular arginine ($^{15}N_{\omega,\omega'}$) in N. crassa.....	85
	II	Assignments of ^{15}N-labeled metabolites observed in N. crassa mycelia	89

LIST OF FIGURES

Part	Figure	Title	Page
I	1	The active site of crystalline carboxypeptidase A	3
	2	The active site of crystalline carboxypeptidase A on binding of Gly-Tyr	4
	3	A probable mechanism of catalysis by carboxypeptidase A	7
	4	The structures of arsanilazotyrosyl-248 carboxypeptidase A (Zn.Azo-CPA) and model compounds	12
	5	^{15}N shifts of arsanilazo-N-acetyltyrosine (DAT) as functions of pH	13
	6	^{13}C shifts of arsanilazo-N-chloroacetyltyrosine as functions of pH	15
	7	^{15}N shifts of tetrazolylazo-N-acetyltyrosine (TAT) and its zinc complex as functions of pH	17
	8	^{15}N spectra of Zn.Azo-CPA at pH 7.0, 8.8, and 9.6.	19
	9	^{15}N shifts of Zn.Azo-CPA, Apo.Azo-CPA, DAT and TAT.Zn complex as functions of pH	20
	10	Probable states of Tyr-248 and Zn in Zn.Azo-CPA...	24

Part	Figure	Title	Page
I	11	^{15}N spectra of Zn.Azo-CPA, its Gly-Tyr and β-phenylpropionate complexes and Apo.Azo-CPA at pH 8.8	26
	12	^{15}N shifts of Zn.Azo-CPA and its Gly-Tyr and β-phenylpropionate complexes as functions of pH ...	29
	13	Possible modes of binding of Gly-Tyr to Zn.Azo-CPA	31
	14	Possible mode of binding of β-phenylpropionate to Zn.Azo-CPA	34
II	1	^{13}C shifts of benzoate carboxyl carbon as a function of pH in 42 mol % dioxane in water.....	49
III	1	The pH dependence of ^{15}N chemical shifts of L-arginine	57
IV	1	^{15}N chemical shift spectrum of intracellular arginine ($^{15}N_{\omega,\omega'}$) in intact N. crassa mycelia.....	75
	2	^{15}N spectra of intracellular arginine ($^{15}N_{\omega,\omega'}$) in N. crassa for NOE measurement	77
	3	a. Plot of NOE against τ_c for nitrogen-15.....	79
		b. Plot of T_1 against τ_c for nitrogen-15.....	79
	4	Representative ^{15}N spectra for the T_1 measurement of arginine ($^{15}N_{\omega,\omega'}$) in N. crassa	81

Part	Figure	Title	Page
IV	5	Plots of $\ln(S_\infty - S_\tau)$ against τ for the T_1 measurement of arginine ($^{15}N_{\omega,\omega'}$) in N. crassa	82
	6	a. ^{15}N spectrum of mycelia suspension of N. crassa ure-1 strain grown in $^{15}NH_4Cl$-containing medium b. ^{15}N spectrum of the same mycelia after additional 2 hours' growth in $^{14}NH_4Cl$ containing medium	87
	7	Anabolic pathways of some nitrogenous metabolites in N. crassa mycelia	90
	8	^{15}N spectrum of cell extracts of N. crassa mycelia...	96
	9	^{15}N spectrum of mycelia suspension of N. crassa ure-1 strain grown in $^{15}NH_4Cl$-containing medium after addition of cycloheximide	99
	10	a. Time course of assimilation of $^{15}NH_4^+$ into glutamine and glutamate in N. crassa am-1 strain b. The same in N. crassa ure-1 strain	105
	11	Comparison of the peak intensities of glutamine N_γ and glutamate N_α as functions of time in N. crassa am-1 and ure-1 strain	108

PART I

A ^{15}N Nuclear Magnetic Resonance Study of the Active-site Conformation of Arsanilazo-carboxypeptidase A

INTRODUCTION

Carboxypeptidase A (CPA) catalyzes the cleavage of C-terminal amino acid from a peptide chain.* Its active-site residues have been identified as zinc, tyrosine (Tyr-248), glutamic acid (Glu-270), and arginine (Arg-145) on the basis of chemical modification[1a-c] and X-ray[2a,b] studies. In recent years, there has been considerable controversy[3a-c] regarding the conformation of the active site, specifically the location of Tyr-248 relative to zinc, because the conformation of the enzyme in solution might be significantly different from that in the crystalline enzyme. According to the most recent interpretation of the electron-density maps, crystalline CPA at pH 7.5 exhibits two conformations; the predominant conformation being the one in which Tyr-248 hydroxyl is at the surface of the molecule and is separated by 17 Å from the zinc (Figure 1), and a second conformation constituting up to 25% of the enzymes in which the tyrosine hydroxyl is within 2 Å of the zinc.[4] On binding of a slowly-hydrolyzing substrate, glycyl-L-tyrosine, to the enzyme, there is a large conformational change of the predominant conformation whereby the tyrosine hydroxyl moves from the surface of the molecule to within 4∿5Å of the zinc and 3Å from the NH group of the scissile peptide bond[2b] (Figure 2). This movement of Tyr-248 has been regarded as one of the most striking examples of the induced-fit theory of enzyme-substrate binding.

---

*The pH dependence of the activity of CPA at ionic strength 0.5 shows a broad plateau of optimum activity in pH 7.0 to 9.0 region, the relative velocity of hydrolysis at pH 8.6 being 93% of that at pH 7.5.[1d]

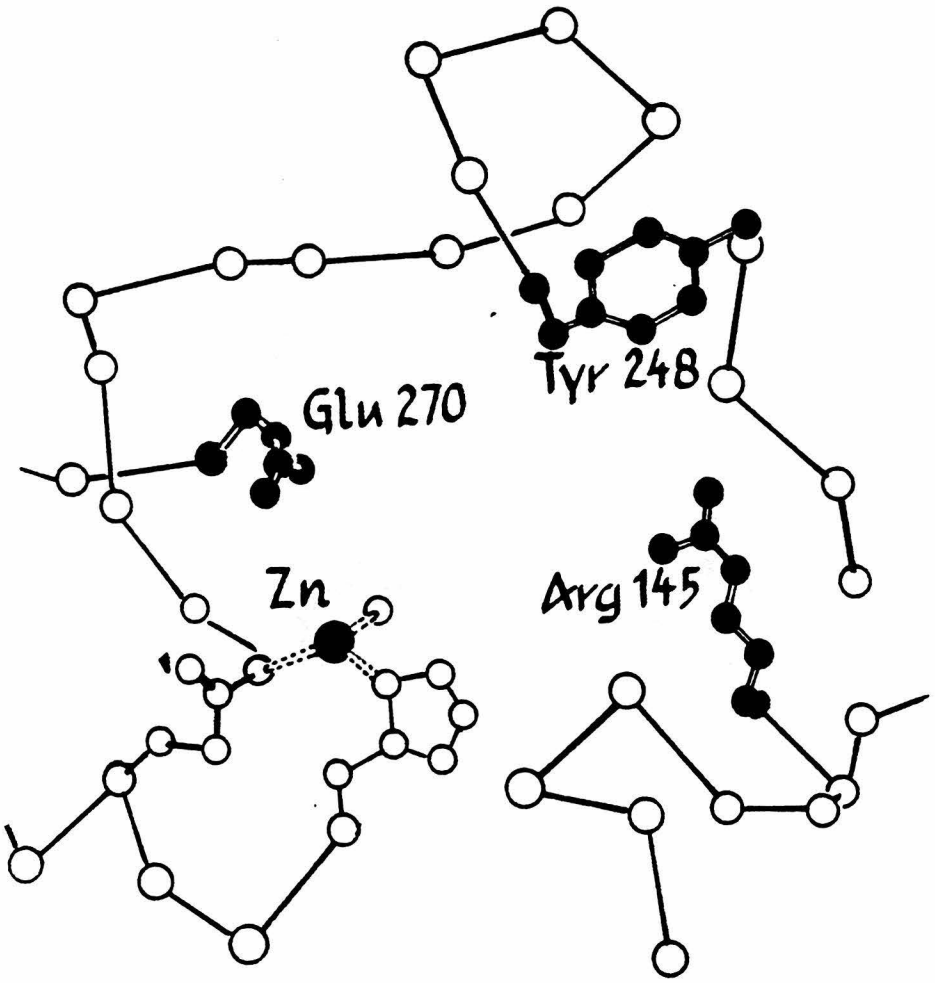

Fig. 1 The predominant conformation of the active site of crystalline carboxypeptidase A according to X-ray structure. The carbon, oxygen and nitrogen atoms of the active-site residues (including the C_α atoms) are shown by filled circles, and parts of the peptide backbones around the active site are shown by blank circles (Adapted from R. E. Dickerson and I. Geis, "The Structure and Action of Proteins,", Harper and Row, New York, 1969)

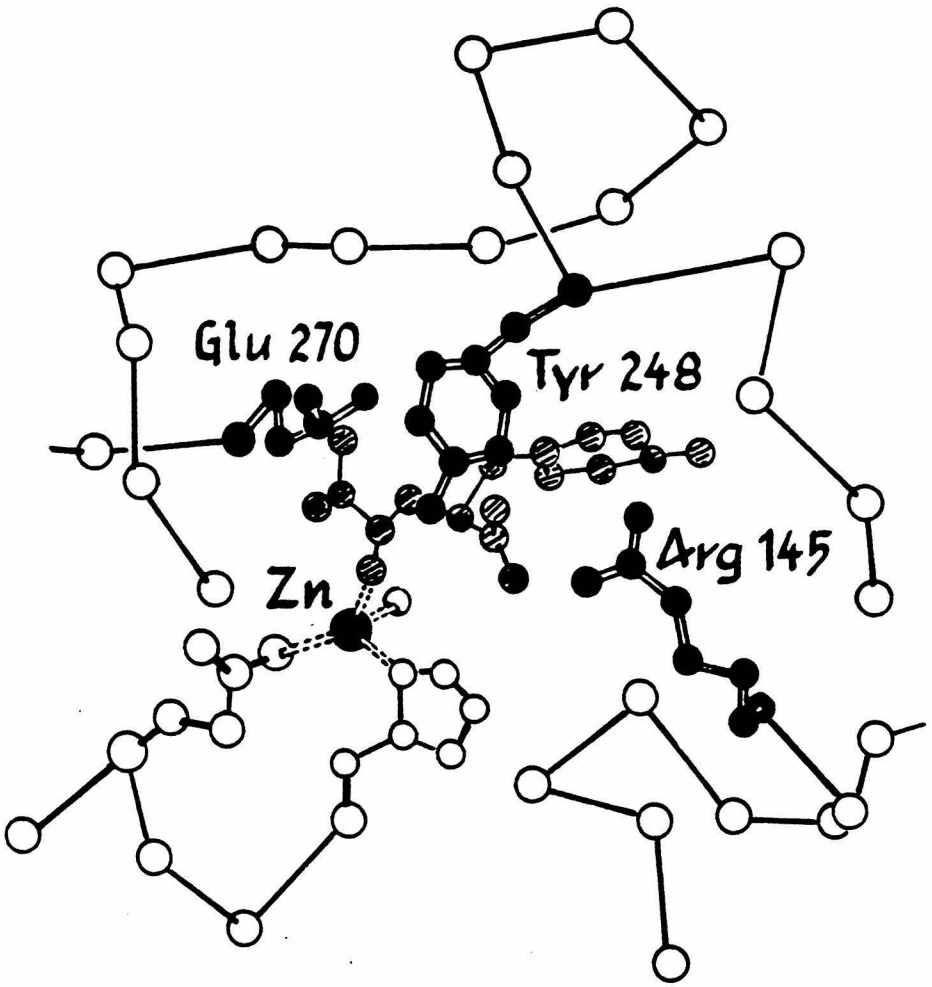

Fig. 2 The active-site conformation of crystalline carboxypeptidase A on binding of a quasi-substrate glycyl-L-tyrosine. Glycyl-L-tyrosine is shown by shaded circles and the active-site residues by filled circles. (Adapted from R. E. Dickerson and I. Geis, "The Structure and Action of Proteins", Harper and Row, New York, 1969)

However, Vallee and coworkers[3a, b] have studied the active-site conformation of the enzyme in solution and proposed that the Tyr-248 hydroxyl is complexed to zinc before substrate binding, and therefore has a conformation significantly different from that of the major conformation of the crystalline enzyme. To determine the conformation in solution, Vallee and coworkers used a modified CPA with the active-site tyrosine-248 residue specifically labeled with an arsanilazo group. The coupling of arsanilazo group to Tyr-248 is selective,[5] and the resulting arsanilazo tyrosyl-248 CPA (Zn.Azo-CPA) has full catalytic activity,[6] indicating that the active-site conformation necessary for catalysis is preserved. Vallee and coworkers showed, by comparison with model azotyrosine compound and their zinc complexes, that Zn.Azo-CPA exhibits visible absorption,[3b, 6] circular dichroic,[3b, 6] and resonance Raman spectra[7] similar to those of azophenol, azophenolate-Zn complex and azophenolate ion at pH 6.2, 8.5 and 10.8 respectively and therefore they proposed that Tyr-248 in Zn.Azo-CPA is complexed to the catalytic zinc around pH 8.5 in solution.

Valuable as the spectral techniques have proved to be, the techniques employed so far provide no unequivocal molecular basis for the observed spectral properties of Zn.Azo-CPA, and if azotyrosine-Zn complexation is taking place, the mode of complexation on molecular level--whether the proximal or the distal azo nitrogen is involved in chelation--is not known. Moreover, previous techniques provide no quantitative estimate of the degree of Tyr-248-Zn complexation, if it is occurring, at the active-site of Zn-Azo-CPA in solution. Another interesting point is the detailed conformational change that occurs at the active-site on binding of a substrate or an inhibitor to Zn.Azo-CPA in solution.

The present research involves the application of ^{15}N nuclear magnetic resonance spectroscopy to study the active-site conformation of arsanilazotyrosyl-248 CPA (^{15}N enriched in both azo nitrogens) (1) as free enzyme in solution, (2) on binding of a quasi-substrate, glycyl-L-tyrosine and an inhibitor β-phenylpropionate, and (3) on removal of the catalytic zinc. The potential of ^{15}N NMR spectroscopy as probe of enzyme active sites has been successfully demonstrated for α-lytic protease.[8] ^{15}N chemical shift is potentially a very sensitive probe of azotyrosine-Zn complexation in arsanilazotyrosyl-248 CPA, because, with a model azotyrosine compound, the azo nitrogen shows an upfield shift of fully 90 ppm on complexation with zinc. The high sensitivity of ^{15}N shift to coordination with zinc permits a semi-quantitative estimate of the degree of azotyrosine-Zn complexation in arsanilazotyrosyl-248 CPA in solution which so far has not been possible by other spectral techniques. With Zn.Azo-CPA ^{15}N enriched in both azo nitrogens, it is also possible to determine which azo nitrogen, if any, is involved in complexation. Moreover, the ^{15}N shifts of azo nitrogens can be a sensitive probe, not only of zinc complexation but also of intramolecular hydrogen bonding with tyrosyl-248 hydroxyl whose catalytic function, according to proposed mechanism of catalysis[9] is to donate a proton to the leaving amine group (Figure 3). Thus, ^{15}N chemical shifts of Zn.Azo-CPA-Gly-Tyr complex were expected to provide important information on the state of hydrogen-bonding of the Tyr-248 hydroxyl in the enzyme-substrate complex in solution.

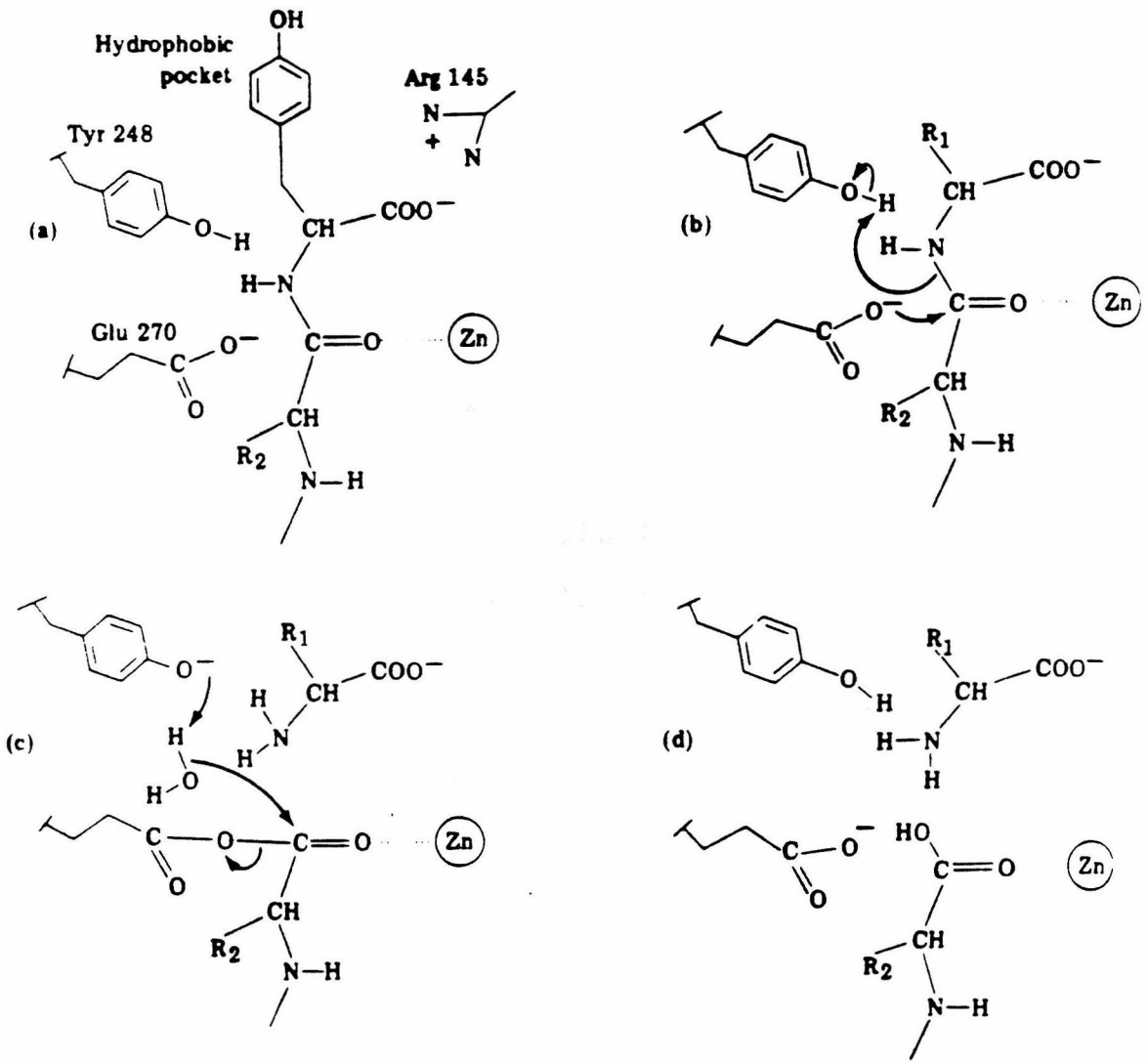

Fig. 3 A probable mechanism for catalysis by carboxypeptidase A (Adapted from R. E. Dickerson and I. Geis. "Structure and Action of Proteins," Harper and Row, New York, 1969)

EXPERIMENTAL

Sodium nitrite (99% enriched in ^{15}N) and p-arsanilic acid (99% enriched in ^{15}N) were obtained from Isotope Labeling Corporation.

Monoarsanilazo-N-acetyltyrosine (DAT) was prepared by reacting diazotized arsanilic acid with N-acetyltyrosine.[7c, 10] Selective nitrogen-15 isotopic enrichment of N_α or N_β was effected by using sodium (^{15}N) nitrite or (^{15}N)p-arsanilic acid, respectively in the diazotization reaction. The ultraviolet-visible absorption spectrum of each preparation of ^{15}N-enriched DAT was carefully examined over the pH range 4.0 to 11.0. In general, all spectral parameters were found to be identical to those reported previously.[7c, 10]

Monotetrazolylazo-N-acetyltyrosine (TAT) was prepared by reacting diazonium-1H-tetrazole with N-acetyltyrosine as described by Sokolovsky and Vallee.[11] The ^{15}N derivative was synthesized by using sodium (^{15}N) nitrite in the preparation of the diazonium-1H-tetrazole. Ultraviolet-visible absorption spectra of the nitrogen-15 enriched product were obtained as a function of pH and of added zinc ion; observed spectral properties agreed closely with those previously reported.[3b]

Carboxypeptidase A[12] was obtained as a crystal suspension from Sigma Chemical Company and was recrystallized before use. Arsanilazotyrosyl-248 carboxypeptidase A was prepared by reacting diazotized p-arsanilic acid with carboxypeptidase A crystals as described by Johansen and Vallee.[3a] Nitrogen-15 enrichment at N_α or N_β was effected through the use of sodium (^{15}N) nitrite or (^{15}N)p-arsanilic acid, respectively, as described above for DAT. Ultraviolet-visible absorption spectroscopy was used to

demonstrate that each preparation of nitrogen-15 enriched azo-enzyme responded to pH, removal of zinc, inhibitors and substrates, and denaturing agents in the manner expected. All spectral properties were in good agreement with previously reported results.

Peptidase activity was determined spectrophotometrically using (furylacryloyl)glycylphenylalanine. Activity of the modified enzyme as measured with this substrate was not discernibly different from that of the unmodified enzyme.

Apoarsanilazotyr-248-CPA was prepared by suspending the crystals of arsanilazotyr-248-CPA (5 mg/ml) in 0.01 M 1,10 phenanthroline, 0.01 M 2-(N-morpholino)ethanesulfonic acid (Mes) buffer (pH 7.0) at 20 °C for 1 hr. for four successive times followed by four 0.5 hr. washings with 0.01 M Mes buffer (pH 7.0).[9b] The apoenzyme prepared by this method contained less than 0.016 g-atom of zinc/mol of enzyme as determined by atomic absorption spectroscopy.

10-Phenylazo-9-phenanthrol was synthesized by refluxing 9,10-phenanthraquinone and phenylhydrazine hydrochloride in acetic acid.[9c] Crystallization from ethanol gave pure 10-phenylazo-9-phenanthrol (melting point 163∿164 °C). Its anion was prepared by addition of 1.5 equivalent of sodium hydroxide in dimethyl sulfoxide.

^{15}N chemical shift spectra were obtained with a Bruker WH180 spectrometer operating at 18.25 MHz. A 1 M solution of $H^{15}NO_3$ in D_2O contained in capillary provided both reference signal and field-frequency lock. For the model compounds arsanilazo-N-acetyltyrosine (DAT), tetrazolylazo-N-acetyltyrosine (TAT) and its zinc complex (TAT.Zn), the spectra were

taken of 5 mM aqueous solution. The operating conditions were 90° pulse and 15 sec. delay. For arsanilazotyrosyl-248-CPA, the spectra were taken of 1.5∿2.0 mM aqueous solutions in 1.0 M NaCl-0.02M tris(hydroxymethyl) aminomethane buffer at 15° C. Glycyl-L-tyrosine (7.5 mM) or β-phenylpropionate (7.5 mM) was added to the enzyme solution to make enzyme-substrate or enzyme-inhibitor complexes, respectively. For apoarsanilazotyrosyl-248-CPA, the spectra were obtained of 0.3 mM aqueous solution in the same buffer at 5° C. Operating conditions for the ^{15}N spectra of the enzyme, its substrate and inhibitor complexes and the apoenzyme were 90° pulse and 0.8 sec. delay and pH 7.0 and 7.8 and 0.29 sec. delay at other pH values. Each spectrum required 8∿16 hours of accumulation time. The stabilities of the enzyme and its complexes during NMR measurement were monitored before and after by the visible absorption spectrum of each solution. All solutions were found to be stable during the NMR measurements. The peptidase activity of Zn.Azo-CPA was checked before and after each NMR measurement. For NMR experiments at pH 7.0∿9.6, there was no appreciable change in activity before and after the experiments. At pH 10.3, Zn.Azo-CPA has no catalytic activity, presumably due to binding of hydroxide ion to catalytic Zn, but the three-dimensional conformation of the enzyme is preserved as indicated by recovery of catalytically active Zn.Azo-CPA on lowering pH.

^{13}C chemical shift spectra were obtained with a Varian XL100 spectrometer operating at 25.14 MHz. Operating conditions were 90° pulse and 3 sec. delay.

Enzyme concentrations were measured by the absorbance at 278 nm, based on a molar absorptivity at 278 nm of 7.32×10^4 M^{-1} $cm.^{-1}$ Visible absorption spectra were obtained on Beckman Acta CIII spectrophotometer, and/or on a Varian 219 spectrophotometer.

RESULTS AND DISCUSSION

Figure 4 shows the structures of arsanilazotyrosyl-248 residue of the modified CPA (Zn.Azo-CPA), and two model compounds arsanilazo-N-acetyltyrosine (DAT) and tetrazolylazo-N-acetyltyrosine (TAT). DAT is the model for free azotyrosine, but because the bidentate DAT does not form a soluble 1:1 zinc complex, the zinc complex of tridentate TAT was used as a model for azotyrosine-Zn complex as in previous studies of arsanilazotyrosyl-248 CPA by visible absorption and resonance Raman spectroscopy.

^{15}N NMR shifts of DAT

The ^{15}N chemical shifts of the two azo nitrogens of DAT in water as a function of pH is shown in Figure 5. The assignment of N_α and N_β nitrogens was straightforward because DAT was ^{15}N-enriched in N_α and N_β separately. While the N_α shift of DAT at -126∿-128 ppm is close to that of azobenzene, -133 ppm,[13] the N_β shift of DAT at -82 ppm is approximately 45 ppm shielded relative to N_α. This shielding is the result of an intramolecular hydrogen bond between N_β and the phenolic proton (Figure 5-I). Although such hydrogen-bond is well-known for o-hydroxy azo compounds,[14,15] it has not been previously determined whether the hydrogen bond is to N_α

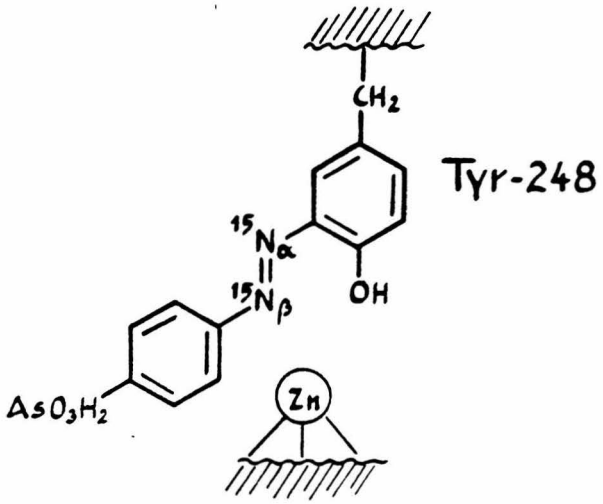

Arsanilazotyrosine-248 carboxypeptidase A
(Zn·Azo-CPA)

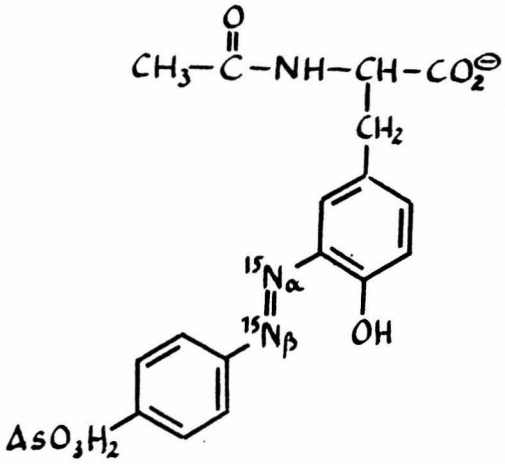

Arsanilazo-N-acetyltyrosine (DAT)

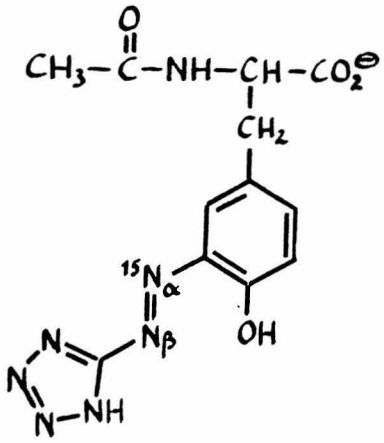

Tetrazolylazo-N-acetyltyrosine (TAT)

Fig. 4 The structures of arsanilazotyrosyl-248 residue of the modified CPA (Zn.Azo-CPA) and the model compounds arsanilazo-N acetyltyrosine (DAT) and tetrazolylazo-N-acetyltyrosine (TAT).

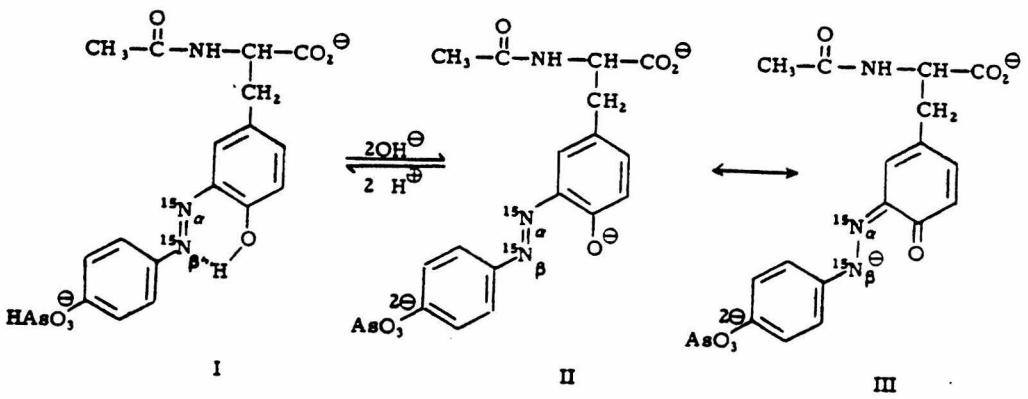

I II III

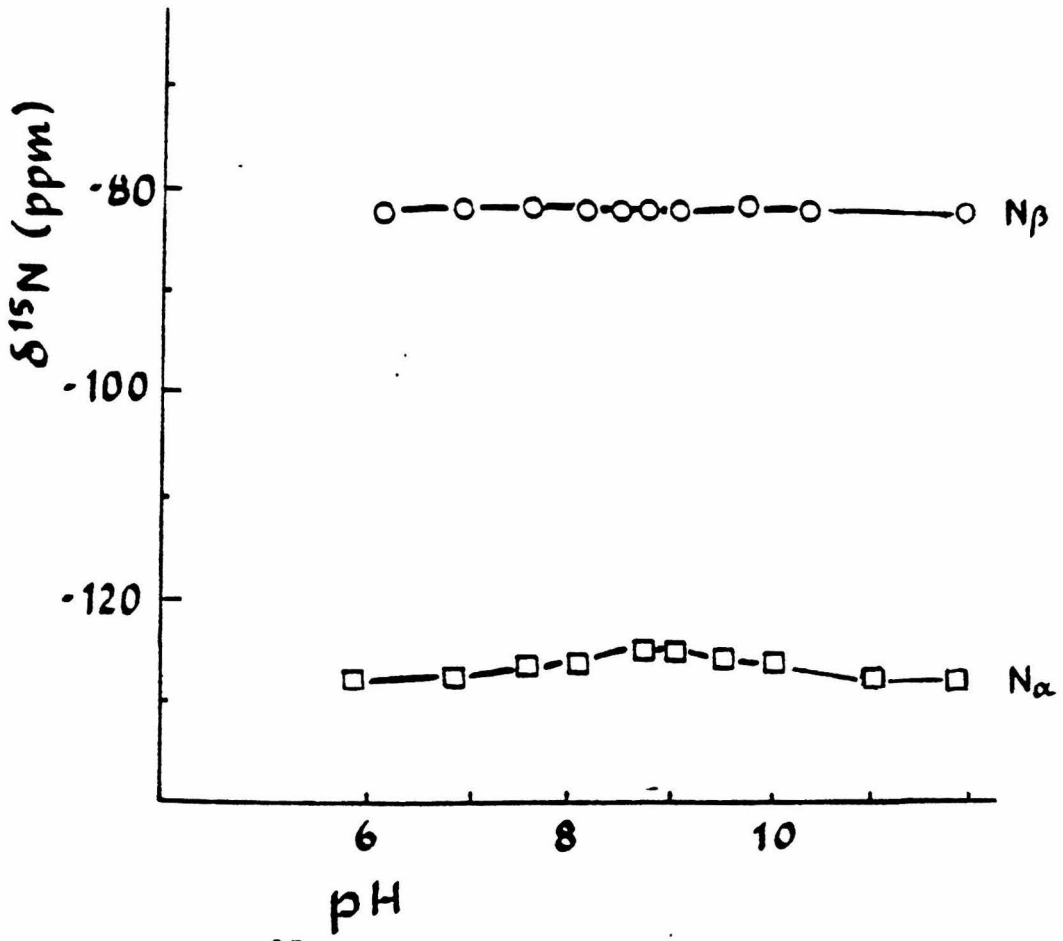

Fig. 5 ^{15}N chemical shifts of the azo nitrogens of arsanilazo-N-acetyltyrosine (DAT) as function of pH in water.

or to N_β in the model compound DAT.[7b] The $^{15}N_\beta$ shifts of DAT in H_2O and in dimethyl sulfoxide (discussed on p.30) clearly establish N_β as the acceptor of the hydrogen bond from the phenolic hydroxyl.

The $^{15}N_\alpha$ chemical shift of DAT shows small but real changes with pH, a shielding of 2.2 ppm between pH 5.8 and 8.8 and a deshielding of 1.7 ppm between pH 8.8 and 11.9. The shielding is probably due to the dissociation of the second proton from the arsonate group, and the deshielding can be attributed to the ionization of the tyrosine hydroxyl. The ^{13}C shift-pH titration curves of arsanilazo-N-chloroacetyltyrosine in H_2O, shown in Figure 6, support this interpretation; between pH 6 and 8.1, only the C4 carbon adjacent to the arsonate group shows appreciable shift change with pH, while at higher pH, the aromatic carbons on the tyrosine moiety show large shift changes with pH, with a pK_α value of approximately 9.5, due to ionization of the tyrosine hydroxyl. For a structurally similar model compound monoarsanilazocresol, pK_α values of 8.4 and 9.5 have been reported for the ionization of the arsonic and the tyrosine hydroxyl respectively.[7b]

The apparent insensitivity of the N_β shift of DAT to ionization of tyrosine hydroxyl is surprising but can be interpreted as follows. When the phenolic proton ionizes, the resulting anion can be represented as a resonance hybrid of the principal structures II and III (Figure 5). If the azophenolate (II) were the dominant resonance form, the loss of the hydrogen bond would cause a significant deshielding of N_β. However, a predominant contribution from structure III would be expected to be

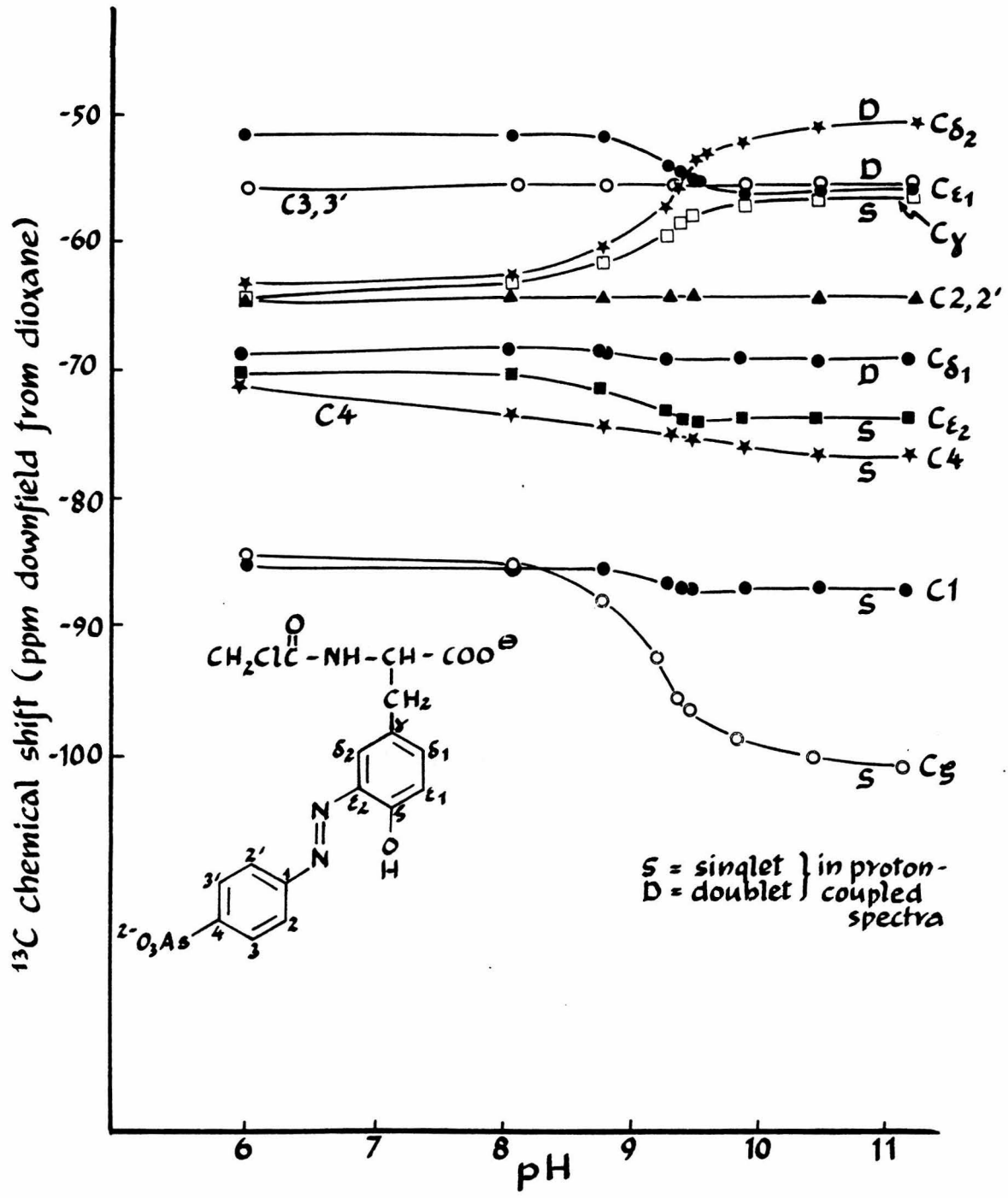

Fig. 6 ^{13}C chemical shifts of arsanilazo-N-chloroacetyltyrosine as function of pH in water. The ^{13}C resonances were assigned by comparison with those of tyrosine, azobenzene and arsanilic acid. The assignments of C_{δ_2} and C_{ε_1} above pH 9.2 are uncertain due to overlap.

associated with a pronounced shielding of N_β. These effects oppose each other and if more or less equal could thus result in an essentially unchanged ^{15}N shift. Further evidence in favor of this interpretation will be presented later in this paper.

^{15}N NMR shifts of TAT and TAT-Zn complex

The $^{15}N_\alpha$ shifts of TAT and its zinc complex as a function of pH are shown in Figure 7. The $^{15}N_\alpha$ shifts of TAT and DAT in the absence of zinc are similar except for the small shielding around pH 7.7 in DAT due to the ionization of the arsonate group. The $^{15}N_\alpha$ resonances of both TAT and DAT show slight deshielding around pH 8.5 due to the ionization of the tyrosine hydroxyl.

On addition of one equivalent of zinc chloride, the ^{15}N resonance of TAT shows a large shielding as pH is increased from 3 to 6; clearly the complexation with zinc is facilitated by ionization of the proton from the tetrazole ring which has an estimated pK_α of 5.4.[7b] Further shielding is observed between pH 8 and 9 on ionization of the phenolic proton. On full zinc complexation at pH 9, the azo nitrogen of TAT is shielded to -40 ppm, an upfield shift of 90 ppm compared to that of TAT alone. Increasing the TAT-Zn ratio to 1:3 caused no further shielding of N_α. Above pH 10.0, hydroxide ions begin to complex with zinc, and precipitation of zinc hydroxide occurs.

It is known that an o-hydroxy azo compound with a heterocyclic substituent such as TAT acts as a tridentate ligand, complexing with most

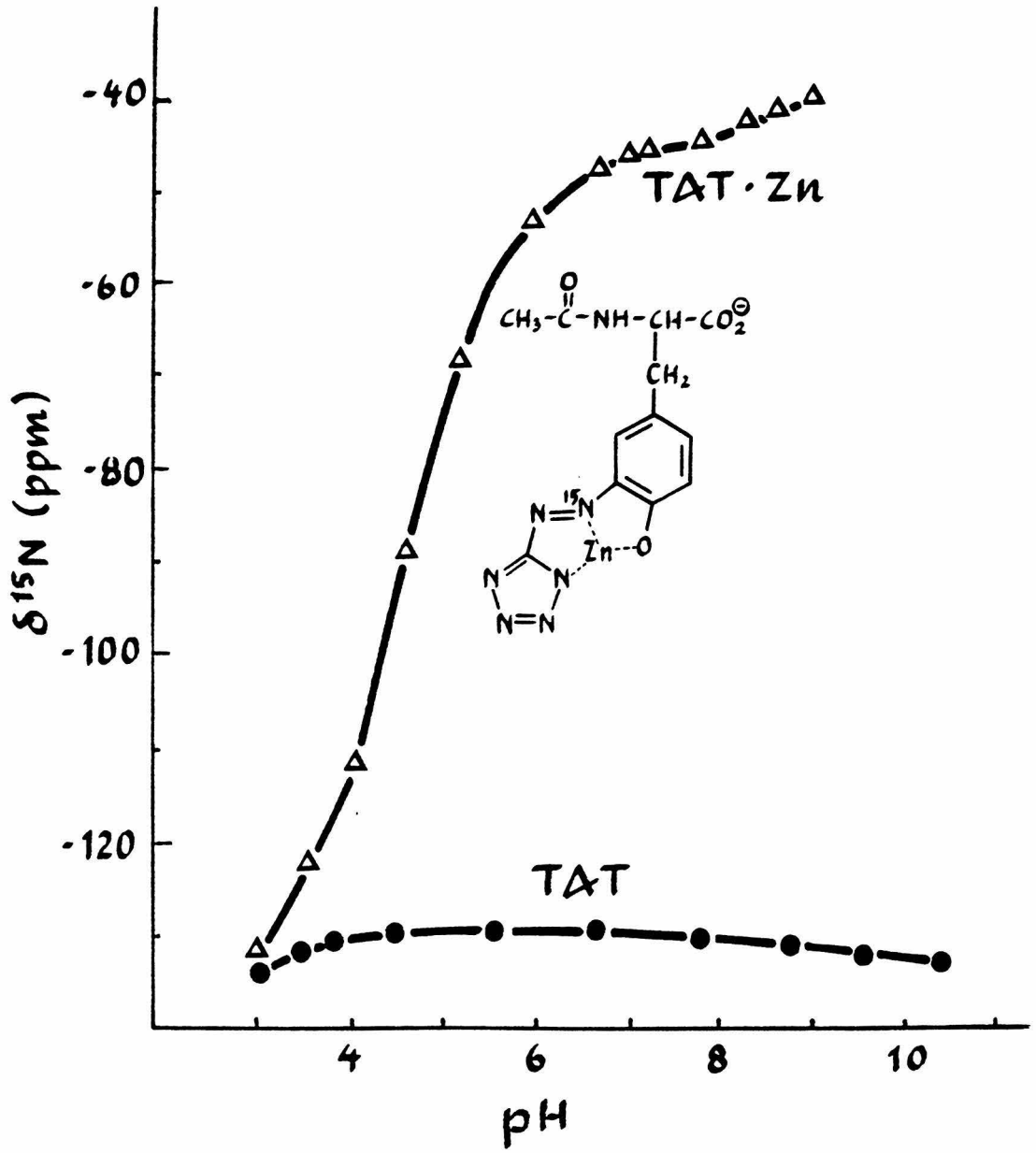

Fig. 7 ^{15}N shifts of tetrazolylazo-N-acetyltyrosine (TAT) and its zinc complex (TAT.Zn) as functions of pH.

metals through the o-hydroxyl group, the azo nitrogen nearest to the phenolic ring (N_α) and the heterocyclic nitrogen atom, giving two stable five-membered chelate rings as shown in Figure 7.[16a, b] Therefore, the shift of N_α in TAT.Zn complex at -40 ppm can be regarded as the shift of an azo nitrogen directly complexed to Zn. Thus, if azotyrosine-Zn complexation actually occurs in arsanilazotyrosyl-248-CPA, we can expect one of the azo nitrogens, the one directly complexed to zinc, to shift upfield to the vicinity of -40 ppm.

^{15}N shifts of arsanilazotyrosyl-248 CPA (Zn.Azo-CPA)

The ^{15}N NMR spectra of arsanilazotyrosyl-248 CPA enriched in ^{15}N at both azo nitrogens, at pH 7.0, 8.8 and 9.6 are shown in Figure 8. This enzyme, with a molecular weight of 34,472[17] is the largest enzyme from which ^{15}N spectra have so far been obtained. The assignment of N_α and N_β was made by first obtaining ^{15}N spectra of arsanilazotyrosyl-248 CPA ^{15}N enriched in N_α only; the ^{15}N shift so obtained was identical to the one assigned to N_α in the doubly enriched enzyme.

The ^{15}N shifts of the two azo nitrogens of arsanilazotyrosyl-248 CPA (Zn.Azo-CPA) as function of pH are compared with those of DAT and TAT.Zn complex in Figure 9, and are listed in Table I. At pH 7.0 and 7.8, the shifts of N_α at -130 ppm and N_β at -78 ppm in the enzyme are very close to the corresponding shifts of DAT without zinc and therefore there is no indication of complexation with zinc at this pH; the shielding of N_β relative to N_α indicates that in the enzyme as in DAT, N_β is hydrogen-bonded to the Tyr-248 hydroxyl.

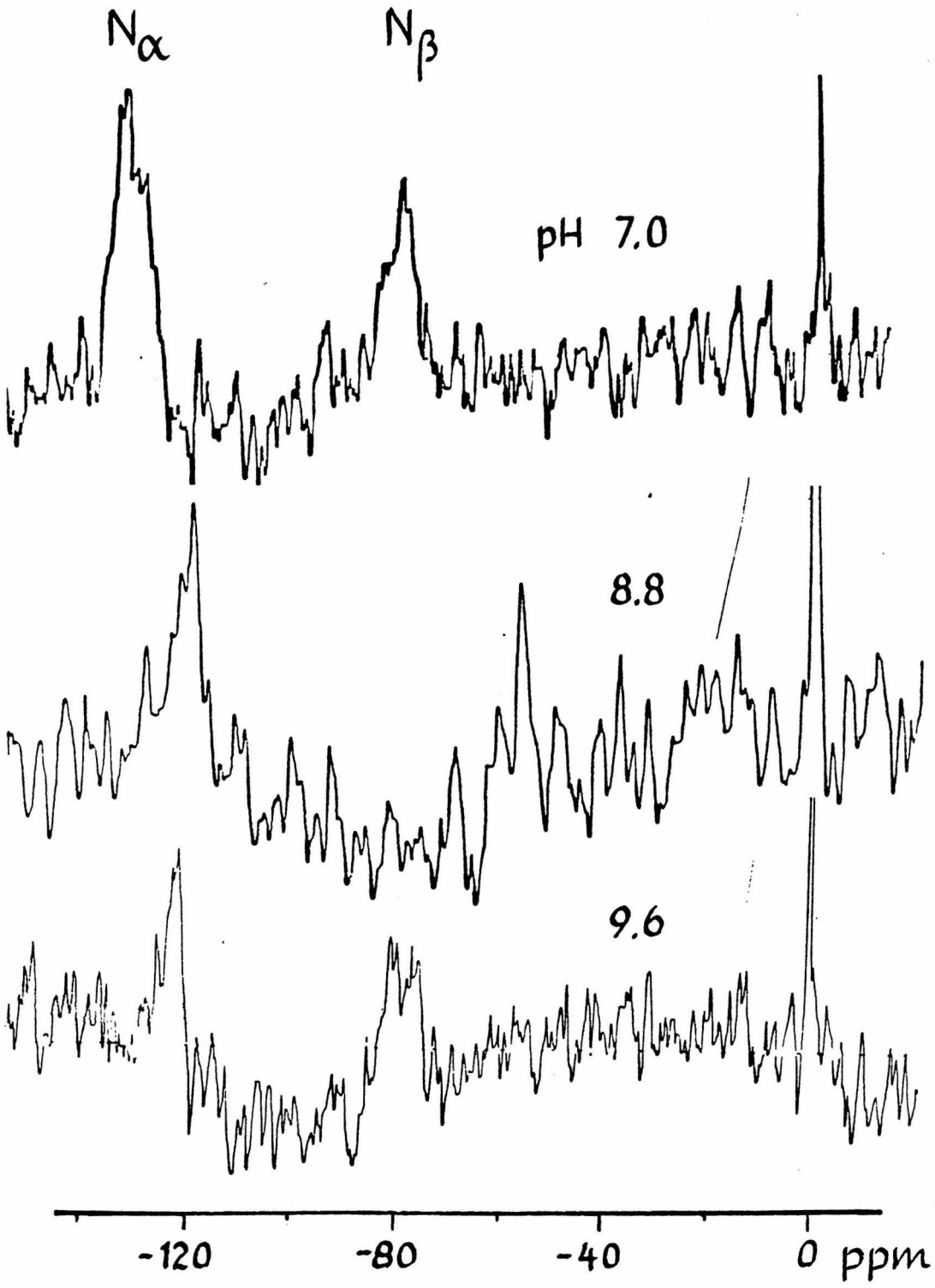

Fig. 8 ^{15}N spectra of arsanilazotyrosyl-248 CPA (Zn.Azo-CPA) enriched in ^{15}N at both azo nitrogens obtained at pH 7.0 (43,799 transients), pH 8.8 (70,010 transients) and at pH 9.6 (52,057 transients).

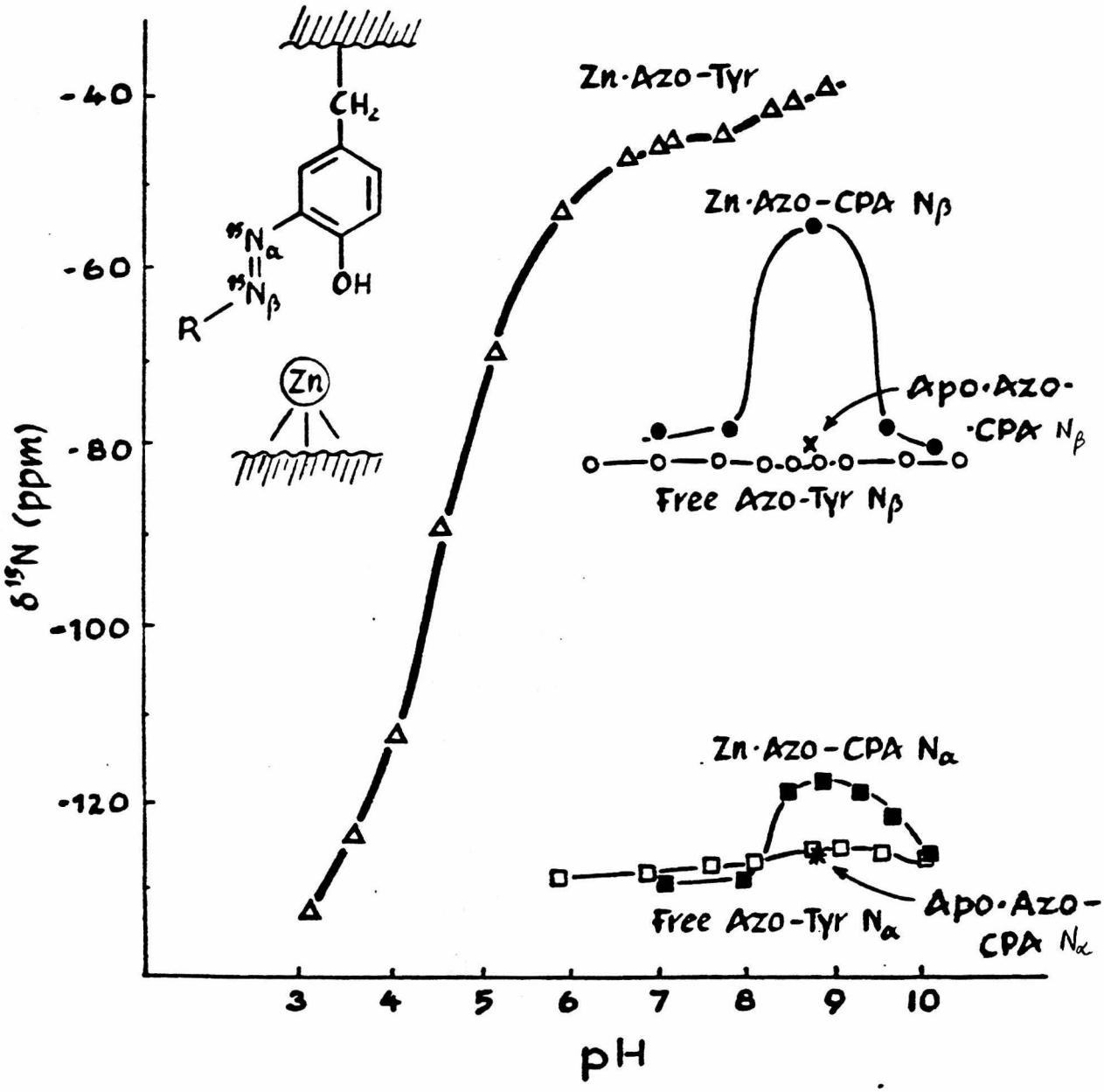

Fig. 9 The pH dependence of the ^{15}N shifts of the two azo nitrogens of arsanilazotyrosyl-248 CPA (Zn.Azo-CPA; ■ : N_α : ● : N_β); apoarsanilazo-tyrosyl-248 CPA (Apo.Azo-CPA, ✳ : N_α; × : N_β), and the model compounds DAT (free Azo-Tyr, □ : N_α; ○ : N_β) and TAT.Zn complex (Zn.Azo-Tyr, △ : N_α)

At pH 8.8, however, the N_β nitrogen shows a large upfield shift to -56 ppm and N_α shows a small upfield shift to -118 ppm. These results strongly suggest that at this pH, the azotyrosine in Zn.Azo-CPA is at least partially complexed with zinc. The larger shift observed for N_β relative to N_α suggests that in arsanilazotyrosyl-248 CPA, zinc complexes to the phenolic oxygen and N_β, resulting in a six-membered ring (Figure 10) as in other bidentate azophenol metal complexes whose structures are known from X-ray studies.[18a, b] This is in contrast to the tridentate TAT where Zn complexes to N_α, phenolic oxygen and heterocyclic nitrogen to form two five-membered rings as mentioned earlier. Because the azo nitrogen directly complexed to zinc is N_α in TAT but N_β in Zn.Azo-CPA, the ^{15}N shifts of these two nitrogens are the ones that should be compared to estimate the extent of zinc complexation in the enzyme, although such estimate will be approximate because of the unknown effect of the presence of the third ligand, the tetrazole nitrogen, on the magnitude of the shielding of the azo nitrogen on complexation with zinc. A semi-quantitative estimate of the extent of complexation in Zn.Azo-CPA can be attempted as follows. One approach is to compare the observed ^{15}N chemical shifts ($\delta^{15}N$) of the free azotyrosine, model azotyrosine-Zn complex and the enzyme. If we assume from Figure 9 that -40 ppm represents the chemical shift of an azo nitrogen fully complexed to zinc, and -82.5 ppm represents that of an azo nitrogen hydrogen-bonded to tyrosine hydroxyl, then the chemical shift of -55.6 ppm observed for the azotyrosine in Zn.Azo-CPA suggests that about 63% of the time, the active-site tyrosine in the enzyme is complexed to catalytic zinc. Another approach is to compare the

magnitude of shielding, $\Delta\delta^{15}N$, on complexation, in the model compound and the enzyme. If we assume that $\delta^{15}N$ of Zn.Azo-CPA in the absence of hydrogen-bonding or zinc complexation is equal to that the N_β of DAT in dimethyl sulfoxide, -103.9 ppm, or of N_β in Zn.Azo-CPA-β-phenylpropionate complex, -107.3 ppm (Table I, discussed on p. 30), and further assume that only zinc complexation contributes to the shielding of N_β in Zn.Azo-CPA, the observed $\delta^{15}N_\beta$ of -55.6 ppm indicates that zinc complexation causes a shielding ($\Delta\delta^{15}N_\beta$) of 48.3 ppm (or 51.7 ppm) in Zn.Azo-CPA. Compared to the $\Delta\delta^{15}N$ of 90 ppm for the azo nitrogen of TAT on full complexation to zinc, the observed $\Delta\delta^{15}N$ in Zn.Azo-CPA indicates 54~57% complexation. The two approaches, based on slightly different assumptions as indicated above, yield reasonably close values, and suggest that the major active-site conformation of Zn.Azo-CPA at this pH is the one in which the active-site tyrosine is complexed to zinc.

Such partial complexation can arise from either (1) the coexistence of at least two different conformations for a flexible tyrosyl-248 side chain in which full zinc-azotyrosyl complex occurs 54∿63% of the time, or (2) a single conformation in which the azotyrosyl-248 Zn complex is weak due to steric constraints at the active site and/or partial neutralization of zinc by other ligands on the enzyme. Although one cannot distinguish between these two possibilities at present, the ^{15}N results clearly show that in solution the conformation of tyrosyl-248 side chain is such as to allow 54∿63% azotyrosyl-Zn complexation at pH 8.8.

At pH 9.6∿10.3, both azo nitrogens in Zn.Azo-CPA shift downfield to values close to those of free azophenolate ion. This is in accord with loss of the azotyrosyl-Zn complexation because of the competition of

hydroxide ions with azophenolate for zinc, just as was observed in TAT.Zn mixtures above pH 10.0.

Figure 10 shows schematically the probable states of the active-site tyrosine and zinc in Zn.Azo-CPA at various pH values. At pH 7.0, the azo nitrogen (N_β) is intramolecularly hydrogen-bonded to the phenolic proton. At pH 8.8, on partial ionization of phenolic proton, the azophenolate complexes with zinc. At pH 10.3, hydroxide ion replaces azophenolate as ligand to zinc.

The X-ray structure of crystalline CPA has been studied only at pH 7.5, and we cannot determine from the ^{15}N results alone whether at this pH the azotyrosyl residue is close to the catalytic zinc but is not complexed because the catalytic zinc does not compete effectively with proton for the azophenolate at that pH, or the tyrosine hydroxyl in solution is more distant from zinc as in crystalline CPA. However, the ^{15}N results clearly indicate that the tyrosine-248 side chain is mobile enough to assume a conformation in which the azophenolate is close enough to zinc to form a complex in the pH range where it is an effective ligand to zinc. Thus, caution is required in interpreting the conformation of crystalline enzyme as being directly applicable to solution conformation.

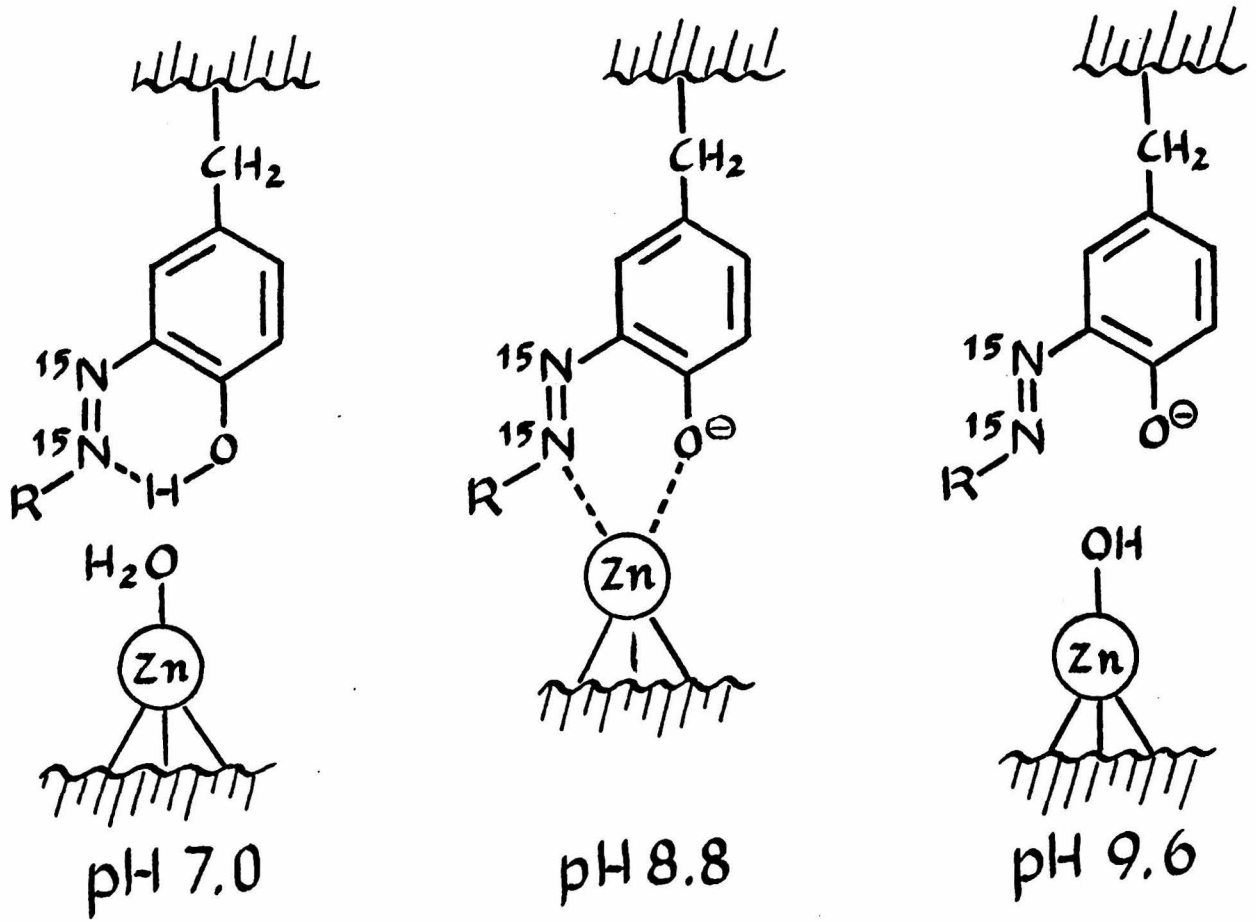

Fig. 10 Schematic diagram of the probable state of the active-site tyrosine and zinc in arsanilazotyrosyl-248 CPA at various pH values.

^{15}N shifts of apoarsanilazotyrosyl-248 CPA (Apo.Azo-CPA)

To investigate whether the observed shielding of the azo nitrogens of arsanilazotyrosyl-248 CPA (Zn.Azo-CPA) at pH 8.8 is caused by complexation with the catalytic zinc and not by possible interactions with other active-site groups, the zinc was removed from the enzyme to obtain apoarsanilazotyrosyl-248 CPA (Apo.Azo-CPA) (Experimental section).

The ^{15}N spectrum of Apo.Azo-CPA at pH 8.8 is shown in Figure 11(D) and the ^{15}N shifts of the two azo nitrogens are compared to those of Zn.Azo-CPA in Figure 9. Removal of zinc causes a 23.5 ppm deshielding of N_β resonance, from -55.6 ppm for the Zn.Azo-CPA to -79.1 ppm for the Apo.Azo-CPA, a value close to that of free azotyrosine DAT (-82.5 ppm). The N_α resonance also shifts downfield, from -117.9 ppm for Zn.Azo-CPA to -126.2 ppm for Apo.Azo-CPA, a value almost identical with that of DAT (-126.0 ppm). These results provide strong evidence that the large shielding of the azo nitrogens observed in Zn.Azo-CPA relative to that of Apo.Azo-CPA and of free DAT at pH 8.8 is caused by partial complexation of the azotyrosyl group of the enzyme with the catalytic zinc.

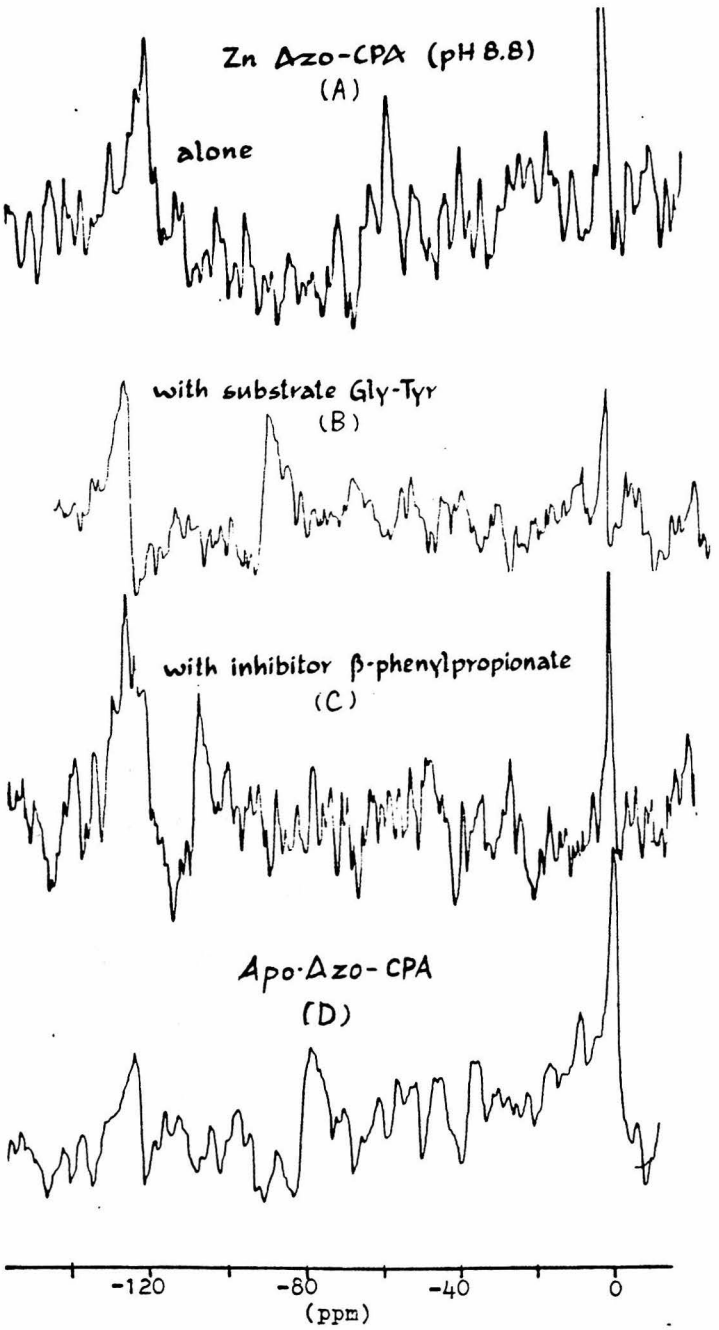

Fig. 11 ^{15}N spectra at pH 8.8 of (a) arsanilazotyrosyl-248 CPA (Zn.Azo-CPA, 70,010 transients); (b) Zn.Azo-CPA with quasi-substrate glycyl-L-tyrosine (245,587 transients); (c) Zn.Azo-CPA with inhibitor β-phenylpropionate (131,054 transients); (d) apoarsanilazotyrosyl-248 CPA (Apo.Azo-CPA, 255,327 transients).

^{15}N shifts of Gly-Tyr and β-phenylpropionate complexes of Zn.Azo-CPA

Further evidence that the shielding of the azo nitrogens of the enzyme at pH 8.8 is due to complexation with zinc is found in the significant changes observed in the ^{15}N shifts on addition of a substrate glycyl-L-tyrosine (Gly-Tyr) or an inhibitor β-phenylpropionate, each of which is known to bind to the active site and cause loss of the absorption maximum at 510 nm which has been attributed to Zn.azotyr-248 complex.[6] The mode of binding of Gly-Tyr to the active-site of carboxypeptidase A, according to X-ray structure at 2 Å resolution,[2b] is shown in Figure 2; zinc is found to be bound to the carbonyl oxygen of the substrate and Tyr-248 has its hydroxyl close to the amide nitrogen of the peptide bond. Therefore the binding of Gly-Tyr is expected to break the azotyrosine-Zn complex and cause deshielding of the azo nitrogens. This is indeed what occurs. Figure 11 shows how the ^{15}N spectrum of Zn.Azo-CPA at pH 8.8 (A) compares with that of the substrate-enzyme complex at the same pH (B). The N_β nitrogen which was shielded to -56 ppm in Zn.Azo-CPA shifts downfield, on binding of Gly-Tyr, to -88 ppm, a value close to that of DAT. The resonance of the N_α nitrogen also shifts downfield to a value characteristic of DAT. These results provide further evidence that the ^{15}N shifts of the azo nitrogens in Zn.Azo-CPA are a sensitive

probe of the formation and dissociation of azotyrosine-zinc complexation.

The inhibitor β-phenylpropionate is also known to bind to the catalytic zinc atom through its carboxylate group and is therefore expected to break the Tyr-Zn association. In presence of the inhibitor at pH 8.8, the N_β peak again is substantially downfield relative to that of the enzyme alone which indicates the expected dissociation of the Tyr-Zn association (Figure 11 (C)).

The ^{15}N shifts of the substrate and inhibitor complexes of Zn.Azo-CPA at pH 8.8 are sensitive probes, not only of the dissociation of azotyrosine-Zn complex, but also of the formation or dissociation of hydrogen bonding of N_β with neighboring groups, and thus provide interesting information as to the changes that occur at the active site of the enzyme in solution on binding of the substrate or the inhibitor. Figure 12 provides a comparison of the ^{15}N shifts of the substrate and inhibitor complexes of Zn.Azo-CPA over the range of pH from 8.8 to 10.3 with those of free Zn.Azo-CPA, Apo-Azo-CPA and DAT. Significantly, at pH 8.8, the N_β shift of the enzyme inhibitor complex is deshielded by 28.2 ppm while that of the enzyme-substrate complex is slightly deshielded by 8.9 ppm relative to that of Apo.Azo-CPA.

In the Gly-Tyr complex of Zn.Azo-CPA, the 8.9 ppm deshielding of the N_β resonance relative to that of Apo.Azo-CPA suggests the

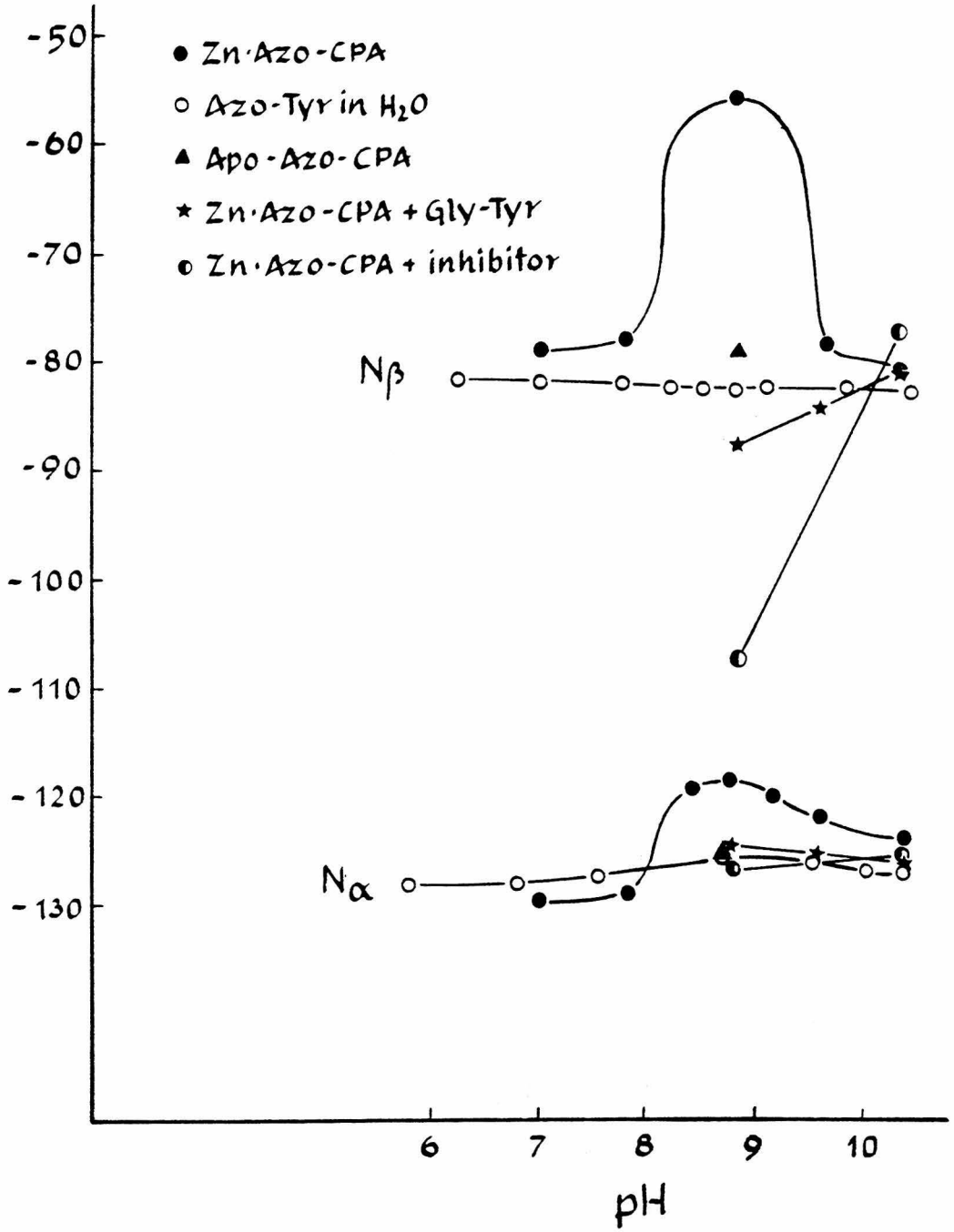

Fig. 12 The pH dependence of the ^{15}N shifts of the two azo nitrogens of arsanilazotyrosyl-248 CPA (Zn.Azo-CPA) and its complex with glycyl-L-tyrosine and with inhibitor β-phenylpropionate. The ^{15}N shifts of apoarsanilazotyrosyl-248 CPA (Apo-Azo-CPA) and of the model compound DAT (Azo-Tyr) are also shown for comparison.

following possibilities.

(1) The dominant conformation at the active site is the one in which N_β is hydrogen bonded to Tyr-248 hydroxyl (Figure 13 Ia) but there is a minor conformation in which Tyr-248 hydroxyl is intermolecularly hydrogen-bonded to another neighboring group, possibly to the NH group of the substrate (Figure 13 Ib). (2) The N_β is hydrogen bonded to NH group of the substrate while the Tyr-248 hydroxyl is hydrogen bonded to the same amide nitrogen (Figure 13 II). If the true catalytic function of Tyr-248 hydroxyl is to donate a proton to the leaving amine group, conformation Ib or II in which the tyrosine hydroxyl is hydrogen bonded to the amide nitrogen of the substrate should occur in Zn.Azo-CPA which has full catalytic activity. Further study is required to distinguish between these possibilities, for example, by use of N-methyl and ester analogues of Gly-Tyr.

In the β-phenylpropionate complex of Zn.Azo-CPA, the N_β resonance is deshielded to -107 ppm at pH 8.8 (Figure 12). This shift is seen to be comparable to that of the N_β of DAT (-103.9 ppm) in dimethyl sulfoxide (Table I). It is also clear that the change in N_β shift of the inhibitor complex, from -107 ppm at pH 8.8 to -76.9 ppm at pH 10.3 closely resembles the change in the N_β shift of DAT in dimethyl sulfoxide from -103.9 ppm to -78.1 ppm * on ionization of Tyr-OH by addition of sodium hydroxide.

* The ^{15}N shift of ionized DAT was measured in dimethyl sulfoxide-water in order to keep the ionized species in solution (see Table I).

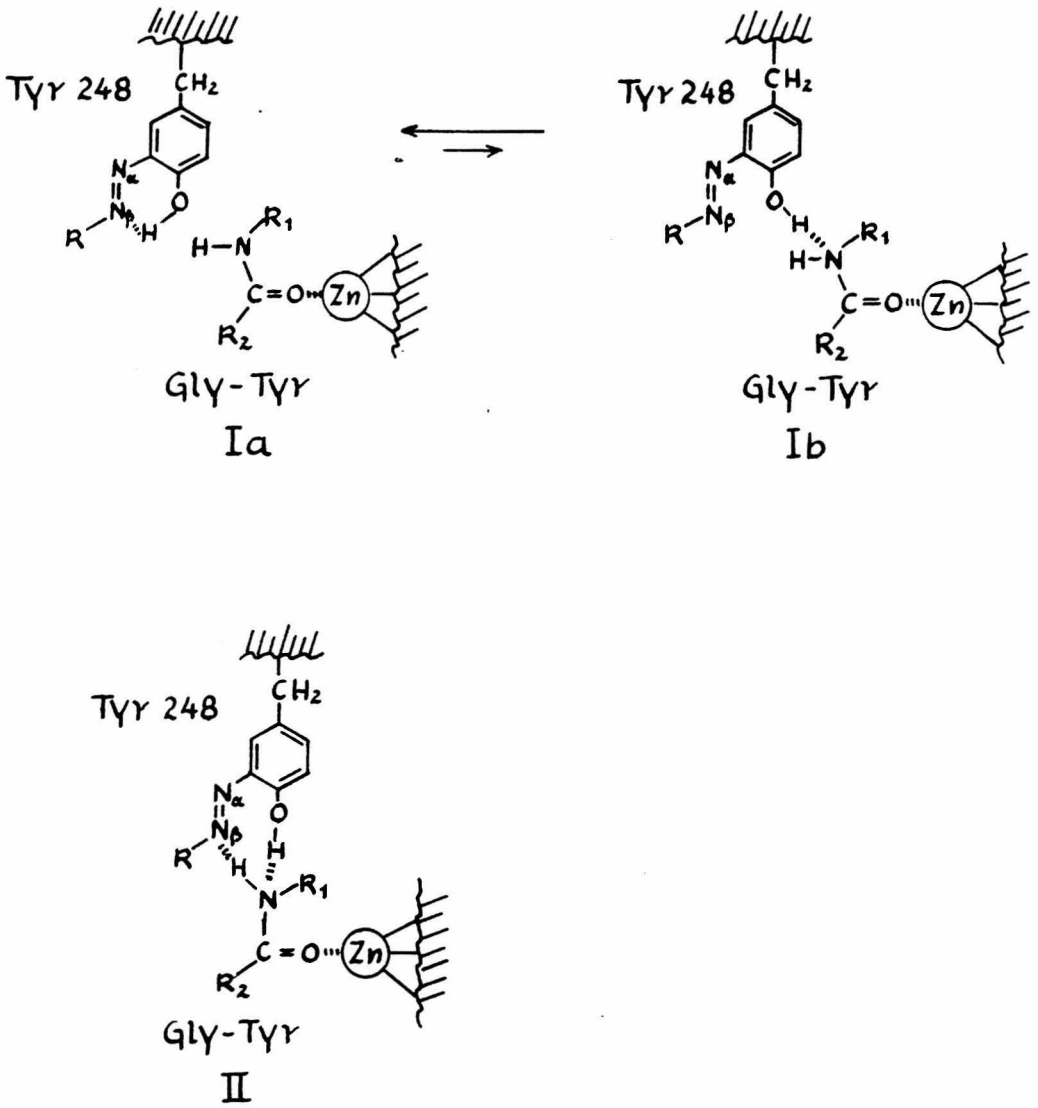

Fig. 13 Possible modes of binding of Gly-Tyr to Zn.Azo-CPA

Table I

^{15}N shifts of Zn.Azo-CPA, its Gly-Tyr and β-phenylpropionate complexes, Apo.Azo-CPA and DAT

pH	$\delta^{15}N$ for N_β (ppm)[a]							
	Zn.Azo-CPA	Zn.Azo-CPA + Gly-Tyr	Zn.Azo-CPA + β-ϕ-propionate	Apo.Azo-CPA	DAT			10-phenyl azo-9-phenanthrol anion (DMSO)
					H_2O	DMSO	DMSO/H_2O 3:1 v/v	
7.0	-78.0				-82.1			
8.8	-55.6	-88.0	-107.3	-79.1	-82.5	-103.9 (phenol)	-101.4	
9.6	-78.5	-84.4			-82.4			
10.3	-80.8	-80.5	-76.9		-82.6		-78.1 (phenolate)	-33.8

pH	$\delta^{15}N$ for N_α (ppm)[a]							
	Zn.Azo-CPA	Zn.Azo-CPA + Gly-Tyr	Zn.Azo-CPA + β-ϕ-propionate	Apo.Azo-CPA	DAT			10-phenyl azo-9-phenanthrol anion (DMSO)
					H_2O	DMSO	DMSO/H_2O 3;1 v/v	
7.0	-129.8				-127.8			
8.8	-117.9	-125.1	-125.9	-126.2	-126.0		-137.0 (phenol)	
9.6	-122.3	-125.5			-126.8			
10.3	-123.8	-125.9	-125.1		-127.4		-130.1 (phenolate)	-110.1

a. from HNO_3. Negative sign indicates downfield.

The N_β shifts of DAT in dimethyl sulfoxide can be interpreted as follows. The position of N_β resonance of DAT in dimethyl sulfoxide at -103.9 ppm is much more deshielded than that in water (-82.5 ppm) because dimethyl sulfoxide is an excellent hydrogen-bond acceptor and can compete effectively with the N_β as the acceptor for the hydrogen bond to the phenolic proton (see Figure 14). Arguing from this, the close similarity between the N_β shift of DAT in dimethyl sulfoxide (-103.9 ppm) and that of the Zn.Azo-CPA- β-phenylpropionate complex (-107.3 ppm) at pH 8.8 strongly suggests that in the enzyme-inhibitor complex, the tyrosine-248 hydroxyl is not hydrogen bonded to N_β but instead is hydrogen bonded to another neighboring group, the most likely acceptor being the second carboxylate oxygen of the inhibitor as shown schematically in Figure 14.

Interaction of the carboxylate group of β-phenylpropionate with the catalytic zinc of CPA has been inferred from (a) X-ray structure of CPA-β-(p-iodophenyl)propionate complex at 6 Å resolution[19]; (b) the decreased rate of exchange of zinc with ^{65}Zn in CPA on inhibitor addition and the failure of the inhibitor to bind to zinc-free CPA.[20] It is further known that the Tyr-248 hydroxyl of the free CPA can be acetylated by treatment with N-acetylimidazole and that this acetylation is blocked if β-phenylpropionate is bound

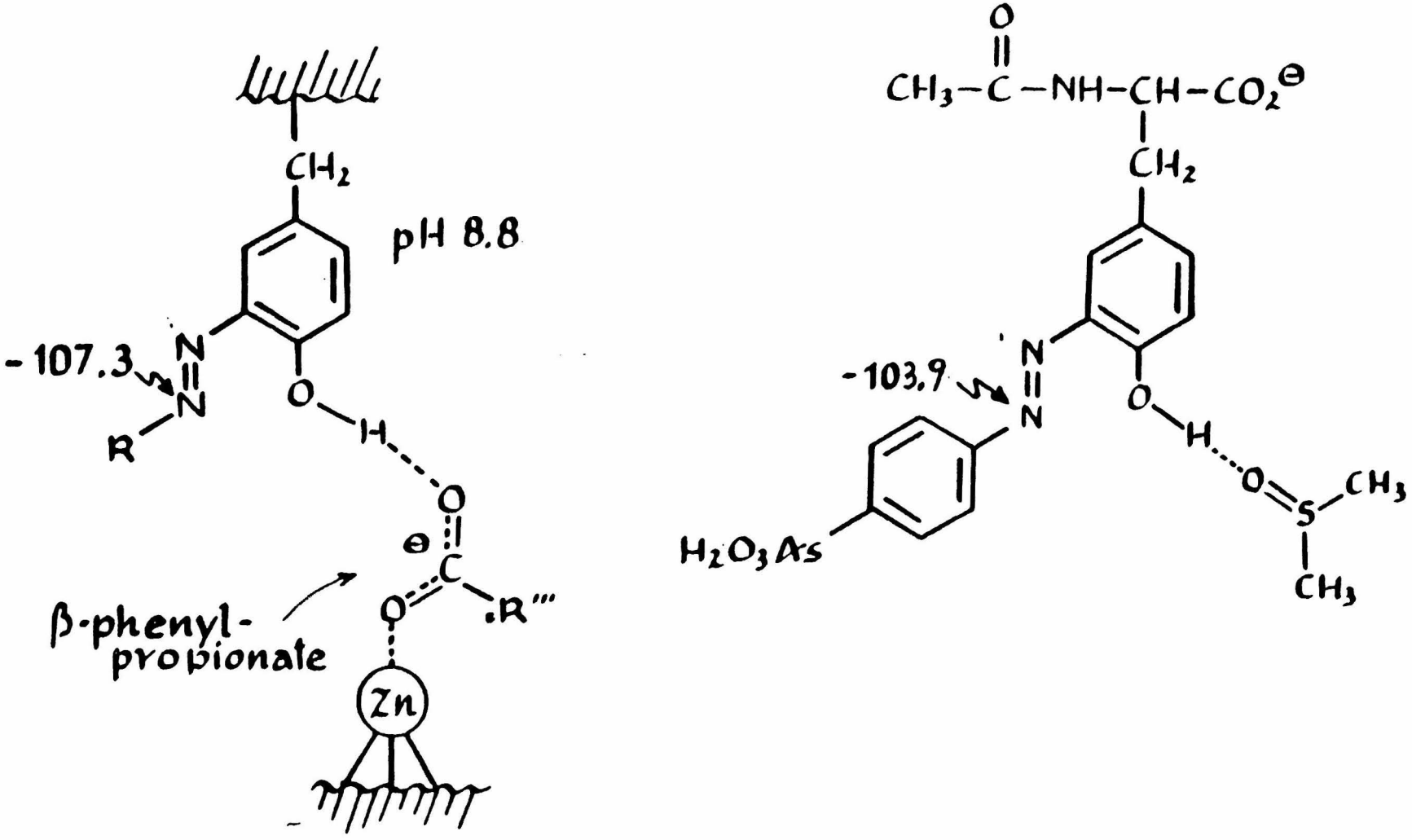

Fig. 14 Probable mode of binding of the inhibitor β-phenylpropionate to the arsanilazotyrosyl-248 residue of Zn.Azo-CPA (left). The observed ^{15}N shifts in the enzyme-inhibitor complex are similar to those of the model compound DAT in dimethyl sulfoxide (right).

to the enzyme;[21] this suggests a close proximity of the carboxylate group of the inhibitor not only to zinc, but also to the Tyr-248 hydroxyl of CPA. Thus the chemical and NMR evidence are consistent in suggesting that the carboxylate group of the inhibitor coordinates with zinc through one oxygen and forms a hydrogen bond with Tyr-248 hydroxyl through the other as shown schematically in Figure 14.

On ionization of the tyrosine hydroxyl, the ^{15}N shift of Zn.Azo-CPA-β-phenylpropionate complex at pH 10.3 shifts upfield to -76.9 ppm, close to the value for ionized DAT in dimethyl sulfoxide/water, -78.1 ppm (Table I). On ionization of the phenolic proton, DAT can be represented as a resonance hybrid of structures such as II and III in Figure 5, and the observed shielding of N_β might be attributed to some contribution of structure III. To obtain an estimate of the N_β shift expected for an ionized hydrazone of structure III, a model compound, the anionic form of 10-phenylazo-9-phenanthrol which is known to exist completely in the hydrazone form,[22] was synthesized and its ^{15}N shifts were measured in dimethyl sulfoxide. Its observed N_β shift of -33.8 ppm (Table I) indicates that N_β resonance of an ionized hydrazone is considerably shielded relative to that of azobenzene (-133 ppm) and suggests that the observed shielding of N_β resonance of DAT from -101.4 ppm to -78.1 ppm on ionization of phenolic proton can be attributed to some contribution from structure III. In water, the ionized DAT shows N_β shift (-82 ppm) very close

to the corresponding shift in dimethyl sulfoxide/water (Table I), suggesting that in water also, the resonance structure III (Figure 5) makes contribution to the phenolate species of DAT.

CONCLUSION

The results presented here clearly indicate that the ^{15}N shifts of azo nitrogens are highly sensitive to both complexation with zinc and to hydrogen-bonding and are therefore useful probes for studying such interactions in model systems and biomolecules. The present study demonstrates that it is feasible, by introducing an ^{15}N-enriched probe, to study the active-site conformation of an enzyme such as carboxypeptidase A (CPA), having molecular weight of $\sim$34,500, by ^{15}N NMR, despite the low sensitivity of ^{15}N nucleus and line broadening expected for slowly tumbling macromolecules. The ^{15}N shifts of an arsanilazo group, specifically coupled to the active site tyrosine-248 of CPA with retention of full catalytic activity, serve as sensitive probes of the possible complexation of azotyrosyl-248 with the catalytic zinc in the enzyme in solution. In arsanilazotyrosyl-248 CPA (Zn.Azo-CPA), the 23.5 ppm and 8.3 ppm shielding observed for the N_β and N_α nitrogens relative to those of apo.Azo-CPA at pH 8.8 clearly indicate that complexation of zinc with azotyrosyl-248, with N_β as ligand to zinc is taking place, and that such complex constitutes the molecular

to the corresponding shift in dimethyl sulfoxide/water (Table I), suggesting that in water also, the resonance structure III (Figure 5) makes contribution to the phenolate species of DAT.

CONCLUSION

The results presented here clearly indicate that the ^{15}N shifts of azo nitrogens are highly sensitive to both complexation with zinc and to hydrogen-bonding and are therefore useful probes for studying such interactions in model systems and biomolecules. The present study demonstrates that it is feasible, by introducing an ^{15}N-enriched probe, to study the active-site conformation of an enzyme such as carboxypeptidase A (CPA), having molecular weight of $\sim$34,500, by ^{15}N NMR, despite the low sensitivity of ^{15}N nucleus and line broadening expected for slowly tumbling macromolecules. The ^{15}N shifts of an arsanilazo group, specifically coupled to the active site tyrosine-248 of CPA with retention of full catalytic activity, serve as sensitive probes of the possible complexation of azotyrosyl-248 with the catalytic zinc in the enzyme in solution. In arsanilazotyrosyl-248 CPA (Zn.Azo-CPA), the 23.5 ppm and 8.3 ppm shielding observed for the N_β and N_α nitrogens relative to those of apo.Azo-CPA at pH 8.8 clearly indicate that complexation of zinc with azotyrosyl-248, with N_β as ligand to zinc is taking place, and that such complex constitutes the molecular

basis for the spectral properties of Zn.Azo-CPA observed in this pH range by visible absorption, circular dichroic and resonance Raman techniques. Moreover, the high sensitivity of $^{15}N_{\beta}$ shift to coordination with zinc permits a semi-quantitative estimate of the degree of azotyrosyl-248-Zn complexation which is calculated to be 54~63% at pH 8.8. Thus the major conformation of Zn.Azo-CPA, and by implication, of CPA in solution at this pH is the one in which the active-site tyrosine is complexed to zinc.

It has generally been accepted on the basis of X-ray structures of crystalline CPA and its substrate complex at pH 7.5 that the major conformation of free CPA is the one in which the Tyr-248 hydroxyl is 17 Å from the zinc and that, on binding of a substrate, a large conformational change involving an inward movement of the Tyr-248 hydroxyl from the surface of the molecule toward zinc takes place. This has been regarded as one of the most striking examples of the induced fit theory of enzyme-substrate binding. The ^{15}N NMR results indicate that, in the absence of substrate binding, the Tyr-248 can assume a conformation in which its hydroxyl is close to the catalytic zinc. Thus caution is required in interpreting the conformation of crystalline enzyme as being applicable to solution conformation.

The ^{15}N shift of azotyrosine is also a sensitive probe of intramolecular hydrogen bonding of this nitrogen with phenolic

proton, as indicated by the large deshielding observed in the model compound DAT on disruption of the hydrogen bond by dimethyl sulfoxide. The binding of a quasi-substrate, glycyl-L-tyrosine to Zn.Azo-CPA not only breaks the azotyrosyl-248-Zn complex but also partially disrupts the intramolecular hydrogen-bonding of N_β with tyrosyl-248 hydroxyl as indicated by the 8.9 ppm deshielding of this nitrogen relative to that of Apo.Azo-CPA at pH 8.8. This result is consistent with partial hydrogen bonding of Tyr-248 hydroxyl, whose postulated catalytic function is to donate a proton to the leaving amine group, with the amide nitrogen of the scissile peptide bond of the quasi-substrate.

The binding of an inhibitor β-phenylpropionate causes a nearly complete disruption of the intramolecular hydrogen bond between N_β and the tyrosyl-248 hydroxyl as indicated by 28.2 ppm deshielding of $N\beta$ relative to that of Apo.Azo-CPA. The greater deshielding of the N_β resonance in the enzyme inhibitor complex than in the enzyme-quasi-substrate complex indicates that the carboxylate group of the inhibitor competes much more effectively with the azo nitrogen for the Tyr-248 hydroxyl than does the quasi-substrate.

REFERENCES

1. a. J. F. Riordan and B. L. Vallee, Biochemistry 2, 1460 (1963)

   b. R. T. Simpson and B. L. Vallee, Biochemistry 5, 1760 (1966)

   c. J. P. Felber, T. L. Coombs and B. L. Vallee, Biochemistry 1, 231 (1962)

   d. R. Lumry, E. L. Smith and R. R. Glantz, J. Am. Chem. Soc. 73, 4330,(1951)

2. a. G. N. Reeke, J. A. Hartsuck, M. L. Ludwig, F. A. Quiocho, T. A. Steitz and W. N. Lipscomb, Proc. Natl. Acad. Sci. USA, 58, 2220 (1967)

   b. W. N. Lipscomb, J. A. Hartsuck, G. N. Reeke, F. A. Quiocho, P. H. Bethge, M. N. Ludwig, T. A. Steitz, H. Muirhead and J. C. Coppola, Brookhaven Symp. Biol. 21, 24 (1968)

3. a. J. T. Johansen and B. L. Vallee, Proc. Natl. Acad. Sci. USA, 68, 2532 (1971)

   b. J. T. Johansen and B. L. Vallee, Proc. Natl. Acad. Sci. USA, 70, 2006 (1973)

   c. F. A. Quiocho, C. H. McMurray and W. N. Lipscomb, Proc. Natl. Acad. Sci. USA, 69, 2850 (1972)

4. W. N. Lipscomb, Proc. Natl. Acad. Sci. USA, 70, 3797 (1973)

5. J. T. Johansen, D. M. Livingston and B. L. Vallee, Biochemistry, 11, 2584 (1972)

6. J. T. Johansen and B. L. Vallee, Biochemistry, 14, 649 (1975)

7. a. R. K. Scheule, H. E. Van Wart, B. L. Vallee and H. A. Scheraga, Proc. Natl. Acad. Sci. USA 74, 3273 (1977)

b. R. K. Scheule, H. E. Van Wart, B. O. Zweigel, B. L. Vallee and H. A. Scheraga, J. Inorg. Biochem. 11, 283 (1979)

c. R. K. Scheule, H. E. Van Wart, B. L. Vallee and H. A. Scheraga, Biochemistry, 19, 759 (1980)

8. W.W. Bachovchin and J. D. Roberts, J. Am. Chem. Soc. 100, 8041, (1978)

9. a. J. A. Hartsuck and W. N. Lipscomb, "The Enzymes " ed. P. D. Boyer, vol. III p. 1 (1971)

b. D. S. Auld and B. Holmquist, Biochemistry 13, 4355 (1974)

c. R. G. R. Bacon and D. C. H. Biggs, J. Chem. Soc. Perkins Trans. 1, 2156 (1974)

10. M. Tabachnick and H.Sobotka, J. Biol. Chem. 234, 1726(1959)

11. M. Sokolovsky and B. L. Vallee, Biochemistry 5, 3574 (1966)

12. D. J. Cox, F. C. Bovard, J. P. Bargetze, K. A. Walsh and H. Neurath, Biochemistry 3, 44 (1964)

13. R. O. Duthaler and J. D. Roberts, J. Am. Chem. Soc. 100, 4969 (1978)

14. S. B. Hendrichs, O. R. Wulf, G. E. Hilbert and U. Liddel, J. Am. Chem. Soc. 58, 1991 (1963)

15. A.Burawoy and I. Markowitsch-Burawoy, J. Chem. Soc. 36 (1936)

PART II

Benzoate Catalysis in the Hydrolysis of *endo*-5-[4'(5')imidazolyl]-bicyclo[2.2.1] hept-*endo*-2-yl *trans*-cinnamate: Implications for the Charge-transfer Mechanism of Catalysis by Serine Proteases

INTRODUCTION

A "charge-relay" mechanism has been postulated to be crucial to the effectiveness of operation of the "catalytic triad (serine, histidine, and aspartic acid residues)" in the enzymatic cleavage of peptide bonds by serine proteases[1]. The key feature of this mechanism (Eq. 1) is formation of tetrahedral intermediate by attack of serine on the peptide carbonyl, assisted by proton transfers from serinyl OH to histidyl imidazole and of H3 of the histidyl imidazole to the aspartate carboxylate anion. That the effectiveness of the second of these transfers requires the aspartate carboxylate to be a stronger base than the histidyl imidazole has been clearly delineated by Hunkapiller et al[2]. However, a ^{15}N NMR investigation [3] of α-lytic protease clearly showed that the histidyl imidazole of this enzyme has a normal base strength and the decrease of activity that occurs at low pH values is fully consistent with protonation of this

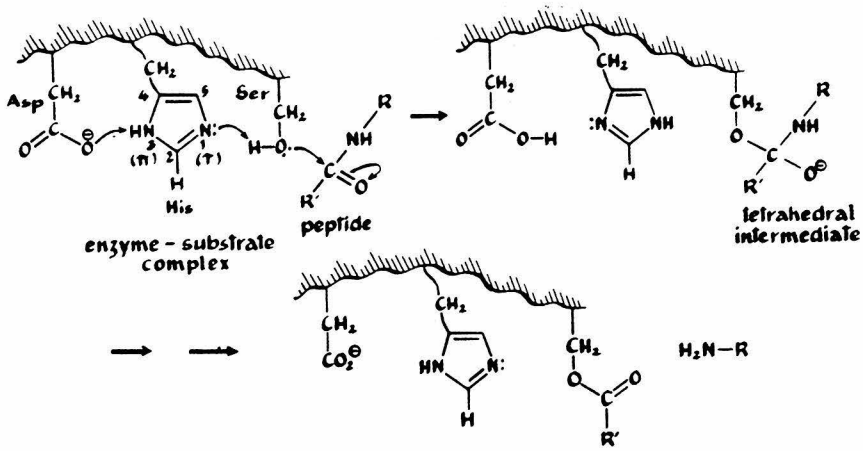

[1]

imidazole rather than the aspartate carboxylate anion of the triad [2],

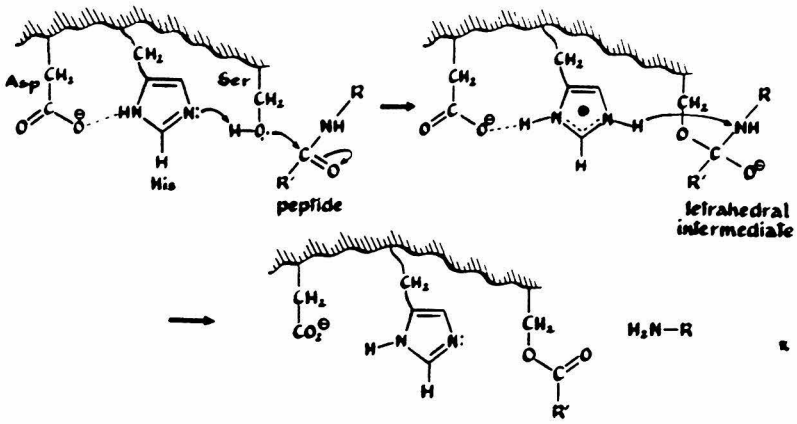

[2]

An alternative mechanism (Eq. 2) has been proposed [3], which might be called a carboxylate-assisted process. This mechanism features (i) a sufficient degree of hydrogen bonding of histidyl imidazole in the tautomeric form with the proton on N3 and the aspartate carboxylate to make this tautomer the predominant one, and (ii) assistance of transfer of the serine proton to N1 of the imidazole by both hydrogen and electrostatic bonding between the resulting imidazolium cation and aspartate carboxylate. This mechanism is completed to the serine ester stage by transfer of a proton from the imidazolium cation to the nitrogen of the leaving RNH — group [3].

The elegant model compound studies by Bender and coworkers [4,5], however, seem to provide strong support for the charge-relay formulation through discovery of a very pronounced benzoate catalysis of the hydrolysis of endo-5-[4'-(5')imidazolyl]bicyclo[2.2.1]hept-endo-2-yl

trans-cinnamate (I). The postulated mechanism is shown in Eq. 3, with water playing the role of serine, the pendant imidazole the role of histidine, and benzoate ion the role of the aspartate carboxylate.

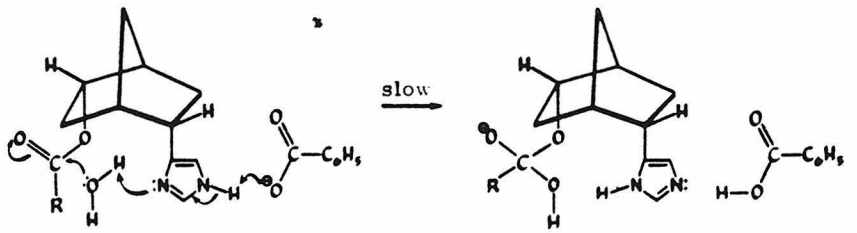

I

[3]

The argument for this mechanism is derived from the fact that, although there is no benzoate catalysis, even at 0.5 M benzoate in water, there is a steadily increasing catalytic effect with increasing dioxane content in the water. This increase in catalytic effectiveness of benzoate ion can be attributed to an increase in the pK_a of the benzoic acid and, thus, a concomitant increase in the basicity of the benzoate ion [5]. Exactly the same kind of argument has been used to account for the postulated effectiveness of the aspartate carboxylate in the charge-relay mechanism--the carboxylate in question being located in a "hydrophobic pocket" of the enzyme [1], thus leading to the expectation of a larger pK_a and greater basicity of the aspartate carboxylate [2].

We believe that there are alternative interpretations of the results. Benzoate ion in 42 mol % dioxane in water has a high catalytic effectiveness. The ratio of catalyzed rate to uncatalyzed rate is about 400 for 0.1 M benzoate (2500 for 0.5 M benzoate)

between pH 6 and 8, where the reported pK_a is 9.4 [5]. Nonetheless, the reported pK_a value of 9.4 implies that the effective concentration of benzoate ion must be small (calculated for a 0.1 M solution to be 0.004 M at pH 8 and 4×10^{-5} M at pH 6). We have used ^{13}C and ^{15}N NMR to probe the species present in the solutions at these concentrations with 4-methylimidazole as model for I.

EXPERIMENTAL SECTION

The ^{13}C NMR spectra were determined at 25.14 MHz with a Varian XL100 spectrometer using the pulse Fourier transform technique with a 35-μsec pulse width and 3-sec repetition rate with proton decoupling, and 12-mm sample tubes. tert-Butyl alcohol and $^{2}H_2O$ in a capillary provided both the shift reference and the lock signal. The ^{15}N NMR spectra were obtained with a Bruker WH180 spectrometer operating at 18.25 MHz, using a 55-μsec pulse width, 5-sec delay, and full proton decoupling [6]. To remove traces of Fe^{3+} and Cu^{2+}, the dioxane was distilled from 8-hydroxyquinoline. This procedure ensured being able to detect the nitrogen resonances of 4-methylimidazole.[3,7]

RESULTS AND DISCUSSION

The use of ^{13}C and ^{15}N NMR spectroscopy to determine the degree of ionization of carboxylic acids and imidazoles, respectively, is well established [3,7,8]. The results obtained for several solutions in 42 mol % dioxane in water containing benzoic acid and 4-methylimidazole at different pH [9] and ionic-strength values are given in Table

I. Clearly, the concentration of benzoate ion in these solutions greatly exceeds that which might be expected from the reported pK_a value. The discrepancy is more real than apparent because the reported pK_a is the thermodynamic value derived with proper regard for the activity coefficients of the ions in this solvent system [5,10]. Concentration equilibrium constants for benzoic acid corresponding to pK_a values of 6.78 and about 6.2 can be derived, respectively, for 0.1 M solutions (with an approximate ionic strength of 0.1) and 0.5 M solutions (ionic strength, 0.5) from the ^{13}C NMR titration curves of Fig. 1. The pK_a values were not changed significantly by addition of equivalent concentrations of 4-methylimidazole. The curve in Fig. 1 for ionic strength 0.5 could not be determined over the whole range of concentrations because of phase separations, but, unquestionably, there is the expected substantial decrease in pK_a with increasing ionic strengths. The pK_a of 4-methylimidazolium cation calculated from the concentrations listed in Table I is 6.4±0.2, which is, within experimental error, the same as the thermodynamic value for I reported by Komiyama *et al* [5]. This is as expected for the ionization of a cationic acid, $BH^+ + H_2O \rightleftharpoons B + H^+_3O$, where changes in the activity coefficient of BH^+ and H^+_3O with solvent and ionic strength will be reasonably parallel.

The hydrolysis rate of I substantially decreases in the absence of benzoate as the proportion of dioxane is increased in the solvent. This decrease has been attributed to preferential solvation of the *trans*-cinnamate group by dioxane, causing steric hindrance to the

Table I. 4-Methylimidazole and benzoic acid (0.5 M each) in 42 mol % dioxane/58% H_2O at 60°C

		Benzoate		4-Methylimidazole		
				$\delta\ ^{15}N$, ppm*		% imidazolium
pH	μ	$\delta\ ^{13}C$, ppm[a]	$\%C_6H_5CO_2^-$[b]	N1	N3	cation†
6.1	0.5[c]	-141.0	56.6	190.6	183.5	60.1
6.4	0.5[c]	-141.8	71.7	188.6	180.9	52.9
6.7	0.5[c]	-142.2	79.2	185.9	177.9	44.0
6.1	0.1[d]	-140.2	41.5	189.4	182.5	56.6

* Upfield from 1 M $H^{15}NO_3$.

† Calculated from the following ^{15}N shifts of 0.5 M 4-methylimidazole (μ=0.1) in 42 mol % dioxane/58% H_2O:

		$\delta\ ^{15}N$, ppm	
	pH	N1	N3
4-methylimidazolium cation	4.3	202.0	197.7
4-methylimidazole	8.5	174.2	161.1

a. Shift of carboxylcarbon downfield of the methyl carbon of tert-butyl alcohol

b. Calculated from the ^{13}C shifts of carboxyl carbon of 0.1 M benzoic acid in Fig. 1

c. $C_6H_5COO^-Na^+$ (0.5 M) and 4-methylimidazole (0.5 M) dissolved in dioxane/H_2O and adjusted to pH by addition of HCl

d. C_6H_5COOH (0.5 M), 4-methylimidazole (0.5 M), and KCl (0.1 M) dissolved in dioxane/H_2O and adjusted to pH by addition of NaOH.

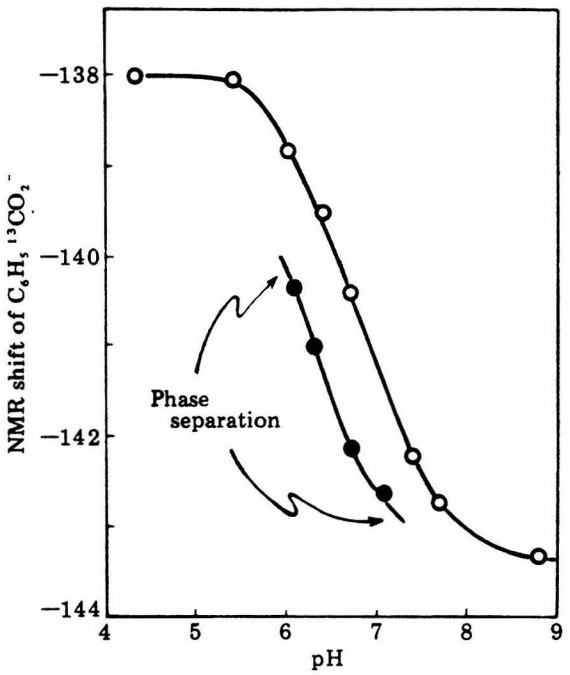

Fig. 1. ^{13}C NMR chemical shifts of benzoate carboxyl carbon as a function of pH at 60°C in 42 mol % dioxane in water. ○, 0.1 M C_6H_5COOH with 0.1 M KCl; the pH was changed by addition of NaOH. ●, 0.5 M $C_6H_5COO^-$ Na^+; the pH was adjusted by addition of HCl. The pH values for this solvent mixture are corrected from glass electrode readings by the procedure of Van Uitert and Fernelius [9]. The shifts are in ppm downfield of the methyl carbon of tert-butyl alcohol. The curves were calculated for pK_a values of 6.78 and 6.2 for 0.1 M and 0.5 M benzoate concentrations, respectively.

concerted attack of water and imidazole, as in Eq. 3. A more important factor is likely to be the decreased ability of the increasingly nonpolar solvent to accommodate the charge separation produced in the formation of the transition state for Eq. 4. In order for benzoate ion to be effective in the mechanisms such as Eq. 3,

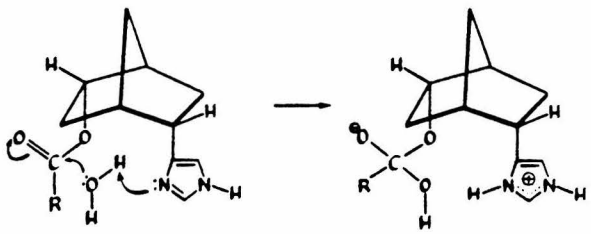

[4]

it should be of comparable basicity to the imidazole group, and, yet, even in 17% mol fraction dioxane in water, where benzoate is only 1/10th as strong a base as imidazole, the rate at 0.5 M benzoate is about 300 times faster than when benzoate is absent [5].

It is our view that benzoate ion can increase the hydrolysis rate of I by virtue of acting much like the asparate carboxylate group in the catalytic triad of a serine protease: first, by hydrogen bonding to the imidazole before the transition state, which will make the imidazole ring more nucleophilic, and, second, by additional stabilization of the transition state by a further degree of hydrogen bonding associated with building up the imidazolium charge as the result of proton transfer (Eq. 5). In addition, there are likely to be secondary influences of benzoate ion at these large concentrations

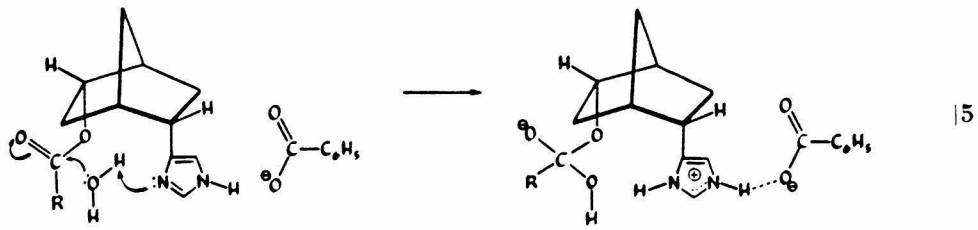

[5]

which contribute to the general polarity of the medium. That the combination of adding benzoate and dioxane could make the reaction rate faster than in pure water is in accord with the speculations of Warshel [11]. Formulations such as given in Eq. 5 also are supported by the failure to obtain evidence for a two-proton transfer mechanism in the benzoate-assisted hydrolysis of I,* although such two-proton transfers have been suggested by proton-inventory studies for some, but not all, reactions catalyzed by α-lytic protease [12] and trypsin [13].

We thank Profs. J. H. Richards and W. W. Bachovchin for many helpful suggestions. This is contribution no. 6173 from the Gates and Crellin Laboratories of Chemistry. These studies were supported by U.S. Public Health Service Grant GM-11072 from the Division of General Medical Sciences and by the National Science Foundation.

* Bender, M. L., presented at the Fourth IUPAC Conference on Physical Organic Chemistry, York, England, September 4-8, 1978.

REFERENCES

1. D. M. Blow, J. J. Birktoft, and B. S. Hartley (1969) Nature (London) 221, 337.

2. M. W. Hunkapiller, S. H. Smallcombe, D. E. Whitaker and J. H. Richards (1973) Biochemistry 12, 4732.

3. W. W. Bachovchin and J. D. Roberts (1978) J. Am. Chem. Soc. 100, 8041.

4. M. Komiyama, T. R. Rosel and M. L. Bender (1977) Proc. Natl. Acad. Sci. USA 74, 23.

5. M. Komiyama, M. L. Bender, M. Utaka and A. Takeda (1977) Proc. Natl. Acad. Sci. USA 74, 2634.

6. D. Gust, R. B. Moon and J. D. Roberts (1975) Proc. Natl. Acad. Sci. USA 72, 4696.

7. I. I. Schuster and J. D. Roberts (1979) J. Org. Chem. 44 3864

8. R. Hagen and J. D. Roberts (1969) J. Am. Chem. Soc. 91, 4504.

9. L. G. Van Uitert and W. C. Fernelius (1954) J. Am. Chem. Soc. 76, 5887.

10. L. G. Van Uitert and C. G. Haas (1953) J. Am. Chem. Soc. 75, 451.

11. A. Warshel (1978) Proc. Natl. Acad. Sci. USA 75, 5250.

12. M. W. Hunkapiller, M. D. Forgac and J. H. Richards (1976) Biochemistry 15, 5581.

13. R. L. Schowen (1977) in Solvent Isotope Effects on Enzyme-Catalyzed Reactions, eds. Cleland, W. W. ,O'Leary, M. H. and Northrop, D. B. (University Park Press, Baltimore, MD), pp. 64-99

PART III

Studies of pH and Anion Complexation Effects on L-Arginine by Natural Abundance ^{15}N Nuclear Magnetic Resonance Spectroscopy [1]

INTRODUCTION

Several enzymes have been found to contain arginyl residues which appear to interact with negatively charged phosphate or carboxylate groups of substrates or cofactors.[2] Chemical modification of positively charged arginyl residues (and the resulting loss of charge) has been shown to result in deactivation of the enzymes[2]. Riordan and co-workers have further suggested that enzymes which interact with anionic substances or cofactors will probably contain arginyl residues at the active site.[3] The binding of DNA with histone and protamine is considered to involve electrostatic interactions between the phosphate anions of DNA and the positively charged arginyl and lysyl residues of these nucleoproteins. The guanidinium group of methylguanidine has been shown by x-ray crystallography to complex with a phosphate anion through multiple hydrogen bonds.[4] The complexation of L-arginine with phosphate and chloride ions in aqueous solution has been studied by ^{31}P and ^{35}Cl nuclear magnetic resonance spectroscopy. Katz and co-workers[5] have reported a downfield shift of 0.5 ppm in ^{31}P chemical shift of methyl phosphate on addition of L-arginine in D_2O solution at pH 6.15. Jönsson and co-workers[6] have measured the pH dependence of ^{35}Cl chemical shift in an aqueous mixture of NaCl and L-arginine and observed a distinct change in ^{35}Cl shift on deprotonation of the guanidinium group. The present study was designed (1) to determine a complete ^{15}N chemical shift-pH titration curve for

L-arginine, and (2) to investigate the utility of ^{15}N NMR for detection and characterization of complexations of guanidinium ion (1) and L-arginine (2) with fluoroborate ions, chloride ions, phosphate ions, and ATP in water solutions.

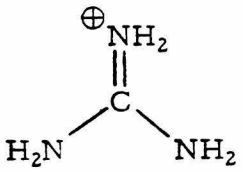

guanidinium ion, 1

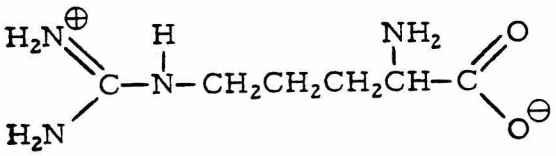

arginine, 2

EXPERIMENTAL SECTION

Natural-abundance ^{15}N NMR spectra were recorded using the pulse Fourier-transform technique with a Bruker WH-180 spectrometer operating at 18.25 MHz. An external 1 M $H^{15}NO_3/H_2O$ capillary reference was used in 25-mm spinning sample tubes. Normal operating conditions for guanidine carbonate and arginine solutions (for spectra other than T_1 measurements) were 55-μs pulses (70° flip angle) with a 15-s pulse delay, and for protamine solutions were 60-μs pulses with a 0.58-s delay. With full proton decoupling, the sample temperatures were about 55°C. Spectra were obtained of 2 M aqueous solutions of guanidine

carbonate with internal D_2O field-frequency locks, and the L-arginine spectra were similarly taken of 1 M aqueous solutions. Protamine sulfate spectra were of 0.0315 M aqueous solutions. L-Arginine was purchased from Sigma Chemical Co., and guanidine carbonate from Matheson Coleman and Bell. Clupeine, a protamine isolated from herring, was obtained as protamine sulfate from the Sigma Chemical Co.

The ^{15}N T_1 values were obtained using the fast inversion recovery (FIRFT) technique.[7] Before measurement of the T_1 values, the solutions were treated with Chelex-100, using the method of Irving and Lapidot,[8] and purged with nitrogen. The pH of each solution was determined with a Radiometer PHM-26C pH meter using a combined glass reference electrode and adjusted with hydrochloric acid and potassium hydroxide. Viscosity measurements were made in an Ostwald viscosimeter immersed in a constant-temperature bath.

RESULTS AND DISCUSSION

Aqueous 1 M solutions of L-arginine show three ^{15}N absorptions. Of these, the resonance at 304 ppm can be assigned to the two equivalent guanidino nitrogens through comparison with the resonance in guanidine carbonate (301.7 ppm); the α-amino nitrogen resonance is surely the one at 342 ppm through comparison with α-amino chemical shifts for other amino acids, and the -NH-absorption is, by elimination, the one at 289 ppm. (A compatible, more rigorous, assignment of peaks has been reported by Pregosin and co-workers.[9])

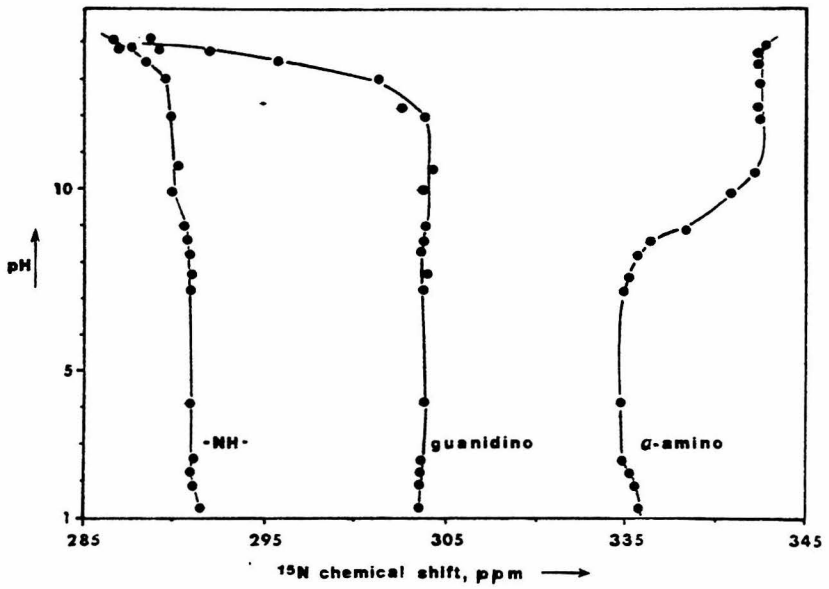

Figure 1. The pH dependence of ^{15}N chemical shifts of L-arginine at 25 ^{o}C. The chemical shifts are in parts per million upfield of $H^{15}NO_3$. The accuracy of pH values is ±0.05 pH unit for pH $\leq$ 13.5. For pH > 13.5, the error may be as much as 0.1-0.3 pH unit because of the high potassium ion concentrations.

The pH dependence of the chemical shift of each of the three resonances is shown in Figure 1. The 8-ppm downfield shift observed for the α-amino nitrogen at 342 ppm as the pH is lowered from 10.6 to 7.3 (pK_a = 9.0 for the α-amino group of L-arginine) [10] is about as expected from decreased shielding of a saturated amine nitrogen on protonation. The 15-ppm upfield shift of the guanidino nitrogens and the 3-ppm upfield shift of the -NH-nitrogen, which result when pH is lowered from 14.1 to 12.0 and protonation occurs, are probably due to a change in the second-order paramagnetic effect of the neutral guanidino nitrogens. Previous studies [11] of the pH dependence of the ^{15}N chemical shift of L-arginine found a similar shift in the highly basic region. However, it was also reported that above pH 13.5 the guanidino nitrogen resonance separates into two resonances, one at approximately 285 ppm and the other at 342 ppm, while the α-amino resonance could not be observed above pH 5.8. The present work and a recent paper by Blomberg and co-workers [12] show clearly that the single resonance at 288 ppm observed in the highly basic region represents the neutral guanidino nitrogens, and that the 342-ppm resonance represents the α-amino nitrogen; the quenching of this nitrogen resonance near its pK_a was almost certainly the result of enhanced relaxation arising from traces of paramagnetic ions, as has been observed for glycine. [13]

On protonation of the carboxyl group (pK_a = 2.2), the α-amino nitrogen resonance shifts 0.6 ppm upfield. This may be due to in-

creased shielding of the nitrogen on loss of hydrogen bonding between the $-NH_3^+$ group and the $-COO^-$ groups as has been suggested by Blomberg and co-workers [12] for glycine. The 0.7-ppm upfield shift of the -NH- group on protonation of the α-amino group (pK_a = 9.0) may be similarly ascribed to increased shielding resulting from the loss of interactions, such as hydrogen bonding, with the neutral α-amino group.

To determine the effects of anions on the resonance of guanidine and L-arginine nitrogens, equivalent amounts of salts or acids were added and the shifts compared to those produced by fluoroborate, which was not expected to complex significantly in aqueous solution. As can be seen from Table I, no very significant changes in shifts were observed on addition of chloride ions. For phosphate-arginine mixtures, the ^{15}N shifts were measured at pH 6.3 at arginine-phosphate mole ratios of 1:1, 1:2, and 1:3 and compared to those produced by fluoroborate. The guanidino nitrogens show a small downfield shift of 0.8 ppm on addition of equimolar phosphate, which may be due to a change in the second-order paramagnetic effect of the guanidino nitrogens on hydrogen bonding with phosphate oxygens. Increasing the phosphate-arginine mole ratio, however, caused no further increase in guanidino nitrogen shifts. Possible effect of phosphate anions on the arginyl residues of protamines was investigated by comparing the nitrogen shifts of arginyl residues in clupeine, a protamine isolated from herring, in the presence and absence of ATP. [14] This protamine has a molecular weight of approximately 5000 and contains 20 arginyl residues per

TABLE I. ^{15}N NMR Shifts[a] of Guanidine Carbonate, L-Arginine, and Protamine Sulfate in Presence of Anions

sample (mole ratio)	pH	guanidine carbonate	1 M arginine -NH-	1 M arginine guanidino	1 M arginine α-NH_2
alone	11.5	301.7	290.3	304.4	342.7
NaCl (1:1)	11.1	301.0	289.7	304.0	342.7
HPO_4^{2-} (1:1)	10.6	300.6	289.6	303.3	341.4
HBF_4 (1:1)	8.9	302.7	291.2	304.2	336.1 [b]
HPO_4^{2-} and $H_2PO_4^-$ [c] (1:1)	7.3		290.5	303.1	334.4 [b]
HCl (1:1)	6.0	301.7	290.8	303.8	335.1 [b]
ATP (1:1)	4.4		291.0	303.7	334.8 [b]
HBF_4	6.3 [d]		290.7	304.0 [e]	.
HPO_4^{2-} and $H_2PO_4^-$ (1:1)	6.3 [d]		290.4	303.2 [e]	334.4 [b]
HPO_4^{2-} and $H_2PO_4^-$ (1:2)	6.3 [d]		290.4	303.0 [e]	334.3 [b]
HPO_4^{2-} and $H_2PO_4^-$ (1:3)	6.3 [d]		290.6	303.1 [e]	334.5 [b]
Protamine	2.8		290.2[g]	303.5 [h]	
alone [f]	2.8		290.4[g]	303.4[h]	
ATP (1:1)[i]					

a Chemical shifts are in parts per million upfield from nitric acid.

b This shift, compared to those above, results from the change in pH

from 11.5 on adding acid (see Figure 1).

c HCl was added to adjust pH to 7.3.

d pH adjusted by NaOH.

e Precision is about ±0.1 ppm.

f Protamine sulfate at 0.03 M. This substance was too insoluble in H_2O to take its ^{15}N spectrum at higher pH values.

g Chemical shift of arginyl -NH- resonances in protamine sulfate.

h Chemical shift of arginyl guanidino nitrogens of protamine sulfate.

i Arginyl residue: ATP = 1:1.

molecule. As can be seen in Table I, no significant changes in shifts were observed on addition of ATP.

If complexation of anions with guanidinium nitrogens does in fact occur in water, the T_1 relaxation times would be expected to be shortened. The T_1 data obtained in the presence and absence of various anions are summarized in Table II. It appears that the pH effect on the nitrogen T_1 values is much more significant than the effects arising from complexation with chloride anions. Protonation changes are not expected to occur in the pH range studied here for guanidino and -NH-nitrogens which have pK_a = 12.48, [10] but possible conformation changes resulting from the deprotonation of the α-amino nitrogen (pK_a = 9.0) and its interaction with the guanidinium group may contribute to the observed change in T_1 of guanidino and -NH-nitrogens between pH 6.0 and 9.4. The T_1 changes may also be due to traces of heavy-metal ions not removed by the Chelex treatment, and such changes in amino acid relaxation times with pH associated with heavy metal ions are well documented. [8,13] Trace metal ions were in fact responsible for the quenching of the α-amino resonance at high pH; after a second treatment with Chelex and addition of 10 mM EDTA, the α-amino resonance was clearly observed at pH 10.1.

On addition of ATP to the arginine solutions, the viscosity increased substantially. In view of the well-known effects of viscosity on T_1, the T_1's of the arginine nitrogens in the presence of ATP were compared at pH 10.1 with those in arginine solutions made isoviscous

TABLE II. T_1 Values for L-Arginine Nitrogens in the Presence of Anions

SAMPLE	concn, [a] M	pH	temp, °C	vis-cosity, cP	T_1, s guani-dino	-NH-	α-ami-no
no addends	1.0	10.1	56	0.66	8.3	14.0	b
L-arginine with NaCl	1.0	9.4	58	0.80	7.7	13.5	b
L-arginine with HCl	1.0	6.0	51	0.82	4.8	9.7	7.1
L-arginine with HCl	1.0	2.7	53	0.85	6.6	9.7	6.9
no addends [c]	2.5	10.1	51	1.33	2.9	5.7	4.5
L-arginine with glycerol [c]	1.0	10.1	51	1.35	3.6	6.6	4.2
L-arginine with ATP [c]	0.6 each	10.1	49	1.32	2.5	5.9	2.3

a Concentration of L-arginine unless otherwise specified.

b No resonance observed.

c 10 mM EDTA added.

with (1) increasing arginine concentration and (2) addition of glycerol. The results provide no evidence for significant changes in T_1 due to complexation with ATP, as can be seen in Table II.

The low sensitivity of guanidino and arginyl nitrogen chemical-shift and T_1 data for aqueous solution toward anionic substances, which have been postulated to complex with such residues of enzymes, do not necessarily mean that ^{15}N NMR cannot be useful for such studies. Arginine in water may well have reduced tendency for complexation compared to arginyl residues in enzymes and, in fact, Borders and co-workers [15] have shown that free arginine reacts with 2,3-butanedione about 15 times more slowly than the essential arginyl residue of creatin kinase. Hydrophobic environments near the active site of the enzyme could very well enhance the binding capabilities of arginyl residues toward anions, and this idea will be investigated further.

REFERENCES AND NOTES

1. Supported by the National Institutes of Health, Public Health Service, Grant GM-11073 from the Division of General Medical Sciences, and by the National Science Foundation.
2. L. Patthy and E. L. Smith, J. Biol. Chem. 250, 565 (1975), and references cited therein.
3. J. F. Riordan, K. D. McElvany, and C. L. Borders, Jr., Science, 195, 884 (1977).
4. F. A. Cotton, E. E. Hazen, Jr., V. W. Day, S. Larsen, J. G. Norman, Jr., S. T. K. Wong, and K. H. Johnson, J. Am. Chem. Soc. 95 2367 (1973).
5. R. Katz, H. J. C. Yeh, and D. F. Johnson, Biochem. Biophys. Res. Commun. 58, 316 (1974).
6. B. Jönsson and B. Lindman, FEBS Lett. 78, 67 (1977).
7. The FIRFT method of T_1 measurement compares quite favorably with the standard inversion recovery method (and less favorably with the progressive saturation method) in studies carried out in this laboratory. See D. Canet, G. C. Levy, and I. A. Peat, J. Magn. Reson. 18, 199 (1975).
8. C. S. Irving and A. Lapidot, J. Am. Chem. Soc. 97, 5945 (1975).
9. P. S. Pregosin, E. W. Randall, and A. I. White, Chem. Commun. 1602 (1971).
10. H. E. Mahler and E. H. Cordes, "Biological Chemistry", Harper and Row, New York, N.Y. 1966, p. 34.
11. T. Suzuki, T. Yamaguchi, and M. Iamanari, Tetrahedron Lett., 1809 (1974).
12. F. Blomberg, W. Maurer, and H. Ruterjans, Proc. Natl. Acad. Sci. U.S.A., 73 1409 (1976).
13. (a) T. K. Leipert and J. H. Noggle, J. Am. Chem. Soc. 97, 269 (1975); (b) H. Pearson, D. Gust, I. M. Armitage, H. Huber, J. D. Roberts, R. E. Stark, R. R. Void, and R. L. Void, Proc. Natl. Acad. Sci. U.S.A. 72, 1599 (1975).

14. The protamine-DNA complex could not be studied because of low solubility in water. See D. E. Olins, A. L. Olins, and P. H. von Hippel, J. Mol. Biol. 33, 265 (1968).

15. C. L. Borders, Jr., and J. F. Riordan, Biochemistry 14, 4699 (1975).

PART IV

A ^{15}N Nuclear Magnetic Resonance Study of Amino Acid Metabolism in Neurospora crassa

INTRODUCTION

Isotopic tracers, radioactive and stable, of C, H, and P have been one of the most valuable tools for studying the pathways and rates of metabolic processes. For nitrogen, which lacks a radioisotope of adequately long lifetime, ^{15}N is of special importance as a tracer of nitrogenous metabolites, and ^{15}N nuclear magnetic resonance spectroscopy is potentially a very powerful technique for use of this isotope. The advantage of nuclear magnetic resonance spectroscopy in stable isotope labeling experiments is that metabolic processes can be studied *in vivo* in intact organisms. Thus the uncertainties encountered in the extraction and separation of labeled metabolites necessary for the detection of the label by mass spectrometry, can be avoided. The advantage of nuclear magnetic resonance spectroscopy in studying *in vivo* systems has been well demonstrated in the application of ^{31}P NMR for the measurement of intracellular pH [1] and for study of adenosine triphosphate metabolism in intact cells and tissues, [2] and in recent ^{13}C NMR studies of glycolysis in microorganisms [2]. There have already been a few reports of ^{15}N NMR studies of intact organisms, although difficulties have been encountered because of

the low sensitivity and relatively long relaxation times of the ^{15}N nucleus. J. Schaefer and coworkers [3] used cross-polarization solid-state ^{15}N NMR to study the change in the relative concentrations of amino acid residues in proteins at various stages of growth of ^{15}N-labeled soybeans. M. Llinas and coworkers have reported the observation of a single peptidyl amide nitrogen resonance in ^{15}N-enriched culture of fungus Ustilago sphaerogena [4]. A. Lapidot and C. S. Irving have studied the dynamic properties of cell wall components of intact bacteria cells by ^{15}N NMR [5]. In these works on microorganisms, only ^{15}N resonances of macromolecules such as proteins and cell-wall peptidoglycan were detected. So far, no ^{15}N NMR studies of small metabolites such as amino acids in intact microorganisms have been reported.

While a wealth of valuable information has been obtained in the past three decades regarding the intermediates and the enzymes involved in amino acid metabolism and the mechanisms of metabolic regulation, there remain intriguing questions about the actual functioning of metabolic processes and their regulation in vivo. Some of the questions that can be studied by labeling the metabolites of micro-

organisms with ^{15}N and tracing their fate *in vivo* by ^{15}N NMR follow.

1. How is a nitrogen source, such as $^{15}NH_4^+$, distributed among competing anabolic pathways?

2. Where alternative pathways from a precursor to a product exist, which pathway is favored?

3. What are the turnover rates of nitrogenous metabolites *in vivo*?

The aim of this study is to explore the potential of ^{15}N NMR as tracer of *in vivo* nitrogen metabolism in microorganisms. The organism chosen for the study is fungus *Neurospora crassa* which has the following advantages.

1. It is easily cultured in the laboratory. Wild-type *Neurospora* can biosythesize all nitrogenous metabolites from NH_4Cl as the sole nitrogen source.

2. It is among the genetically most extensively studied organisms; a number of well-characterized mutant strains, each deficient in an enzyme for a specific metabolic reaction, are known.

3. Unlike procaryotes in which intracellular pools of amino acids are maintained at low levels, this eucaryotic organism contains large free pools of several amino acids [6]. This facilitates the study of their metabolic fates by ^{15}N NMR.

This paper describes some preliminary results which demonstrate the feasibility of observing small ^{15}N-labeled metabolites such as glutamine, glutamate and arginine in intact *N. crassa* mycelia and the

types of information on *in vivo* metabolism that can be obtained by ^{15}N nuclear magnetic resonance spectroscopy. The following experiments are described.

1. The ^{15}N chemical shift, the spin-lattice relaxation time T_1, and nuclear Overhauser enhancement (NOE) of intracellular arginine (enriched in ^{15}N at $N_{\omega,\omega'}$) in intact *Neurospora* mycelia were measured to determine the optimum NMR operating conditions for observing ^{15}N resonances of small metabolites in intact mycelia.

2. ^{15}N spectra of *N. crassa* mycelia grown in minimal medium with $^{15}NH_4Cl$ as the sole nitrogen source were obtained, and the distribution of $^{15}NH_4^+$ into various anabolic pathways of nitrogenous cell components was studied under different growth conditions. The turnover times of some ^{15}N-labeled metabolites were studied by the isotope dilution method.

3. The time course of assimilation of $^{15}NH_4^+$ into ^{15}N-labeled metabolites was studied *in vivo*. With aeration, the mycelia were found to metabolize at an observable rate in a "miniature culture" within the NMR tube. The time dependence of the formation of glutamine and glutamate was compared in two *Neurospora* strains, one capable of synthesizing glutamate directly from $^{15}NH_4^+$ and α-ketoglutarate and one incapable of this synthesis, with the purpose of finding out whether an alternative pathway of glutamate synthesis *via* glutamine occurs *in vivo*.

EXPERIMENTAL

The mutant strains of Neurospora crassa used in these experiments are ure-1 allele 9 (FGSC 1230) (ureaseless) and aga UM906 (FGSC 1699) (arginaseless) obtained from R. H. Davis, and am allele 32213 (FGSC 521) (glutamate dehydrogenase deficient) obtained from the Fungal Genetics Stock Center at Arcata, California. The medium used was Vogel's minimal medium supplemented with 1.5% sucrose [7]. When we speak of a "nitrogen-free medium", we mean the same medium without ammonium nitrate. The $^{15}NH_4Cl$ (99% enriched in ^{15}N) and L-arginine hydrochloride (99% enriched in ^{15}N at $N_{\omega,\omega'}$) were purchased from KOR Isotopes.

Cultures were inoculated with an aqueous suspension of washed conidia to a final concentration of $1x10^7$ conidia/ml. Conidia were germinated in 1 liter baffled flasks containing 500 ml of minimal medium with aeration provided by shaking at 150 rpm at 16°C for 16 ∿ 20 hours. The temperature was then raised to 30°C for 3 hours or until logarithmic growth was established as judged by turbidity. In some cases, mycelia were exposed to $^{15}NH_4$ Cl (0.2%) for the entire germination period. Alternatively, the mycelia were transferred to nitrogen-free medium for 3 hours prior to the addition of $^{15}NH_4$ Cl. Where specified, cycloheximide was added to the culture medium to a final concentration of 20 μg/ml, a few minutes before the addition of $^{15}NH_4$ Cl or ^{15}N-labeled arginine, to inhibit the incorporation of ^{15}N-labeled amino acids into proteins.

The mycelia suspension for the NMR measurements was prepared

by collecting the mycelia by filtration and resuspending them in enough medium to make 18 ml of mycelia suspension in 25 mm-diameter NMR tube. The volume ratio of mycelia pellets to the medium in NMR sample was approximately 1:1, unless otherwise specified.

The ^{15}N NMR spectra were obtained with a Bruker WH-180 spectrometer operating at 18.25 MHz. Chemical shifts are reported in ppm upfield of a 1 M solution of $H^{15}NO_3$ made by dissolving in D_2O and used as an external standard. The operating conditions, unless otherwise specified, were 70 μsec pulses (90^o flip angle) with a 2-sec delay and with full proton decoupling. The sample temperature was maintained at 10 ± 2^oC.

To check the viability of mycelia during the NMR experiments, the doubling time and the ability to take up arginine from the medium were compared in mycelia before and after exposure to similar environment; no change was observed in either cellular property. We conclude that the mycelia are fully viable under these conditions.

RESULTS AND DISCUSSION

1. The ^{15}N shift, the spin-lattice relaxation time and the nuclear Overhauser enhancement of intracellular arginine ($^{15}N_{\omega,\omega'}$) in N. crassa

Wild-type N. crassa, cultured on minimal medium with ammonium nitrate as the nitrogen source, accumulate large pools of amino acids such as arginine (8 mM in cell water) and ornithine.[8] On addition of high levels of arginine to the growth medium, the intracellular arginine pool expands; the increase is several-fold during steady-state growth in arginine-supplemented medium[9].

To test the feasibility and determine the optimum conditions for observing small nitrogenous metabolites in N. crassa, it is advantageous to start with mycelia which have incorporated arginine (^{15}N-labeled at $N_{\omega,\omega'}$) and in which the intracellular level of free arginine is maintained at a constant level, without degradation by arginase or incorporation into cellular proteins. Thus the aga (arginaseless) strain of N. crassa was grown in 500 ml of minimal medium and 200 mg of L-arginine (^{15}N-enriched in $N_{\omega,\omega'}$) was added to the culture medium after addition of cycloheximide. After approximately 90% of arginine ($^{15}N_{\omega,\omega'}$) had been taken up (1-2 hours), the mycelia were collected by filtration, washed extensively with water and resuspended in arginine-free medium for NMR measurement.

Figure 1 shows the proton-decoupled ^{15}N spectrum of intracellular arginine ($^{15}N_{\omega,\omega'}$) in intact N. crassa mycelia. An intense ^{15}N

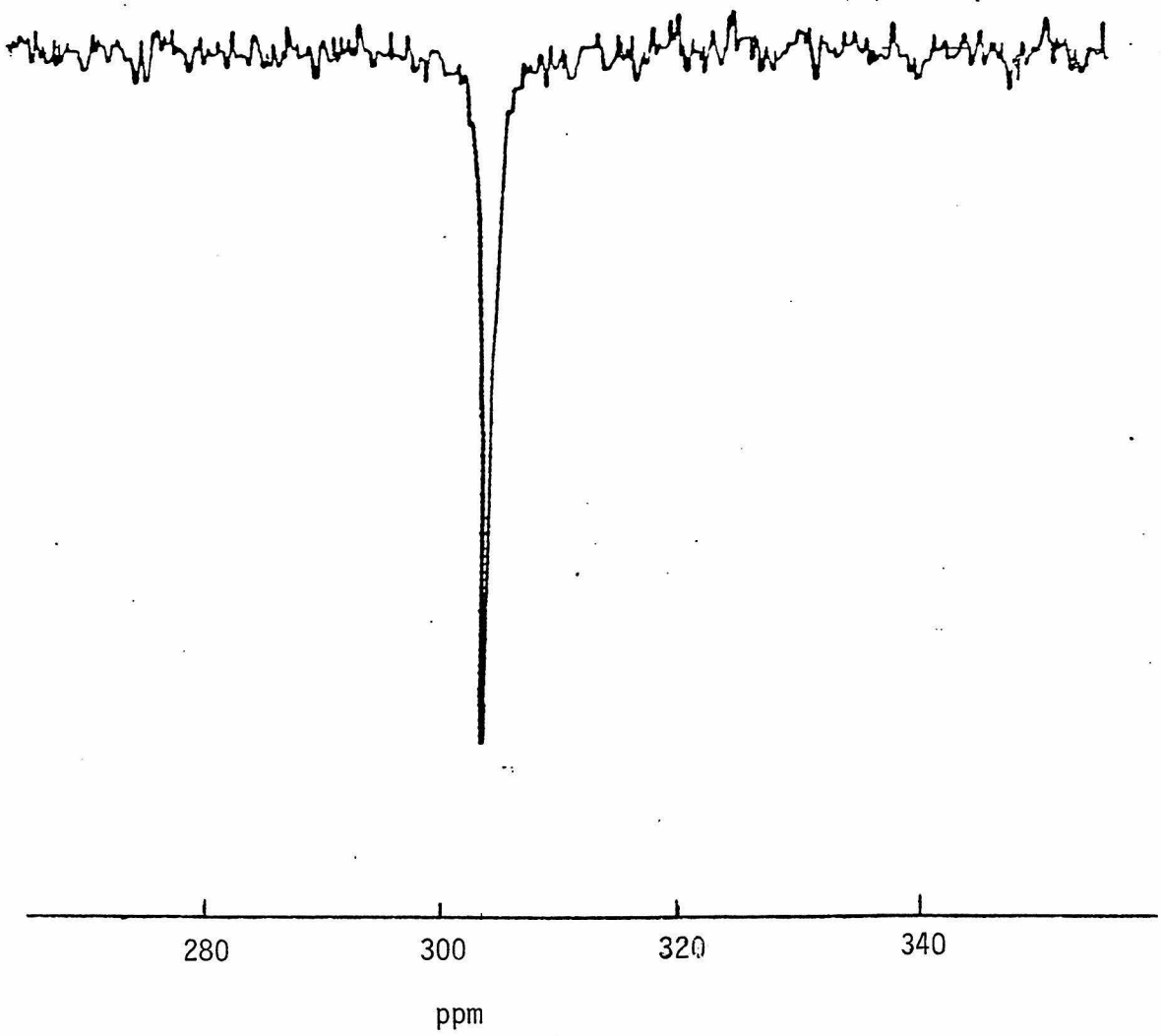

Figure 1. Proton-decoupled ^{15}N chemical shift spectrum of intracellular arginine ($^{15}N_{\omega,\omega'}$) in intact N. crassa mycelia. The spectrum was obtained in 100 transients, with 70° pulse and 4-sec delay.

resonance at 303.5 ppm is observed after only 100 scans (7 minutes of accumulation time) [10]. The ^{15}N shift of 303.5 ppm for intracellular arginine ($^{15}N_{\omega,\omega'}$) in N. crassa is only 0.3 ppm downfield of that of arginine ($^{15}N_{\omega,\omega'}$) in the mycelia free medium (Table 1). Thus an intracellular environment causes no significant change in the $^{15}N_{\omega,\omega'}$ shift of arginine.

These results demonstrate the feasibility of observing small ^{15}N-labeled metabolites in intact mycelia by ^{15}N nuclear magnetic resonance spectroscopy. The observation is facilitated by (1) the high level of free intracellular amino acids in eucaryotic cells and (2) the high sensitivity of our Bruker WH180 spectrometer which has been described elsewhere [11]. The high sensitivity gives a good signal-to-noise ratio in a relatively short time even when a relatively long repetition rate of 4 sec is used. In previous ^{15}N NMR studies of microorganisms, [4,5] ^{15}N resonances of small metabolites were not detected presumably because these nuclei have relatively long relaxation times and were saturated as a result of using fast repetition rates.

To obtain information on the correlation time τ_c of intracellular arginine and to estimate the optimum NMR operating condition for obtaining its ^{15}N spectra efficiently, the nuclear Overhauser enhancement (NOE) and the spin-lattice relaxation time (T_1) of $^{15}N_{\omega,\omega'}$ of intracellular arginine were measured.

Figure 2 compares the ^{15}N spectra of intracellular arginine

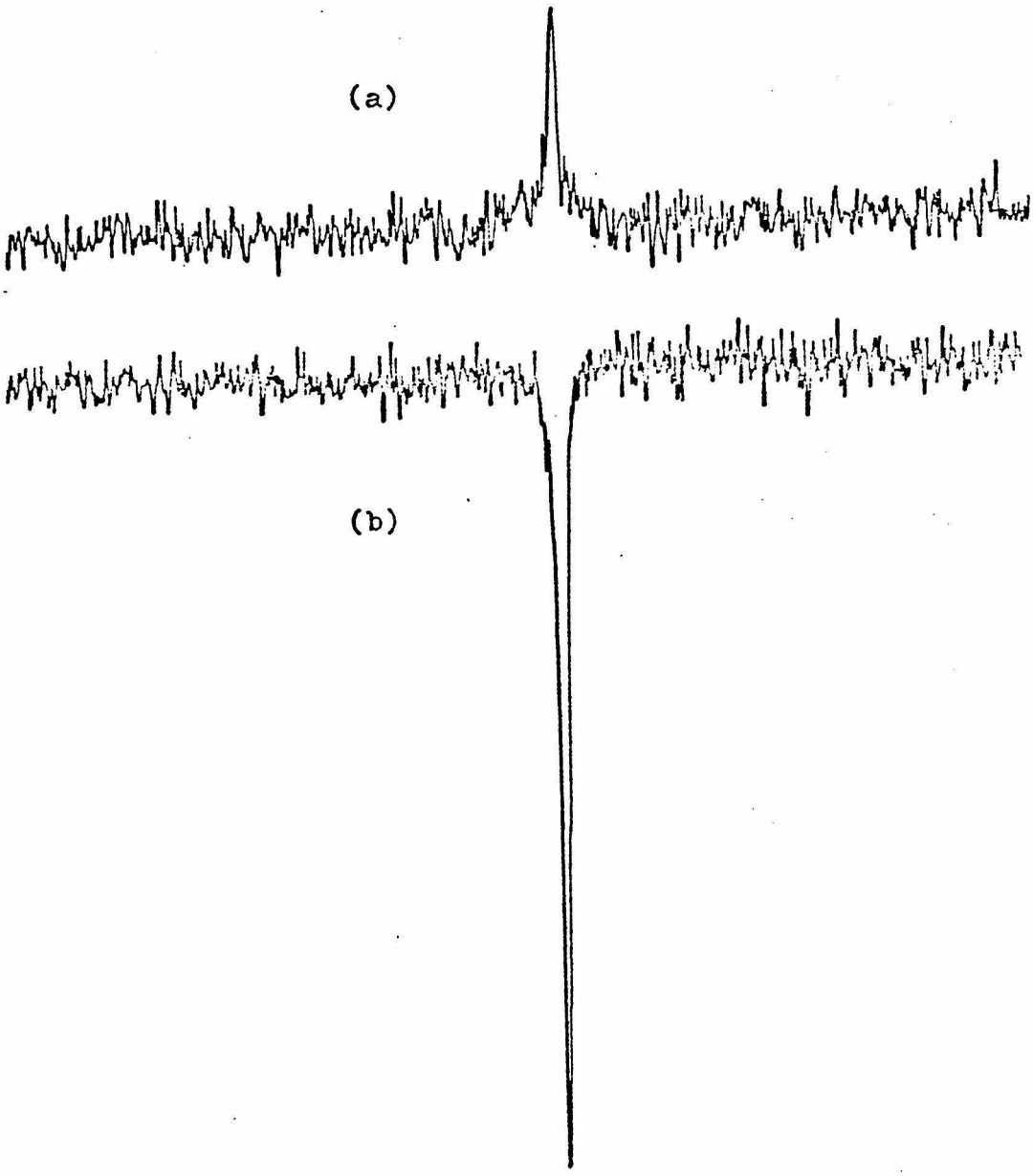

Figure 2. ^{15}N spectra of intracellular arginine ($^{15}N_{\omega,\omega'}$) in N. crassa for NOE measurement, obtained in 80 transients with 90° pulse and 32-sec delay (a) with gated proton decoupling (b) with continuous proton decoupling.

obtained with gated proton decoupling (2a) and continuous proton decoupling (2b) for NOE measurement. The NOE value, calculated from the ratio of the two peak intensities is -3.6 ± 0.2. The NOE value can be used to determine the dipolar contribution to relaxation by the equation

$$T_{1dd} = T_{1obs} \frac{NOE_{max}}{NOE_{obs}} \qquad (1)$$

where T_{1obs} is the measured T_1 value and T_{1dd} is the dipolar contribution to T_1. Substituting $NOE_{max} = -3.96$ [9] and $NOE_{obs} = -3.6$, we obtain

$$\frac{T_{1obs}}{T_{1dd}} = 0.92$$

This indicates that the relaxation of $^{15}N_{\alpha,\omega'}$ of intracellular arginine is predominantly by dipole-dipole interaction with protons, with little contribution from other relaxation mechanisms. On the assumption that only dipolar relaxation to protons is important and that isotropic reorientation depends on the correlation time τ_c, the dependence of NOE on τ_c at 42 kG has been calculated by D. Gust, R. B. Moon and J. D. Roberts [11] and is shown in Figure 3a. From the observed NOE of -3.6 for $N_{\omega,\omega'}$ of intracellular arginine in N. crassa, its correlation time can be estimated to be less than 4×10^{-10} sec.

The spin-lattice relaxation time T_1 of $^{15}N_{\omega,\omega'}$ of intracellular arginine in N. crassa was measured by the fast-inversion-recovery

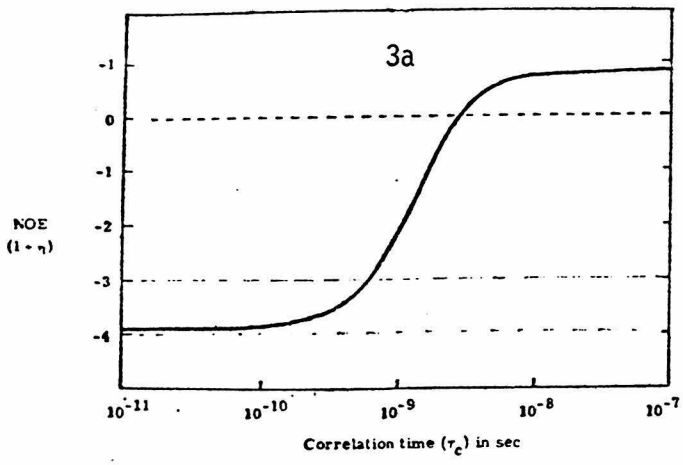

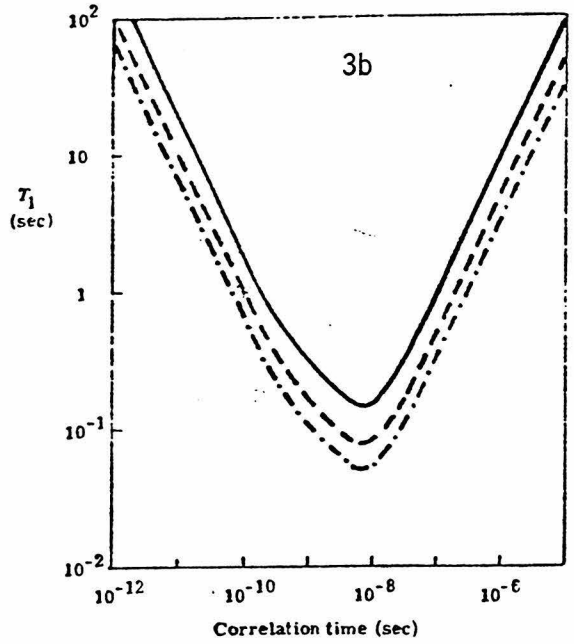

Figure 3a. Plot of NOE against τ_c for nitrogen-15, assuming dipolar relaxation from protons and isotropic rotation. (After Figure 3 in reference 11)

Figure 3b. Plot of T_1 against τ_c for nitrogen-15 at 18.25 MHz, assuming dipolar relaxation and isotropic rotation:—, relaxation to one proton with internuclear distance of 1.02 Å; ----, relaxation to two protons with internuclear distance 1.03 Å; —·—·— relaxation to three protons with internuclear distance 1.03 Å. (After Figure 4 in reference 11)

method,[12] using the pulse sequence $(180^{o} - \tau - 90^{o} - T)_{n}$. Some representative spectra from which the signal intensity S was measured as a function of τ are shown in Figure 4. Semilogarithmic plots of $(S_{\infty} - S_{\tau})$ vs τ are shown in Figure 5. The T_1 value of $^{15}N_{\omega,\omega'}$ of intracellular arginine calculated from the slope of the computer-fitted least-squares line through the plots is 1.06 sec, with a correlation coefficient of 0.9986. The dependence of T_1 on correlation time τ_c at 42 kG has been calculated [11], assuming isotropic reorientation and dipolar relaxation to protons, and is shown in Figure 3b. From the observed T_1 of 1.06 sec for $^{15}N_{\omega,\omega'}$ of intracellular arginine in N. crassa, its correlation time can be estimated to be approximately 1×10^{-10} sec.

The large negative NOE of -3.6 and the relaxation time of 1.06 sec observed for the $N_{\omega,\omega'}$ of intracellular arginine indicate that to obtain spectra of protonated nitrogens of arginine, and by inference, of other small metabolites in N. crassa, it is advantageous to use continuous proton decoupling and a repetition rate of a few seconds. These operating conditions were used throughout the remaining experiments.

The T_1 value of 1.06 for the $^{15}N_{\omega,\omega'}$ of intracellular arginine in N. crassa is considerably shorter than the T_1 value of 4.25 sec obtained for $^{15}N_{\omega,\omega'}$ of 12 mM arginine in the mycelia-free medium at the same temperature (Table I). Assuming dipolar relaxation, T_1 depends on molecular size and the viscosity of the medium, because

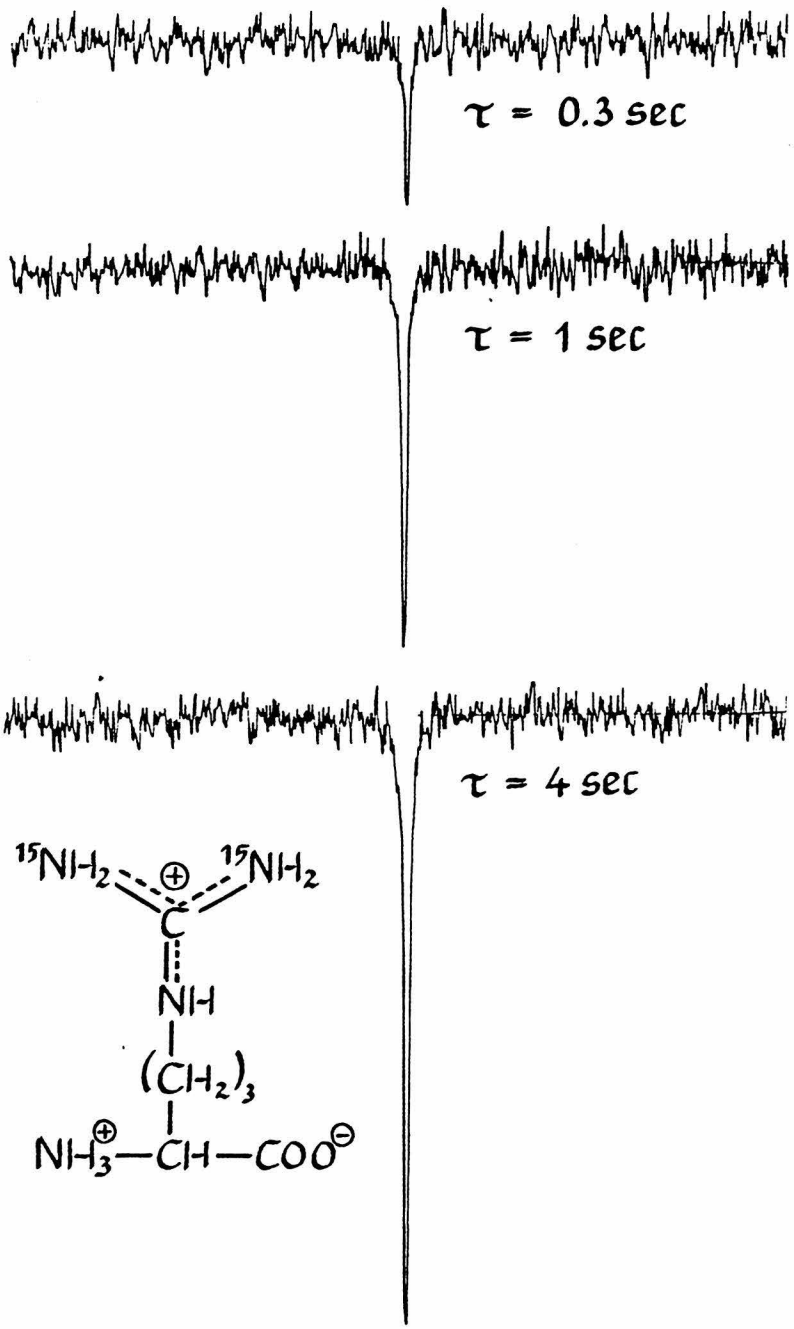

Figure 4. Representative ^{15}N spectra for the measurement of T_1 of $^{15}N_{\omega_\delta\omega'}$ of intracellular arginine in N. crassa. The pulse sequence $(180^0 - \tau - 90^0 - T)_n$ was used, with T = 4 sec and τ = 0.1, 0.3, 0.7, 1, 2, 4, and 32 sec. Each spectrum represents an accumulation of 80 transients.

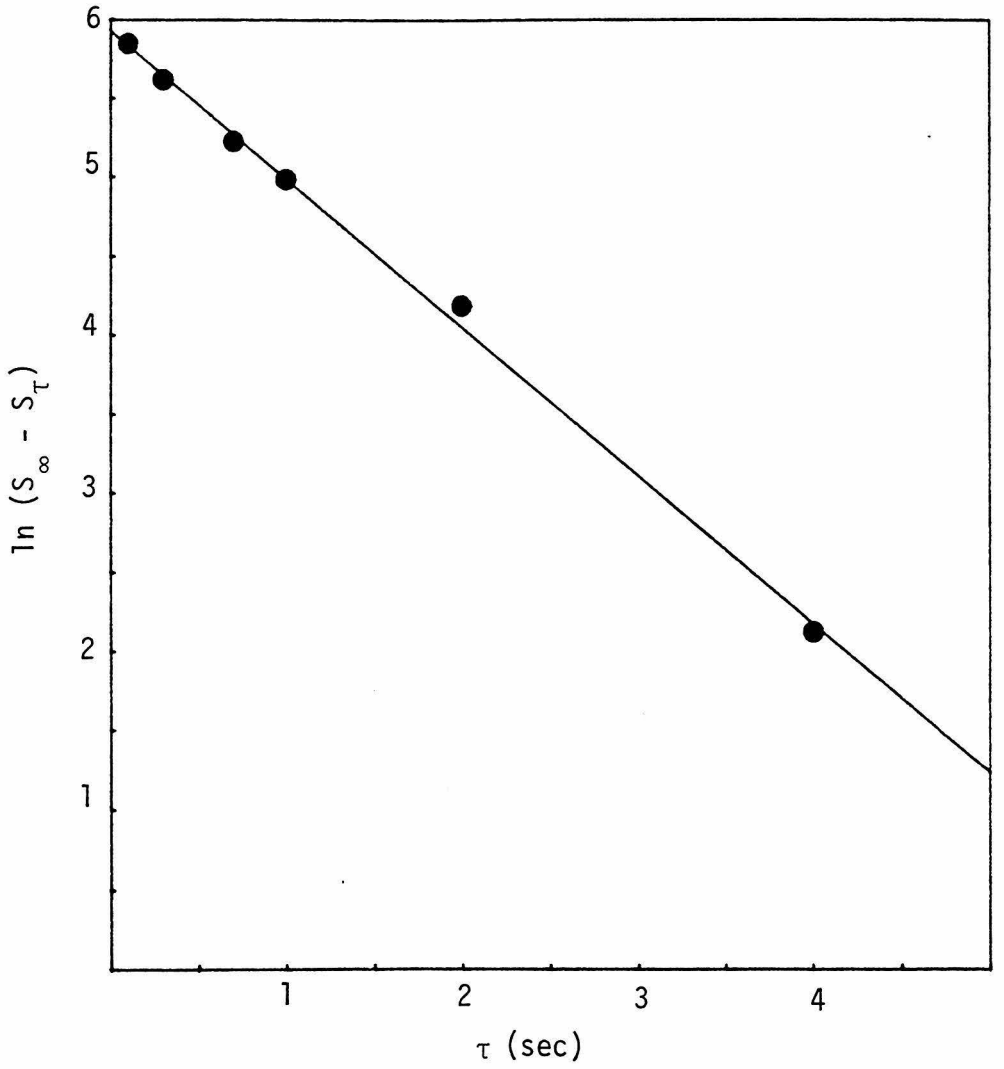

Figure 5. Plots of $\ln(S_\infty - S_\tau)$ against τ for the T_1 measurement of $^{15}N_{\omega,\omega'}$ of arginine in Neurospora. S_τ represents the signal intensity at each τ value shown, and S_∞ is the signal intensity at τ = 32 sec. From the slope of the least-squares line through the plots, T_1 of 1.06 ±0.02sec was obtained.

$$\frac{1}{T_{1dd}} \propto \tau_c$$

in mobile liquids where the relation $\tau_{eff}^2(\omega_N + \omega_H)^2 << 1$ holds, and τ_c is given to a first approximation by

$$\tau_c = \frac{4\pi\eta\, a^3}{3kT}$$

where η is the viscosity of the liquid, a is the radius of the molecule (assumed to be spherical), T is the absolute temperature and k is the Boltzmann's constant. Thus the shorter T_{1dd}, and the longer τ_c, of $^{15}N_{\omega,\omega'}$ of intracellular arginine could be due to the higher viscosity of intracellular environment and/or association of arginine with other cellular components which increases the effective molecular radius a. It has been demonstrated that the bulk intracellular pool of arginine in N. crassa is sequestered in vacuoles [13]. Because the subcellular fraction representing the vacuole contains large quantities of polyphosphates as well as arginine, it has been speculated that the positively-charged guanidino groups of arginine are associated with the negatively-charged polyphosphates in the vacuole; the estimated concentration of arginine in the vacuole is approximately 1M and that of polyphosphate equivalent to approximately 1M of monophosphate units [14]. In this regard, it is significant that a T_1 value of 0.96 sec was obtained for 1M aqueous solution of arginine in the presence

of 0.2M sodium pentaphosphate (arginine-monophosphate ratio of 1:1) (Table I). This value is quite close to the T_1 of 1.06 sec obtained for intracellular arginine in N. crassa.

TABLE I

Comparison of the ^{15}N shifts and T_1 values of intracellular and extracellular arginine ($^{15}N_{\omega,\omega'}$) in N.crassa

Sample	Solvent & Addends	pH	Temp (^{o}C)	Viscosity (cp)	$\delta^{15}N$ (ppm)	T_1 (sec)
Intracellular arginine in N. crassa	mycelia suspended in minimal medium	medium 5.8	10		303.5	1.06
Arginine (12 mM)	in minimal medium	5.8	10		303.8	4.25
Arginine (1 M)	Aqueous solution with 0.2M $Na_7P_5O_{16}$	5.8	10	2.3		0.96

2. ^{15}N Spectra of Intact N. crassa Mycelia Cultured in $^{15}NH_4^+$-Containing Medium

To investigate the types of ^{15}N-labeled metabolites in N. crassa that can be observed in vivo by ^{15}N NMR, spectra were taken of intact mycelia grown in $^{15}NH_4Cl$-containing medium. The ure-1 strain of N. crassa was grown in minimal medium containing 0.2% $^{15}NH_4Cl$ for 20 hours, and the mycelia suspension for NMR measurements was prepared as described in the experimental section.

Figure 6a shows the broadband proton-decoupled ^{15}N spectrum of the mycelia. A number of well-resolved resonances of ^{15}N-labeled intermediates and products are observed. The assignments of the ^{15}N resonances of the intracellular metabolites by comparison with those of the corresponding compounds in aqueous solution are summarized in Table II. The structures of these metabolites and the anabolic pathways by which they are synthesized from $^{15}NH_4^+$ and carbon sources in N. crassa are shown in Figure 7. The intense peaks observed in the spectrum in Figure 6a are the side-chain nitrogens of amino acids (both as free amino acids and residues in proteins), viz glutamine N_γ (262.4 ppm), arginine N_δ (291.0 ppm) and $N_{\omega,\omega'}$ (303.5 ppm), and lysine N_ε and/or ornithine N_δ (342.6 ppm), as well as the α-amino nitrogens of free amino acids such as proline and/or hydroxyproline (321.9 ppm), alanine (∿ 332.3 ppm), glutamate, glutamine, lysine, and arginine (∿ 334.3 ppm), and valine and/or serine (338.9 ppm) [18]. The most shielded peak at 354.5 ppm represents ammonium ion.

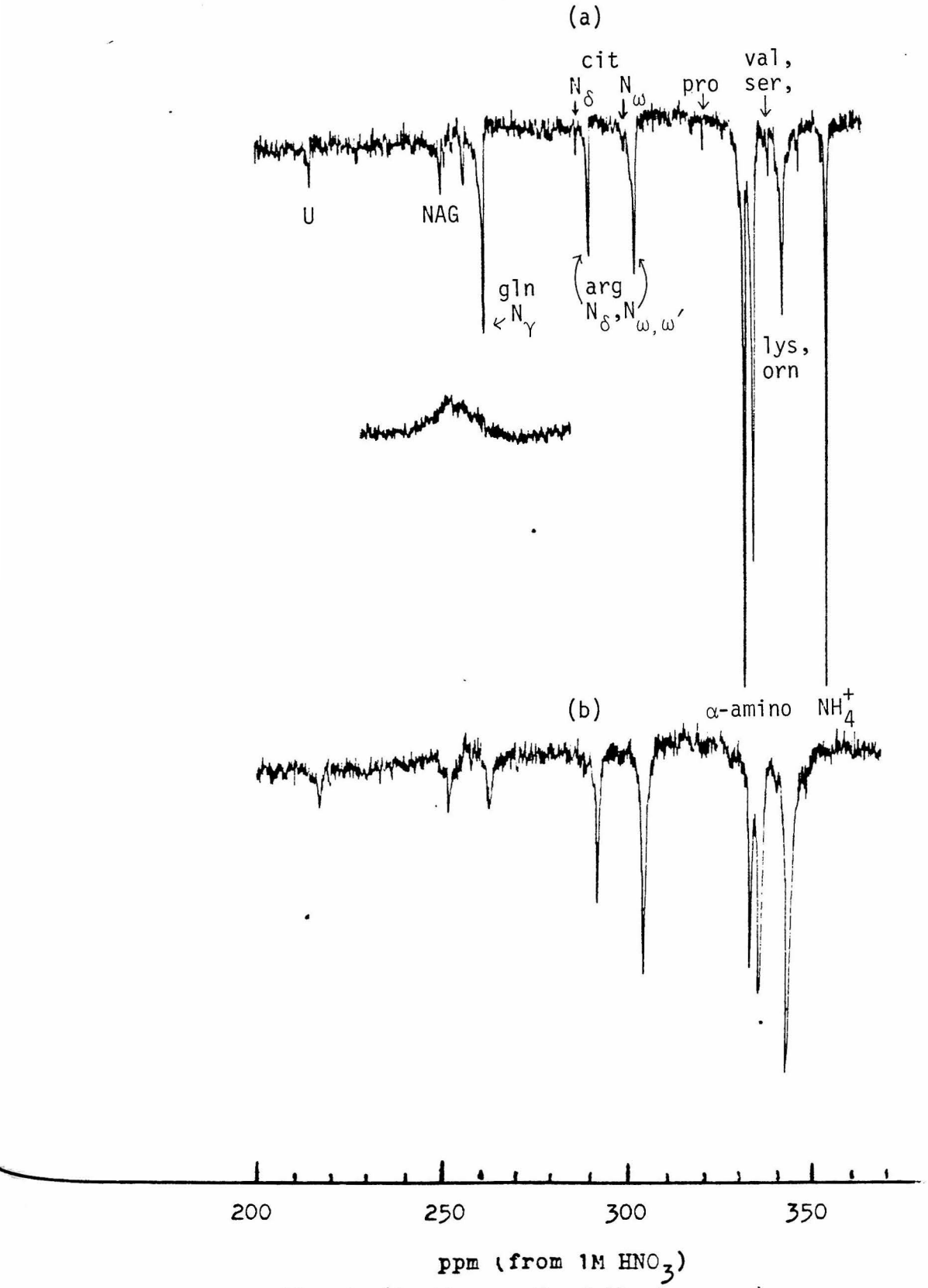

Fig. 6 (Caption on the following page)

Fig. 6. (a) Broadband proton-decoupled ^{15}N spectrum of intact mycelia suspension of N. crassa ure-1 strain grown in $^{15}NH_4Cl$ containing medium for 20 hours. The spectrum represents an accumulation of 5867 transients. The inset shows the amide region of the same sample obtained with gated proton decoupling using 4-sec repetition rate. (b) Broadband proton-decoupled ^{15}N spectrum of the same mycelia after additional 2 hours' growth in $^{14}NH_4Cl$-containing medium. The spectrum represents an accumulation of 21,790 transients. Abbreviations: U:uridine; NAG:N-acetyl-glucosamine; gln:glutamine; cit:citrulline; arg:arginine; pro:proline; lys:lysine; orn:ornithine; ser:serine; val:valine.

Table II

Assignments of ^{15}N-labeled metabolites observed in N. crassa mycelia grown in $^{15}NH_4Cl$-containing medium

Metabolites	$\delta^{15}N$ (ppm from 1 M HNO_3)		
	N. crassa		H_2O
	Intact mycelia grown with $^{15}NH_4Cl$ (Figure 6a)	Cell extract after heat treatment (Figure 8)	
Uridine N3	216.7[a]	217.8	216.5[c]
Guanosine N1		228.8	229.0[h]
Uridine N1			
N-acetylglucosamine	251.5[a,b]		252.4[d]
Peptide amide N		253.2	
Glutamine N_γ	262.4[a,b]	263.3	263.1[e]
Cytidine NH_2		281.8	282.0[h]
Citrulline N_δ	287.7		287.9[e]
Arginine N_δ	291.0[a,b]	291.2	290.6[f]
Adenosine NH_2		297.3	297.9[h]
Citrulline N_ω	300.6		300.8[e]
Guanosine NH_2		303.1	303.2[h]
Arginine $N_{\omega,\omega'}$	303.5[a,b]	304.5[24]	303.8[f]
Proline N_α	321.9		319.8[e]
4-hydroxyproline N_α			322.8[g]
Alanine N_α	332.3[a,b]	332.8	332.3[g]
Lysine N_α			334.1[f]
Glutamate N_α	334.3[a,b]	334.9	334.3[e]
Glutamine N_α			334.7[f]
Arginine N_α			334.9[f]
Valine N_α	338.9	337.3	339.0[g]
Serine N_α			339.0[g]
Lysine N_ε/Ornithine N_δ	342.6	343.4	341.7[f]
Glycine N_α of dipeptides	347.2	348.1	348.1[g]
Ammonium ion	354.5	354.8	354.5

a. Resonances also observed in the mycelia after isotope dilution by further growth on $^{14}NH_4Cl$ (Figure 6b)

b. Resonances also observed in mycelia grown on $^{14}NH_4Cl$-containing medium after cycloheximide addition (Figure 9)

c. Reference 15

d. Reference 16

e. Measured by the author in mycelia-free, nitrogen-free medium at 25°C

f. Measured by the author in aqueous solution at pH 5-7

g. Reference 17

h. Shifts of nucleotides in yeast transfer RNA (Reference 11)

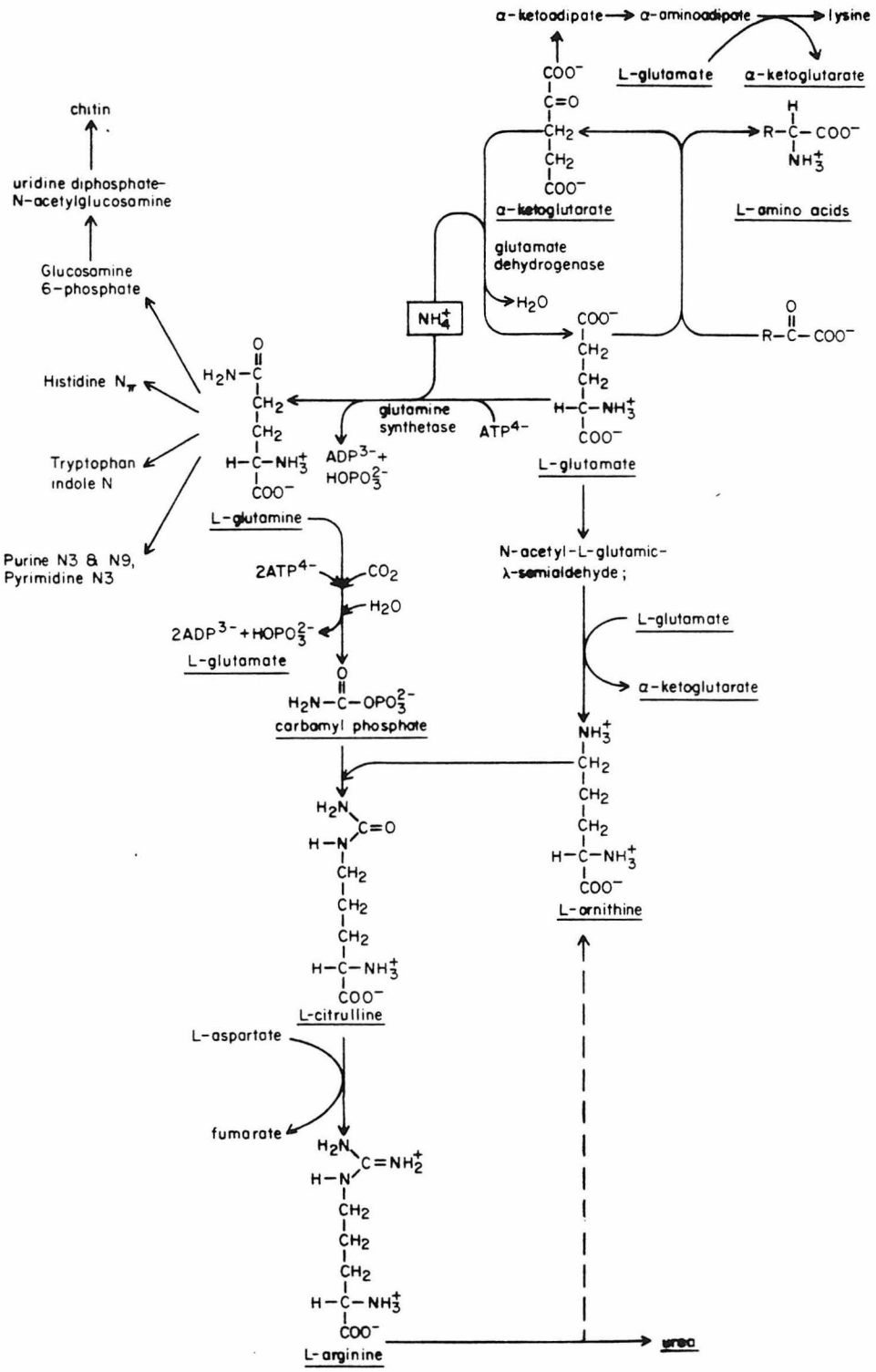

Fig. 7. Anabolic pathways of some nitrogenous metabolites in N. crassa.

Significantly, one can also detect small ^{15}N resonances from some intermediate in arginine biosynthesis such as citrulline N_{δ} (287.7 ppm) and N_{ω} (300.6 ppm).

Observed resonances from other cellular components include N-acetyl-D-glucosamine (NAG, 251.5 ppm) which is a component of fungal cell wall; N. crassa cell wall contains 4.9 mg glucose polymer and 0.5 mg chitin, a homopolymer of N-acetyl-D-glucosamine, per 10 mg cell wall [19]. Among the nitrogens in cellular nucleic acids and free nucleotides, only the N3 resonance of uridine (U, 216.7 ppm) is observed; this probably arises from uridine diphosphoacetyl-glucosamine (UDP-GNAc) and uridine diphosphoglucose (UDP-glucose) which are intermediates in the biosynthesis of chitin and have been reported to occur in significant amounts (60 μmoles UDP-GNAc and 45.5 μmoles UDP-glucose compared to 7.8 μmoles ATP per 100 g wet-weight cell) in N. crassa [20].

The broadband proton-decoupled ^{15}N spectrum in Figure 6a shows no peaks corresponding to the numerous backbone amide nitrogens of cellular proteins, although they appear as a broad peak around 253 ppm when the spectrum is obtained with gated proton-decoupling as shown for comparison in the inset. The nulling of these resonances on broadband proton decoupling could be the result of the amide nitrogens of cellular proteins having on the average an NOE value of approximately zero. A similar effect was observed in the ^{15}N spectra of bacterial cell walls [5a]. The relatively sharp resonance at 257.7 ppm can be due to the amide nitrogen of dipeptides such as leucylglycine (257.1 ppm), although one would expect a much broader peak from a variety of oligopeptide amide

nitrogens present in growing mycelia, on the basis of marked dependence of the amide ^{15}N shifts on the nature of the adjacent amino acid (ranging from 242.6 ppm ~ 260.4 ppm for aliphatic dipeptides [21].) Alternatively, the peak can represent the pyridine ring nitrogen of reduced nicotinamide adenine dinucleotide (256.8 ppm in D_2O), [22] which is an important cofactor in a number of oxidation-reduction reactions. Definitive assignment of the 257.7 ppm resonance must await further study.

The anabolic pathways by which these ^{15}N-labeled metabolites are synthesized from $^{15}NH_4^+$ and carbon sources in N. crassa are summarized in Figure 7. Glutamate and glutamine play crucial roles in assimilating NH_4^+ and acting as precursors for many important nitrogenous cellular components. Glutamate, synthesized from NH_4^+ and α-ketoglutarate, acts (1) as an α-amino group donor in the synthesis of essentially all the common amino acids, (2) as a precursor for the ornithine backbone of arginine, and (3) as the source of nitrogen for the $N_\varepsilon H_3^+$ group of lysine. Glutamine is synthesized from NH_4^+ and glutamate. Its amide nitrogen is the source of nitrogen (1) for one of the guanidino nitrogens ($N_{\omega,\omega'}$) of arginine (via carbamyl phosphate and citrulline), (2) for N-acetyl-D-glucosamine, (3) for imidazole N_π of histidine and the indole nitrogen of tryptophan, and (4) for N3 and N9 of purines and N3 of pyrimidines.

The ^{15}N spectrum of intact N. crassa mycelia in Figure 6a clearly demonstrates the feasibility of observing ^{15}N resonances of the important intermediates, glutamine and glutamate, as well as some

intermediates in the biosynthesis of arginine and chitin. It is to be noted, however, that in this spectrum, the ^{15}N resonances of amino acid side chains such as glutamine N_γ, arginine N_δ and $N_{\omega,\omega'}$ and lysine N_ε represent contributions from both free amino acids and amino acid residues in proteins.

An interesting way to check whether free amino acids or protein residues make predominant contribution to the resonances is to test, by the isotope dilution method, how rapidly the components represented in these resonances turn over. For this purpose, the ^{15}N-labeled mycelia whose spectrum is shown in Figure 6a were collected by filtration, washed and resuspended in $^{14}NH_4Cl$-containing medium (500 ml) for additional 2 hours' growth. During this period, degradation of ^{15}N-labeled cellular proteins is expected to be negligible since most proteins turn over slowly with half lives of the order of days [23]. By contrast, free ^{15}N-labeled amino acids that metabolize rapidly into other cellular components would be expected to show decrease in ^{15}N peak intensities due to dilution of ^{15}N by ^{14}N as the result of metabolic turnover. Figure 6b shows the proton-decoupled ^{15}N spectrum of those mycelia. The most significant change compared to Figure 6a is the marked loss in the intensities of the glutamine N_γ peak (262.4 ppm) and the N_α peaks (332.3, 334.3 ppm) of amino acids [24], compared to other peaks. This result clearly indicates that the glutamine $^{15}N_\gamma$ peak observed in Figure 6a before isotope dilution arose predominantly from free intracellular glutamine molecules, and not from glutaminyl residues in proteins. Moreover, the glutamine N_γ

shows a very rapid turnover rate. It is clear, from a comparison of the glutamine N_γ peak intensities in Figures 6a and 6b (after correction for the difference in the number of transients accumulated), that the half-life of this nitrogen of free glutamine in N. crassa growing in NH_4Cl must be less than 1 hour, although for a more accurate determination, it is necessary to determine the exact, albeit small, contribution of glutamine residues in proteins to the peak intensities. It is also interesting to note that the intermediates in arginine biosynthesis such as citrulline N_δ and N_ω turnover rapidly as indicated by the disappearance of these ^{15}N peaks in Figure 6b. The decrease in the intensities of the α-amino nitrogen resonances of amino acids is no doubt mainly due to their incorporation into proteins, and to transaminations of the glutamate α-amino group to other nitrogenous metabolites. This preliminary result suggests that ^{15}N NMR can be a valuable technique for studying the in vivo turnover time of metabolically important functional groups such as the amide nitrogen of glutamine and α-amino groups of amino acids which are not amenable to radioisotope labeling.

It is useful to check whether any ^{15}N-labeled cellular components that were present in sufficient quantities in the intact mycelia could not be detected in the broadband proton-decoupled spectrum of Figure 6 because of unfavorable NOE caused by low mobility and long correlation time (Figure 3a). The mobility of cellular components such as globular proteins and transfer RNA's can be increased by heat denaturation [11]. Thus the mycelia suspension whose spectrum is shown

in Figure 6b was subsequently heated at 100°C for one hour, and after removal of the mycelia by filtration, the filtrate containing soluble cell extracts was studied by ^{15}N NMR. Figure 8 shows the broadband proton-decoupled ^{15}N spectrum obtained at 50°C. The broad peak around 253.2 ppm can be assigned to the amide nitrogens of soluble oligopeptides which have greater mobility, and hence larger negative NOE, than the globular cellular proteins in intact mycelia. In addition, several new peaks are distinctly observable, and can be assigned to N1 of uridine and guanosine (228.8 ppm), cytidine NH_2 (281.8 ppm), adenosine NH_2 (297.3 ppm), and guanosine NH_2 (303.1 ppm) which appears as a distinct shoulder on the larger arginine $N_{\omega,\omega'}$ peak (304.5 ppm) [25] (Table II.) The uridine N3 resonance (217.8 ppm) is also substantially increased in intensity. Thus the resonances of all the protonated nitrogens of the four major bases of ribonucleic acids are observable in the cell extracts. These probably represent bases in transfer RNA's which, on loss of base-pairing by heat denaturation, assumed a more flexible conformation in which the individual nitrogen nuclei have shorter correlation times, and hence larger negative NOE [11].

The fact that in intact mycelia resonances from the less mobile, structured cellular components such as tRNA, DNA and the peptide backbone of globular proteins cannot be detected in proton-decoupled spectrum places a restriction on the types of cellular components that can be studied <u>in vivo</u> by ^{15}N NMR. Yet, for the study of non-specifically ^{15}N-labeled intact microorganisms, this has the advantage of facilitating the observation and assignment of smaller, metabolically

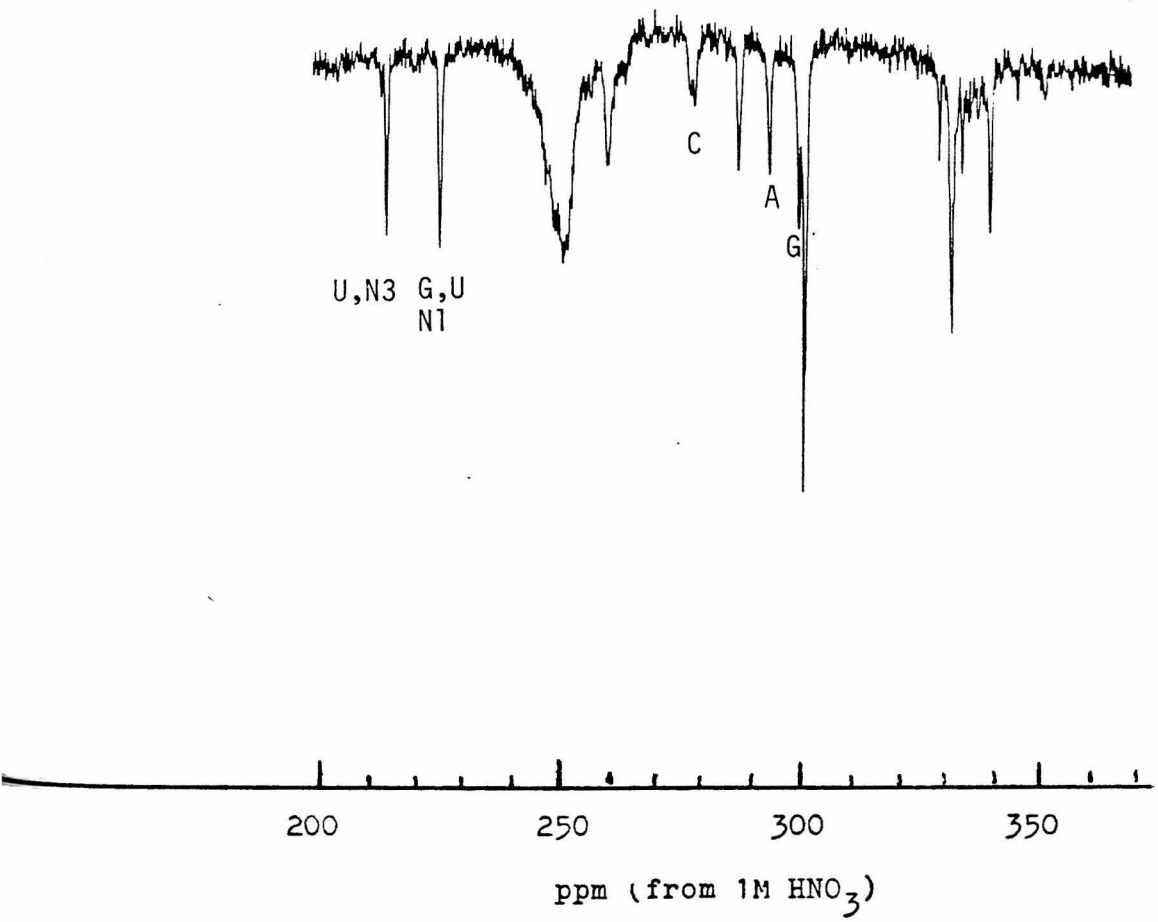

Fig. 8. Broadband proton-decoupled ^{15}N spectrum of the cell extracts obtained by heat treatment of the mycelia in Fig. 6b. The spectrum represents an accumulation of 17,607 transients. Abbreviations: A:adenine; C:cytidine; G:guanosine; U:uridine;(the three labeled upfield peaks are the NH_2 resonances of the specified base).

interesting molecules such as amino acids.

In the intact N. crassa mycelia, it is possible to study the assimilation of $^{15}NH_4^+$ into free amino acids, while restricting their incorporation into proteins. This can be achieved by the addition of cycloheximide to the culture medium before the addition of $^{15}NH_4Cl$ to inhibit protein synthesis; under such conditions, the mycelia can biosynthesize metabolites such as amino acids from $^{15}NH_4Cl$ with preexisting enzymes, but the de novo synthesis of proteins using ^{15}N-labeled amino acids will be inhibited. Thus the biosynthesis of free ^{15}N-labeled amino acids in vivo can be studied by NMR, unobscured by the contributions of ^{15}N-labeled amino acid residues in proteins. Possible effects of the inhibition of protein synthesis on regulation of cellular metabolism are as follows:

1. If the biosynthesis of an amino acid is regulated through a feedback inhibition of regulating enzymes at or near the beginning of the pathway by the amino acid already formed, the biosynthesis will cease as the intracellular amino acid concentration approaches the K_i value of the regulatory enzyme. Such feedback inhibition can occur sooner or later in all N. crassa mycelia growing in $^{15}NH_4Cl$, either with or without cycloheximide addition, but with cycloheximide, the inhibition may occur sooner because the synthesized amino acid is not utilized for protein synthesis.

2. If a metabolic pathway is regulated by induction or repression of the enzyme(s) involved, no de novo synthesis of inducible enzymes can occur, even in the presence of the inducer, after

cycloheximide has been added. However, because most known inducible enzymes are involved in catabolic, not anabolic pathways, the rate of biosynthesis of an amino acid is not likely to be affected by this factor. It is possible, however, that an individual enzyme (as a protein) may have a rapid turnover rate; then the addition of cycloheximide would lead to decrease in the concentration of that enzyme. Repression, which results in the inhibition of enzyme synthesis, will have no additional effect on mycelia in which protein synthesis is already inhibited by cycloheximide.

N. crassa ure-1 strain was grown in minimal medium for 17 hours, then on nitrogen-free medium for 3 hours to deplete the intracellular pool of unlabeled amino acids. [26] After addition of cycloheximide (20 μg/ml), the mycelia were grown in a medium containing 0.4% $^{15}NH_4Cl$ as the sole nitrogen source for 3 hours. Figure 9 shows the proton-decoupled ^{15}N spectrum of the mycelia. The most conspicuous differences from the spectra of mycelia grown without cycloheximide in Figure 6a are that (1) the glutamine N_γ peak (262.4 ppm) is much larger relative to those of arginine N_δ (291.0 ppm) and $N_{\omega,\omega'}$ (303.5 ppm) and (2) the peak corresponding to lysine N_ε and/or ornithine N_δ (342.6 ppm) is extremely small, being just distinguishable from the baseline (the right inset).

Glutamine can be biosynthesized in a large quantity as observed by the intense N_γ peak in Figure 9 because the enzyme catalyzing its synthesis, glutamine synthetase, is not feedback inhibited by glutamine itself [27]. The larger pool of glutamine observed in Figure 9 compared

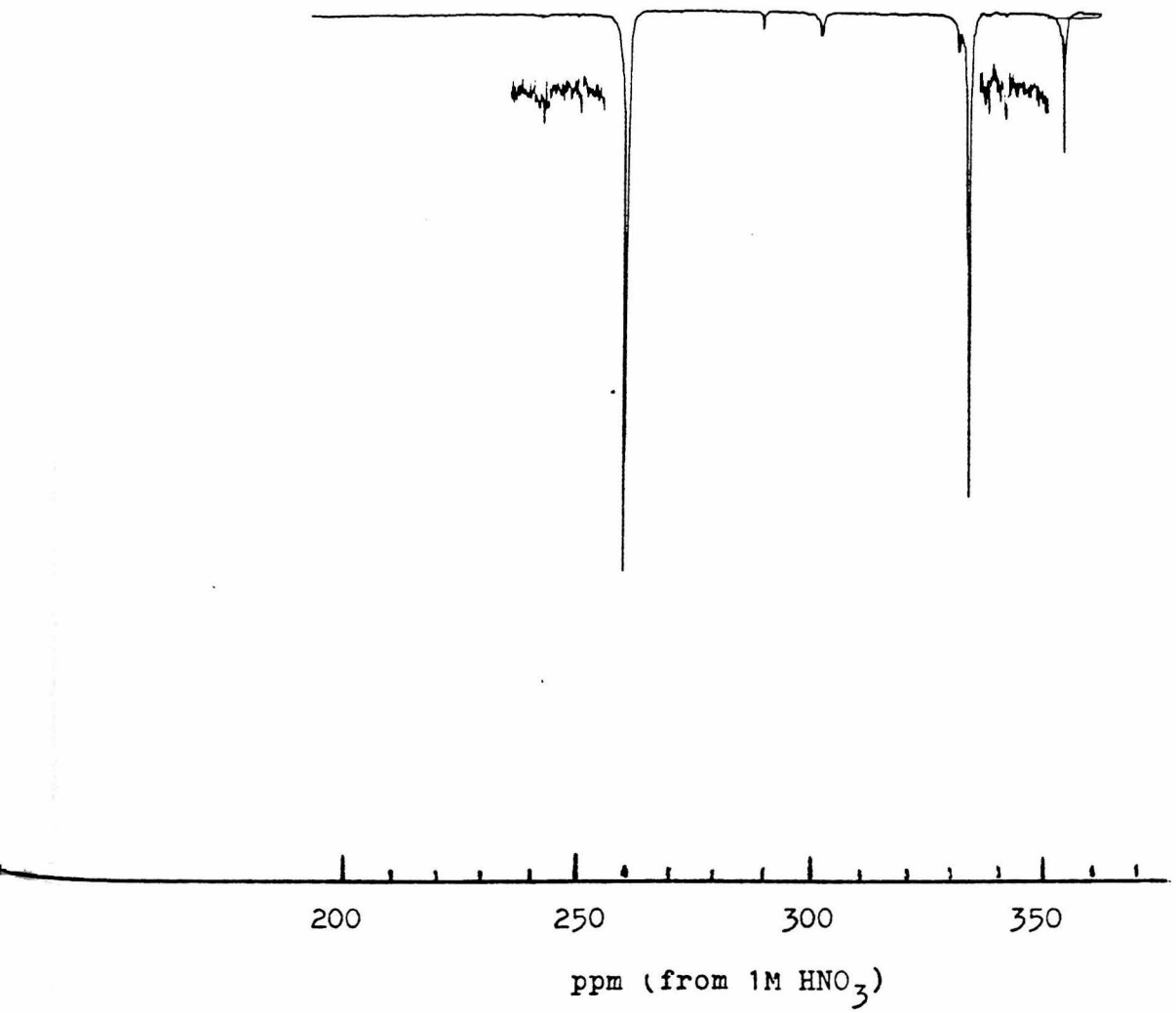

Fig. 9. Broadband proton-decoupled ^{15}N spectrum of intact mycelia suspension of N. crassa ure-1 strain grown in $^{15}NH_4Cl$-containing medium after addition of cycloheximide. The spectrum represents an accumulation of 4854 transients.

to Figure 6a could be due to decreased outflow of glutamine for the synthesis of cellular components such as chitin when growth is restricted by cycloheximide addition.

Arginine, too, is biosynthesized under these conditions as observed in Figure 9. Significantly, this occurs despite the presence of a feedback inhibition mechanism. In N. crassa, arginine biosynthesis is controlled by feedback inhibition of an enzyme acetylglutamate kinase [28] and repression of carbamylphosphate synthetase [29]. Both regulatory responses react to the cytosolic arginine concentration. This concentration is maintained at a low level because most of the arginine pool of cells growing in minimal medium is sequestered in vacuoles [12]. Thus, large pools of arginine must be accumulated before the cytosolic level of the amino acid is high enough to be an effective inhibitor.

By contrast, neither ornithine nor lysine occurs in significant quantities in those mycelia as observed by the very small peak at 342.5 ppm. Because ornithine $^{15}N_{\delta}$ is a precursor for arginine $^{15}N_{\delta}$ (Figure 7), the presence of arginine $^{15}N_{\delta}$ peak (291.0 ppm) in Figure 9 indicates that ornithine was synthesized but has been mostly utilized for arginine synthesis. Because, under normal growth condition, ornithine is accumulated in vacuoles, [8] and a small pool of lysine is also accumulated, the above result suggests that cycloheximide may have the effect of preventing the accumulation of these amino acids.

These results indicate that cycloheximide addition is useful for observing the assimilation of $^{15}NH_4^+$ into amino acids such as glutamine, glutamate and arginine which can be biosynthesized in large quantities without inhibiting its own synthesis. For these amino acids, the addition of cycloheximide has the advantage of permitting normal synthesis and yet restricting their outflow into proteins.

3. The time course of assimilation of $^{15}NH_4^+$ into glutamine and glutamate in two N. crassa strains.

As indicated in the previous section, glutamate and glutamine play central roles in assimilating NH_4^+ and acting as precursors for other nitrogenous metabolites (Figure 7). For many years, it was assumed that the primary metabolic pathway for the biosynthesis of glutamate involved the reductive amination of α-ketoglutarate, catalyzed by nicotinamide adenine dinucleotide phosphate (NADP)-dependent glutamate dehydrogenase:[31]

$$\alpha\text{-ketoglutarate} + NH_4^+ + NADPH + H \rightleftharpoons \text{L-glutamate} + NADP^+ + H_2O \quad (1)$$

Recently, interest has been shown for an alternate pathway for glutamate biosynthesis because a previously unknown enzyme, glutamate synthase, has been found in procaryotes,[32] yeast,[33] and higher plants.[34]

This enzyme catalyzes the formation of two molecules of L-glutamate from α-ketoglutarate and L-glutamine (reaction 3). By coupling this reaction with glutamine synthetase (reaction 2), an essentially irreversible pathway for the formation of glutamate from NH_4^+ and α-ketoglutarate is achieved (reaction 4).

$$\text{L-glutamate} + \text{ATP} + NH_4^+ \longrightarrow \text{L-glutamine} + \text{ADP} + \text{P} \qquad (2)$$

$$\alpha\text{-ketoglutarate} + \text{L-glutamine} + \text{NAD(P)H} \longrightarrow 2\ \text{L-glutamate} + \text{NAD(P)} \qquad (3)$$

$$\text{Sum: } \alpha\text{-ketoglutarate} + NH_4^+ + \text{ATP} + \text{NAD(P)H} \longrightarrow \text{L-glutamate} + \text{ADP} + \text{P} + \text{NAD(P)}^+ \qquad (4)$$

Because of the irreversibility and the high affinity of bacterial glutamine synthetase for ammonia, this pathway can function in a very efficient manner when the cellular levels of free ammonia are low. By contrast, the reaction catalyzed by glutamate dehydrogenase is freely reversible and proceeds towards biosynthesis of glutamate only in the presence of relatively high concentration of ammonium salts.[35] The cellular regulation of reaction (4) in procaryotes suggests that its primary function in these organisms is for the synthesis of glutamate when growth is limited by the availability of ammonia.[32] In plants, by contrast, reaction (4)

is suggested as the primary pathway for ammonia assimilation and glutamate formation; recent studies on the changes in the specific activities of glutamine synthetase, glutamate synthase and glutamate dehydrogenase in response to the availability of nitrogen source in the medium support this suggestion.[34d]

Very recently, glutamate synthase was partially purified from N.crassa and shown to catalyze reaction (3) in vitro.[36] It is therefore of great interest to investigate whether this reaction is coupled with the glutamine synthetase reaction to form an alternate pathway for the assimilation of NH_4^+ into glutamate in vivo. This can be studied using the am-1 strain of N.crassa which lacks NADP-dependent glutamate dehydrogenase for catalyzing reaction (1). If this strain is found to assimilate exogenous NH_4^+ to form glutamate, this would provide strong support for the occurrence of glutamate biosynthesis via reaction (4). in vivo.

^{15}N NMR spectroscopy can be a valuable technique for such studies. If N. crassa am-1 strain is first germinated in medium containing unlabeled glutamate, and then is transferred to minimal medium containing $^{15}NH_4^+$ as the sole nitrogen source, only glutamate synthesized from exogenous $^{15}NH_4^+$, and not the preexisting unlabeled glutamate, would give rise to a ^{15}N resonance. Moreover, if the incorporation of ^{15}N-label into the glutamine amide nitrogen and glutamate N_α is

studied as a function of time, one might obtain interesting clues as to whether glutamate biosynthesis occurs *via* glutamine as postulated in reaction (4).

N. crassa *am*-1 strain was cultured in minimal medium containing unlabeled glutamate for 17 hours, transferred to nitrogen-free medium for 3 hours, then, after addition of cycloheximide (20 μg/ml), $^{15}NH_4Cl$ was added to the medium to the final concentration of 0.2% at time zero. Figure 10a shows the proton-decoupled ^{15}N spectra of the mycelial suspension, prepared as described in figure caption, as a function of time starting from the $^{15}NH_4Cl$ addition. The course of the assimilation of $^{15}NH_4^+$ (resonance at 354.5 ppm) into the amide nitrogen of glutamine (262.4 ppm) and glutamate N_α(334.3 ppm)[37] is clearly observed. Clearly the *N. crassa* *am*-1 strain, which is incapable of glutamate synthesis *via* reaction (1), is capable of using an alternate pathway for assimilating $^{15}NH_4^+$ into glutamate. Because wild-type *N. crassa* carries all the genes that are functional in a mutant, wild type *N. crassa* too must be capable of using this pathway.

To obtain clues as to whether the alternate pathway of $^{15}NH_4^+$ assimilation occurs *via* glutamine as postulated in reaction (4) in *am*-1 strain, a comparison ^{15}N spectrum was obtained for *ure*-1 strain of *N. crassa* which is capable of reaction (1). The *ure*-1 strain was grown on minimal medium for 17 hours, transferred to nitrogen-free medium for 3 hours, then after addition of cycloheximide (20 μg/ml),

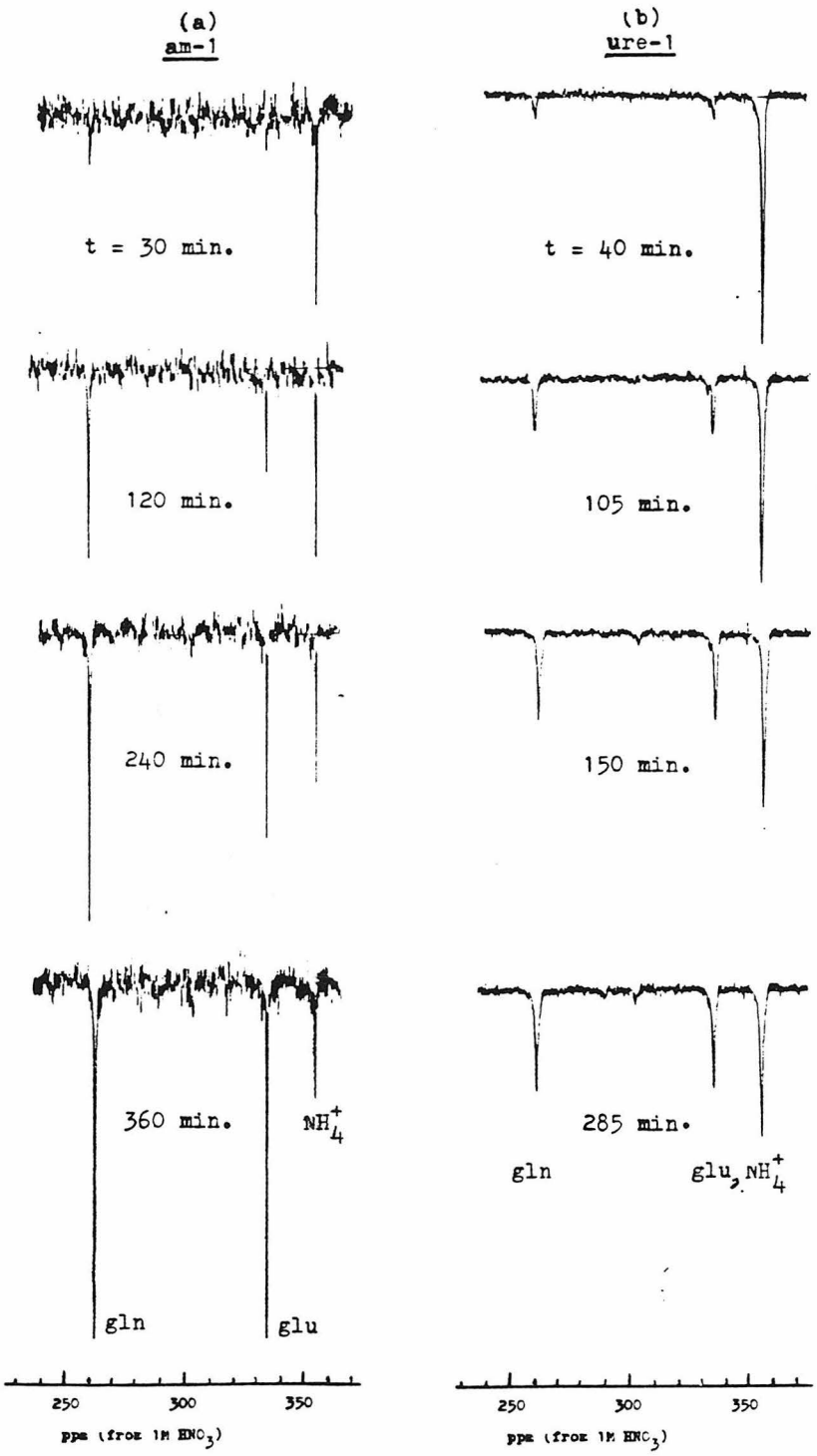

Fig. 10 (Caption on the following page)

Fig. 10 (a) The proton-decoupled ^{15}N NMR spectra of N. crassa am-1 strain as a function of time from $^{15}NH_4Cl$ addition. The mycelia were suspended in 500 ml of nitrogen-free medium in a flask and aerated by bubbling air through them at 25 -30°C. $^{15}NH_4Cl$ (1g) was added to the culture medium at time 0. The NMR sample was prepared by collecting the mycelia by filtration and adding to the mycelia pellets, 9 ml of the culture medium to make 18 ml of mycelia suspension in the NMR tube. After each NMR measurement, the mycelia were resuspended in the same culture medium for further assimilation of $^{15}NH_4Cl$. Each spectrum represents 143 transients accumulated in 5 minutes.
(b) The proton-decoupled ^{15}N NMR spectra of N. crassa ure-1 strain at 28°C as a function of time from $^{15}NH_4Cl$ addition. The cells were suspended in 18 ml of nitrogen-free medium in the NMR tube and were aerated by bubbling in air throughout the NMR measurement. $^{15}NH_4Cl$ (200 mg) was added directly to the NMR sample at time 0. Each spectrum represents 1004 transients accumulated in 33 minutes. The time given for each spectrum indicates the middle of the accumulation period referred to $^{15}NH_4Cl$ addition.
Both spectra were obtained with 70 μsec pulse width and 2-sec delay.
Abbreviations: gln:glutamine; glu:glutamate.

$^{15}NH_4^+$ was added to the mycelia suspension to a final concentration of 1% at time zero. Figure 10b shows the ^{15}N spectrum of ure-1 strain as a function of time from $^{15}NH_4^+$ addition, obtained with the same NMR parameters as in Figure 10a. Comparison of the two spectra (Figures 10a and 10b) clearly indicates that the rate of increase of resonance intensities of glutamine N_γ and glutamate N_α are different for the two strains; in am-1 strain, the resonance intensity of glutamine N_γ increases faster than that of glutamate N_α during the first 120 min., whereas in ure-1 strain, the resonance intensities of glutamine N_γ and glutamate N_α increase at the same rate. This can also be seen in Figure 11a and b which plot the resonance intensities of glutamine N_γ and glutamate N_α as function of time for am-1 and ure-1 strain respectively.

In general, the intensities of resonances in the broadband proton-decoupled ^{15}N spectra cannot be used as a measure of the absolute concentrations of the metabolites because the pulse repetition time may not be long enough to allow full relaxation of all nuclei observed, and the NOE contributions to the intensities may be different for each resonance. However, because the two spectra in Figure 10 were obtained with the same pulse width and repetition rate, the following equation is valid at a given time t:

$$\frac{(S_{gln}/S_{glu})_{am\text{-}1}}{(S_{gln}/S_{glu})_{ure\text{-}1}} = \frac{([gln]/[glu])_{am\text{-}1}}{([gln]/[glu])_{ure\text{-}1}} \qquad (5)$$

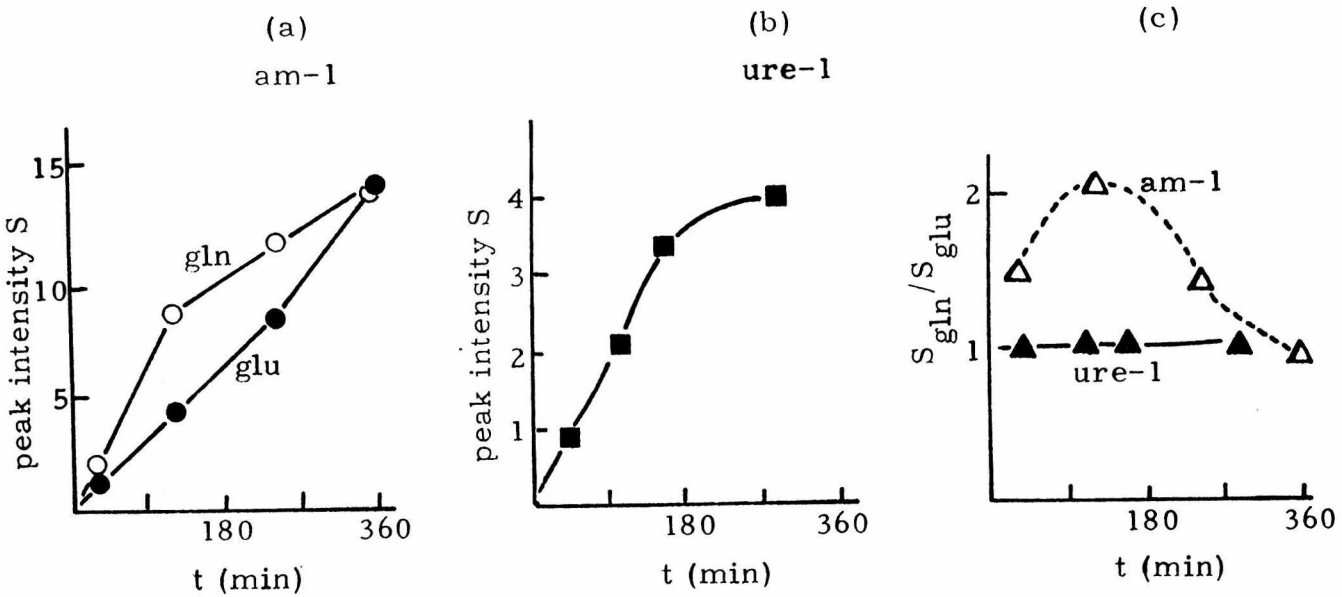

Fig. 11 (a) Peak intensities S of the observed ^{15}N resonances in N. crassa am-1 strain as a function of time from $^{15}NH_4Cl$ addition, taken from Fig. 10a; O:glutamine amide nitrogen; ●: glutamate α-amino nitrogen. Peak intensities are given in arbitrary units.

(b) The same for N. crassa ure-1 strain; ■: glutamine amide nitrogen and glutamate α-amino nitrogen which have the same intensities as can be seen in Fig. 10b.

(c) The peak intensity ratio S_{gln}/S_{glu} as a function of time in am-1 and ure-1 strains where S_{gln} and S_{glu} are the peak intensities of glutamine amide nitrogen and glutamate α-amino nitrogen respectively, taken from Fig. 11a and b. S_{gln}/S_{glu} is proportional to the concentration ratio [gln]/[glu] (see text)

where S_{gln} and S_{glu} are the peak intensities of glutamine N_γ and glutamate N_α and [gln] and [glu] are the intracellular concentrations of the indicated species, and the subscripts am-1 and ure-1 refer to the respective strain. From Figure 10b, we can see that $(S_{gln}/S_{glu})_{ure-1} = 1$ throughout the observed period, indicating that $([gln]/[glu])_{ure-1}$ must have remained constant during this period. Therefore, from equation 5, $(S_{gln}/S_{glu})_{am-1}$ is proportional to $([gln]/[glu])_{am-1}$. Therefore, the peak intensity ratio S_{gln}/S_{glu} can be used as a measure of the concentration ratio [gln]/[glu] for each strain.

Figure 11c compares $(S_{gln}/S_{glu})_{am-1}$ and $(S_{gln}/S_{glu})_{ure-1}$ as function of time. Clearly, in am-1 strain, glutamine concentration increases at a faster rate than glutamate concentration during the first 120 min,. then over the next 240 min., the rate of glutamate synthesis speeds up relative to that of glutamine synthesis. By contrast, in ure-1 strain, the relative rates of glutamine and glutamate synthesis are constant through the entire observed period (285 min.). This result gives support to the hypothesis that in am-1 strain $^{15}NH_4^+$ is assimilated *via* the glutamine amide nitrogen to form the α-amino group of glutamate. Moreover, our result with am-1 strain indicates that *in vivo* the assimilation of $^{15}NH_4^+$ into glutamate by the alternate pathway occurs at a relatively high ammonium ion concentration of 35 mM

in the medium whereas *in vitro* the partially purified glutamate synthase was reported to be inhibited by the presence of 2.5 mM NH_4^+.[36] Although the intracellular $^{15}NH_4^+$ concentration may be different from that in the medium, our result demonstrates that *in vivo* the enzyme is active in *N. crassa* mycelia growing in excess NH_4^+ and suggests that in wild-type *N. crassa* too, NH_4^+ assimilation by the alternative pathway (4) may make greater contribution to glutamate biosynthesis than has been inferred from *in vitro* studies.[38]

The spectrum in Figure 10b shows, for the first time, that it is possible to follow the time course of the assimilation of $^{15}NH_4^+$ into nitrogenous metabolites in intact mycelia suspension growing in a "miniature culture" in an NMR tube; the mycelia were found to assimilate $^{15}NH_4^+$ at an observable rate at 28° C when they are aerated by bubbling air through the sample and when the volume ratio of mycelia pellet to medium is approximately 1:10. Because of the large sample volume (18 ml) used in our wide-bore Bruker WH180 spectrometer, such mycelia concentration is sufficient to give ^{15}N resonances of the major metabolites with good signal-to-noise ratios in a reasonable amount of time.

The preliminary results described in this paper suggest that ^{15}N NMR can be a promising new technique for studying *in vivo* nitrogen

metabolism and its regulation in intact microorganisms. It is particularly valuable for tracing the metabolism of nitrogenous groups such as the amide group of glutamine, the α-amino group of glutamate and the guanidino group of arginine which play crucial roles in intermediary nitrogen metabolism but are not amenable to the traditional method of radioisotope labeling. This paper demonstrates the feasibility of (1) tracing the time course of the biosynthesis of these metabolites from NH_4^+ *in vivo* in intact *N. crassa* mycelia by the noninvasive ^{15}N NMR technique; (2) estimating their turnover time; and (3) measuring their relaxation times T_1 and negative Overhauser enhancements NOE in the intracellular environment.

A few of the numerous areas to which this technique can be applied are as follows.

1. Valuable information on the functioning of metabolic regulation *in vivo* can be obtained by comparing the patterns of the distribution of NH_4^+ into competing anabolic pathways such as is shown in the spectrum in Figure 6a under different nutritional conditions such as the availability of the nitrogen source and the presence of specific repressors or inducers. For major metabolites such as glutamine, glutamate and arginine, their peak intensities in the ^{15}N spectrum can be used to obtain a quantitative estimate of the relative amounts of $^{15}NH_4^+$ channeled into their biosynthesis under a specific condition,

if we first measure the intracellular T_1 and NOE of the ^{15}N nuclei of these metabolites, then use a pulsing rate that permits full relaxation of all nuclei under consideration and correct for the different contributions of NOE to the peak intensities.

2. ^{15}N NMR is particularly useful for distinguishing between alternative pathways from a precursor to a product, and for obtaining clues to the existence of a previously unknown or suspected pathway, in cases where the pathways result in different labeling patterns for the product. A specific example for N. crassa is the following.

N. crassa cultured on minimal medium biosynthesize free glutamine far in excess of their immediate need for this metabolite as a protein component and as a precursor for other nitrogenous cellular components.[30] (Figure 6). Unlike arginine, only a small part of the accumulated glutamine is localized in vacuoles, the bulk of glutamine pool being found in the cytosol.[30] Does the organism store up glutamine as a nitrogen reservoir to be mobilized during nitrogen deficiency, for the synthesis of glutamate and other amino acids, in addition to other metabolites for which it is a known precursor?

Glutamine can be converted to glutamate either by reaction (3) or, in many organisms, by simple hydrolysis by glutaminase:

$$\text{glutamine} + H_2O \xrightarrow{\text{glutaminase}} \text{glutamate} + NH_4^+ \qquad (6)$$

Although glutaminase occurs in a wide variety of bacteria, and some species of fungi,[39] glutaminase activity has not been reported in N. crassa to date. However, it is conceivable that glutaminase is produced in N. crassa but has not been detected because a significant level of production occurs only during certain phases of growth as in E. Coli B,[40] or in the presence of an inducer.

One known pathway by which the amide nitrogen of glutamine is released as NH_4^+ in N. crassa is:[41]

$$\text{glutamine} \xrightarrow[\text{asparagine}]{\alpha\text{-keto-succinamate}} \alpha\text{-ketoglutaramate} \longrightarrow NH_4^+ + \alpha\text{-ketoglutarate} \qquad (7)$$

Recently, G. Espin and coworkers[42] proposed, on the basis of studies on the changes in the intracellular concentrations of glutamine, glutamate and arginine and release of NH_4^+ during nitrogen deficiency, that glutamine amide nitrogen is degraded to NH_4^+ by reaction (7) during nitrogen starvation and reutilized for glutamate synthesis. However, in the absence of isotope labeling, it is uncertain whether the released NH_4^+ derives from glutamine or from other nitrogenous metabolites such as arginine and purine which are known to degrade via urea to NH_4^+ during nitrogen starvation.[26]

^{15}N NMR, combined with ^{13}C NMR, can provide a definitive method for elucidating the pathway(s) of glutamine utilization during nitrogen deficiency *in vivo*. *N. crassa* *am*-1 strain can be grown on glutamine and arginine as nitrogen source.[43] The mycelia can then be transferred to medium containing ($^{15}N_\gamma$)glutamine as the sole nitrogen source and the metabolic fate of the ^{15}N-label can be traced as function of time. Incorporation of the ^{15}N-label mainly into the α-amino group of glutamate and other amino acids would provide strong evidence that the primary pathway for glutamate synthesis from glutamine is *via* reaction (3):

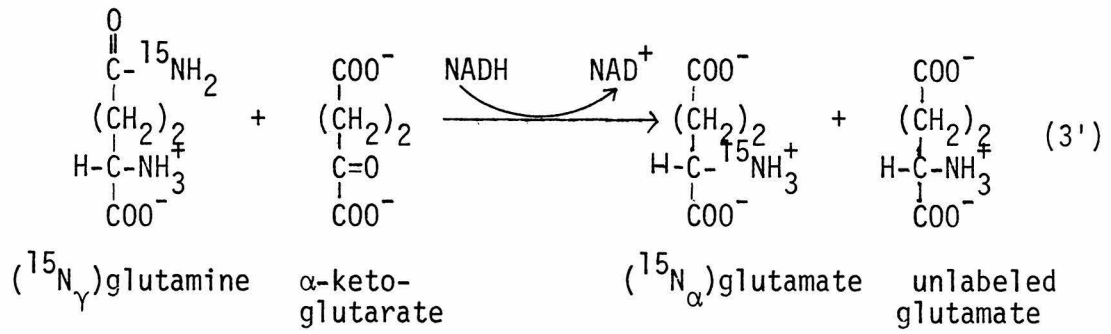

(3')

On the other hand, appearance of the ^{15}N-label mostly as $^{15}NH_4^+$ would imply that the glutamine amide group was hydrolyzed by one of the following processes:

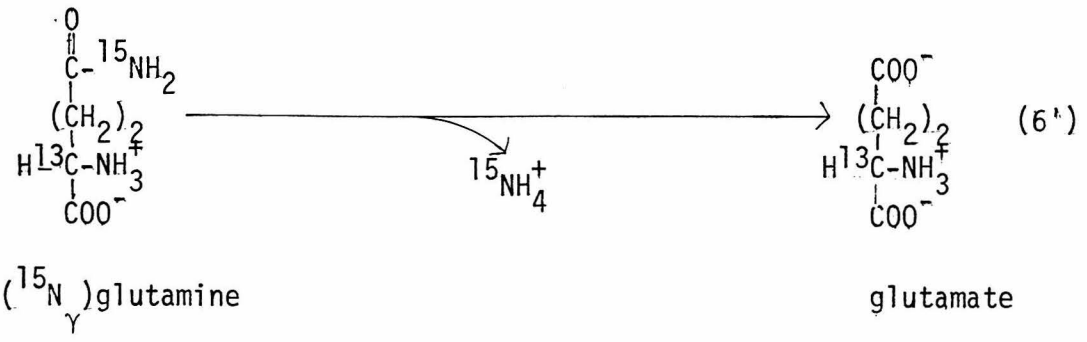

($^{15}N_{\gamma}$)glutamine glutamate (6')

or

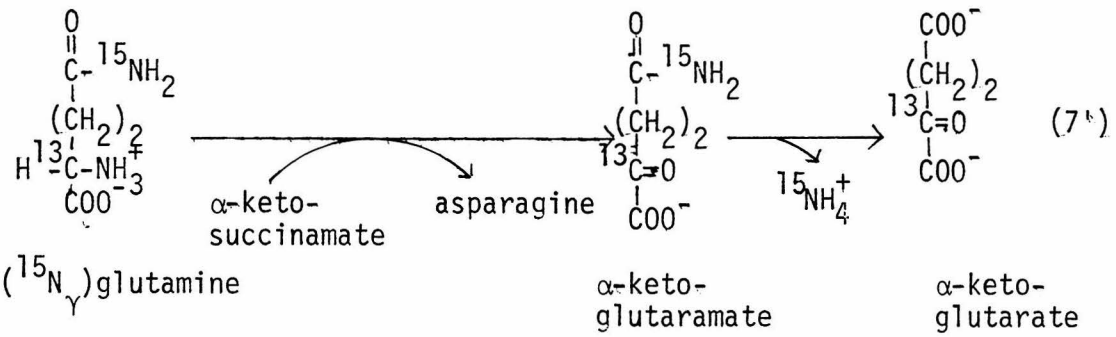

($^{15}N_{\gamma}$)glutamine α-keto-glutaramate α-keto-glutarate (7')

Pathways (6') and (7') can be distinguished by repeating the experiment with ($^{13}C_{\alpha}$)glutamine and monitoring the appearance of the ^{13}C label as either ($^{13}C_{\alpha}$)glutamate or as carbonyl ^{13}C of α-ketoglutaramate and α-ketoglutarate.[44] If $^{15}NH_4^+$ and ($^{13}C_{\alpha}$)glutamate are found to be released from glutamine, this would provide strong evidence for the existence of glutaminase activity in N. crassa. Since $^{15}NH_4^+$ would be partly released into the medium, it is important that the entire metabolic process takes place within a miniature culture medium in the NMR tube. The feasibility of such experiment by Bruker WH180 spectrometer has been demonstrated. Thus ^{15}N and ^{13}C NMR can be used to distinguish

between alternative metabolic pathways where they result in different labeling patterns for the products, and possibly provide evidence for the existence of previously unknown pathways.

REFERENCES AND NOTES

1. R. B. Moon and J. H. Richards, J. Biol. Chem. 248, 7276 (1973).
2. R. G. Schulman, T. R. Brown, K. Ugurbil, S. Ogawa, S. M. Cohen, J. A. den Hollander, Science, 205, 160 (1979) and references cited therein.
3. J. Schaefer, E. O. Stejskal, R. A. McKay, Biochem. Biophys. Res. Commun. 88, 274 (1979).
4. M. Llinas, K. Wuthrich, W. Schwotzer and W. von Philipsborn, Nature 257, 817 (1975).
5. a. A. Lapidot and C. S. Irving, Proc. Natl. Acad. Sci. USA 74, 1988 (1977).
   b. A. Lapidot and C. S. Irving, Biochemistry 18, 704 (1979).
   c. A. Lapidot and C. S. Irving, Biochemistry 18, 1788 (1979).
6. R. L. Weiss and R. H. Davis, J. Biol. Chem. 248, 5403 (1973).
7. T. J. Facklam and G. A. Marzluf, Biochem. Genet. 16, 343 (1978).
8. R. L. Weiss, J. Bacteriol. 126 (3), 1173 (1976).
9. R. H. Davis, M. B. Lawless and L. A. Port, J. Bacteriol. 102, 299 (1970).
10. When the mycelia are extensively washed prior to suspension in arginine-free medium, no leakage of intracellular ^{15}N-arginine into the medium occurs during the NMR measurement. This was checked by recovering the mycelia by filtration and checking the filtrate for the presence of ^{15}N-arginine.

11. D. Gust, R. B. Moon and J. D. Roberts, Proc. Natl. Acad. Sci. USA 72, 4696 (1975).

12. D. Canet, G. C. Levy and I. A. Peat, J. Magn. Reson. 18, 199 (1975).

13. R. L. Weiss, J. Biol. Chem., 248, 5409 (1973).

14. a. C. E. Cramer, L. E. Vaughn and R. H. Davis, (1980) in preparation.

    b. E. Martinoia, U. Heck, Th. Boller, A. Wiemken and Ph. Matile, Arch. Microbiol. 120, 31 (1979).

15. V. Markowski, G. R. Sullivan and J. D. Roberts, J. Am. Chem. Soc. 99, 715 (1977).

16. R. E. Botto and J. D. Roberts, J. Org. Chem. 42(13), 2247 (1977).

17. A. Abe, Ph. D. Thesis, California Institute of Technology.

18. Although asparagine N_β has a very similar shift to that of glutamine N_γ, its concentration in N. crassa mycelia has been found to be less than 5% of that of glutamine (see also reference 30). Similarly, amino acids which have N_α shifts in the regions specified but are known to occur in very low amounts relative to the others in N. crassa are not included in the assignments.

19. N. de Terra and E. L. Tatum, Science 134, 1066 (1961).

20. E. J. Smith and R. W. Wheat, Archives Biochem. Biophys. 86, 267 (1960).

21. T. B. Posner, V. Markowski, P. Lotus and J. D. Roberts, J. S. C. Chem. Commun. 768 (1975).

22. N. J. Oppenheimer & R. M. Davidson, Org. Mag. Res. 13, 14 (1980).

23. E. Martegani and L. Alberghina, J. Biol. Chem. 254, 7047 (1979).

24. To ascertain that no leakage of ^{15}N-labeled metabolites into the $^{14}NH_4Cl$-containing medium had occurred, the medium used for washing and growing the ^{15}N-labeled mycelia was concentrated and its ^{15}N spectrum was taken. No ^{15}N resonance was detected after 3000 transients.

25. The higher chemical shift of 304.5 ppm observed for $N_{\omega,\omega'}$ of arginine in cell extract at 50°C compared to 303.5 ppm in mycelia at 10°C is probably due to the higher temperature since for $N_{\omega,\omega'}$ of free arginine in aqueous solution, too, a shift of 304.4 ppm is observed at 55°C (Table I, in Part III) compared to 303.8 ppm at room temperature. Thus the peak at 303.1 ppm can most reasonably be assigned to guanosine NH_2.

26. T. L. Legerton and R. L. Weiss, J. Bacteriol. 138, 909 (1979)

27. J. Hubbard and E. R. Stadtman, J. Bacteriol. 93, 1045 (1967).

28. E. Wolf and R. L. Weiss (in press).

29. J. Cybis and R. H. Davis, J. Bacteriol. 123, 196 (1975).

30. Y. Mora, G. Espin, K. Willns and J. Mora, J. Gen. Microbiol. 104, 241 (1978).

31. Wild-type N. crassa synthesizes two glutamate dehydrogenases; one specific for nicotinamide adenine dinucleotide phosphate (NADP-GDH) and the other specific for nicotinamide adenine dinucleotide (NAD-GDH). NADP-GDH is biosynthetic, while NAD-GDH is oxidative.

32. D. W. Tempest, J. L. Meers and C. M. Brown in "Enzymes of Glutamine Metabolism", eds. S. Prusiner and E. R. Stadtman, Academic Press, N.Y. 1973.

33. R. J. Roon, H. J. Even and F. Larimore, J. Bacteriol 118, 89 (1974)

34. a. P. J. Lea and B. J. Miflin, Nature 251, 614 (1974)

    b. M. J. Boland and A. G. Benny, Eur. J. Biochem. 79, 355 (1977)

    c. B. J. Miflin and P. Lea in "Progress in Phytochemistry" 4, eds. L. Reinhold, J. B. Harborne, and T. Swain, Pergamon Press, Oxford, 1977

    d. J. Y. Chiu and P. D. Shargool, Plant Physiol. 63, 409 (1979)

35. P. P. Trotta, K. E. B. Platzer, R. H. Haschemeyer and S. Meister, Proc. Natl. Acad. Sci. USA, 71, 4607 (1974)

36. G. Hummelt and J. Mora, Biochem. Biophys. Res. Commun. 92, 127, (1980)

37. In addition to N_α of glutamate, N_α of other amino acids, synthesized from glutamate by transamination (Figure 7) may make small contribution to this resonance at later stage in the experiment. Only the N_α of lysine and glutamine, however, have ^{15}N shifts within $\pm$0.4 ppm of that of glutamate (Table II), and concentration of lysine has been shown to be very low in N. crassa growing under these conditions (p.100)

38. Little is known about the regulation of formation of glutamate synthase in response to the availability of NH_4^+ in other organisms. The enzyme level is higher in limited NH_4^+ than in excess NH_4^+ in some bacterial strains, whereas the reverse has been reported for other strains (see B. Tyler, Ann. Rev. Biochem. 47, 1127 (1978))

39. A. Imada, S. Igarasi, K. Nakahama and M. Isono, J. Gen. Microbiol. 76, 85 (1973)

40. P. D. Boyer "Enzymes" vol. 4, 1971, p.81 , Academic Press, New York

41. C. Monder and A. Meister, Biochem. Biophys. Acta 28, 202 (1958)

42. G. Espin, R. Palacios and J. Mora, J. Gen. Microbiol. 115, 59 (1979)

43. G. Vaca and J. Mora, J. Bacteriol. 131, 719 (1977)

44. Although $^{13}C_{\alpha}$-glutamate in reaction 6' can be metabolized to ^{13}C-α-ketoglutarate by subsequent transamination, such process would occur after release of $^{15}NH_4^+$ in reaction 6' whereas in reaction 7' appearance of ^{13}C-α-ketoglutaramate would precede the appearance of $^{15}NH_4^+$.

PROPOSITION I

A ^{15}N nuclear magnetic resonance study of the ionization states of the coenzyme pyridoxal phosphate and quasi-substrate at the active site of aspartate aminotransferase

Pyridoxal phosphate-dependent aminotransferases, which play an essential role in intermediary nitrogen metabolism, catalyze the reversible transfer of the α-amino group of an amino acid to an α-keto acid, with the coenzyme pyridoxal phosphate acting as an intermediary carrier of the amino group. The pyridoxal phosphate-enzyme complex (PLP-E) accepts an amino group from an amino acid, via two intermediate Schiff's bases, to form the pyridoxamine phosphate-enzyme complex (PMP-E) which then donates its amino group to an α-keto acid (Figure 1).

Of the aminotransferases, aspartate aminotransferase, which catalyzes the reaction, L-aspartate + α-ketoglutarate $\rightleftarrows$ oxaloacetate + L-glutamate, has been studied most extensively. Aspartate aminotransferase from pig-heart cytosol is a dimer (MW $\sim$ 90,000) consisting of two identical subunits; each subunit contains one molecule of the coenzyme, pyridoxal phosphate (PLP), bound to the ε-amino group of Lys-258 in an aldimine linkage (Figure 2a).

A dynamic model for the mechanism of catalysis of aspartate aminotransferase developed by Karpeisky and coworkers [1] with partial revision in the light of more recent evidence [2,3], is shown in Figure 2. A key feature of the model is the assumption that cooperative proton

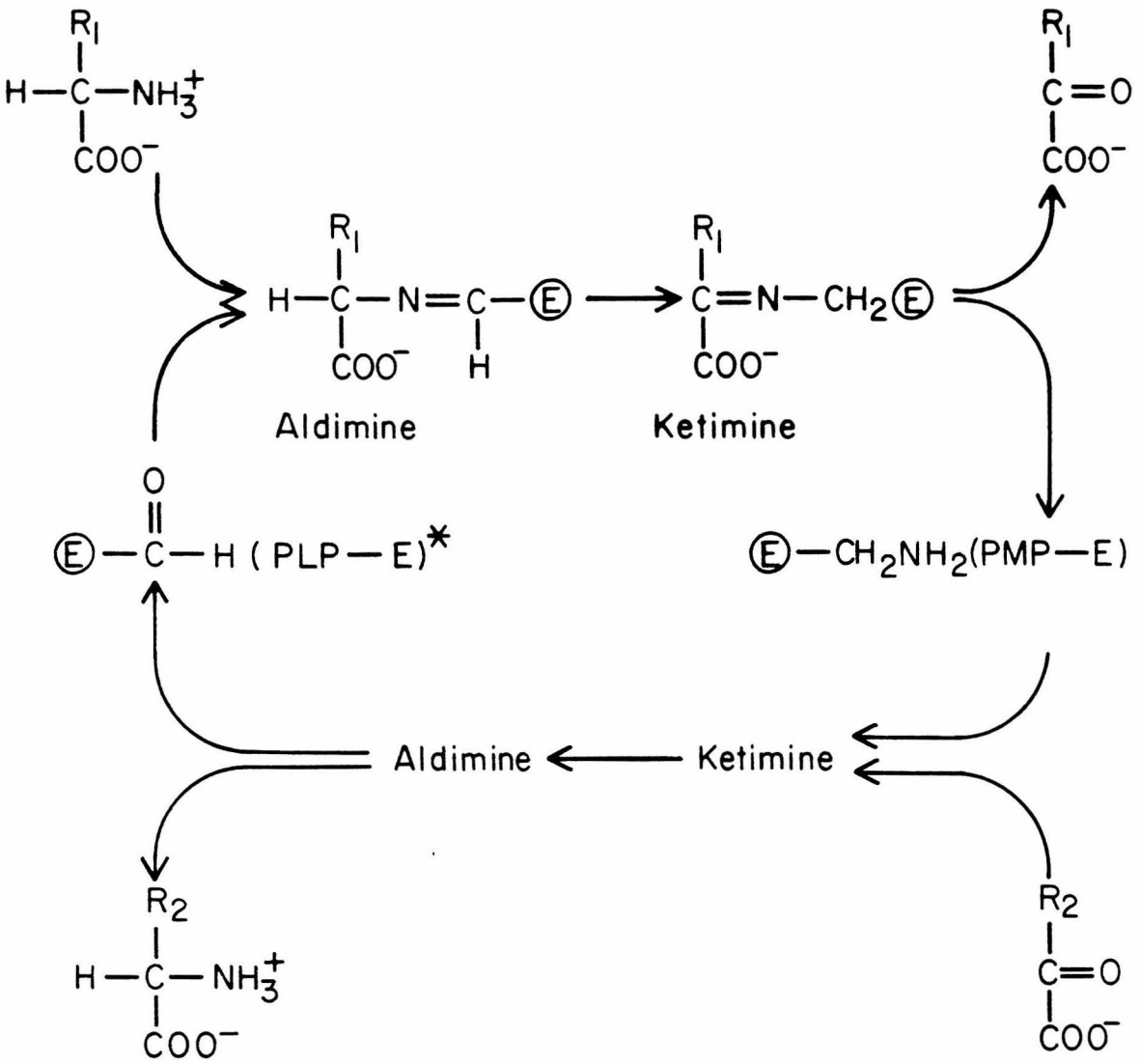

Figure 1

* The aldehyde group of the pyridoxal phosphate forms a Schiff's base with the ε-amino group of a lysine residue of the enzyme whenever it is not occupied by an amino group of the substrate.

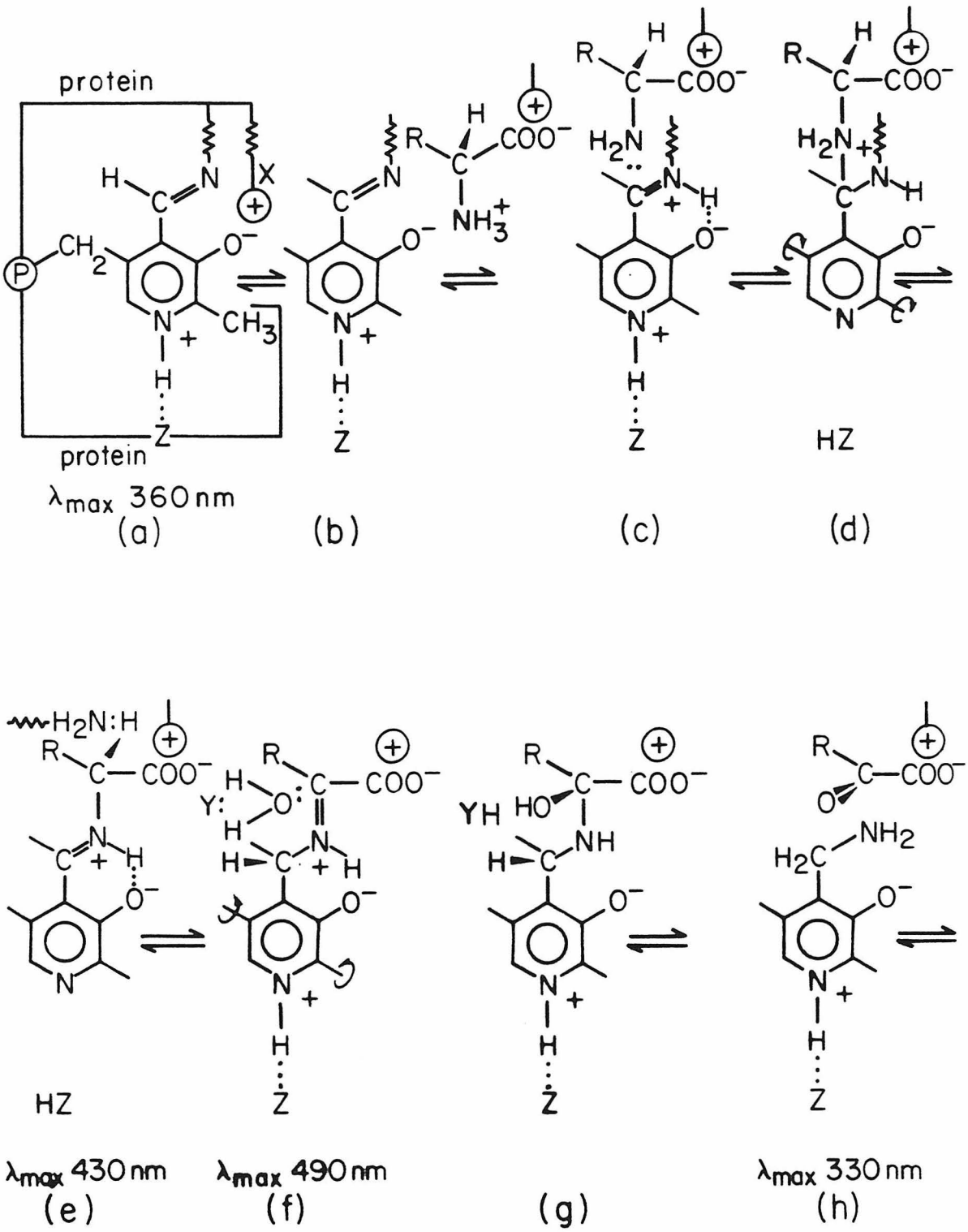
protein
protein
HZ
λmax 360 nm
(a)
(b)
(c)
(d)
HZ
λmax 430 nm
λmax 490 nm
λmax 330 nm
(e)
(f)
(g)
(h)

Figure 2

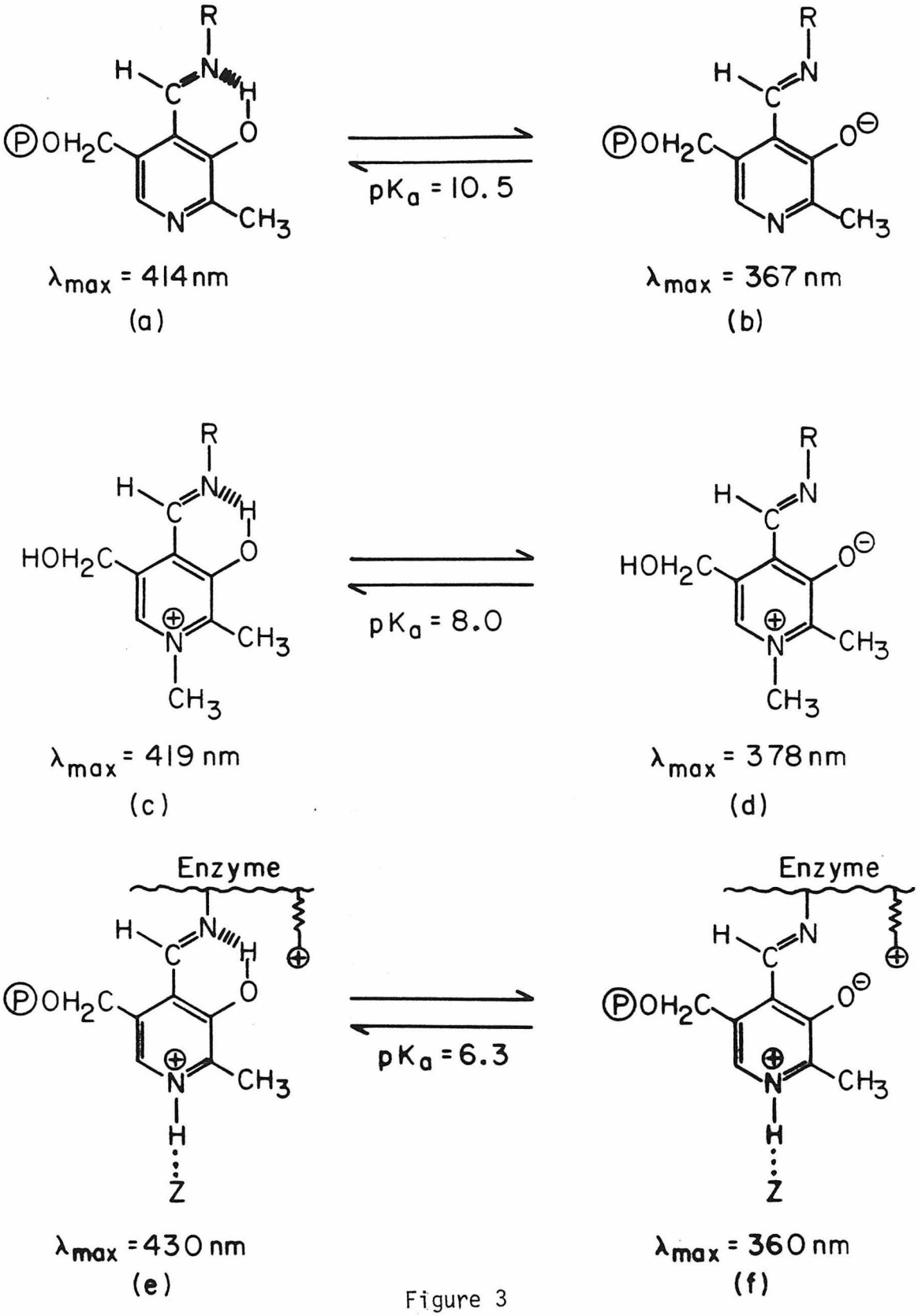
R
H
N
C
H
O
POH_2C
N
CH_3
pK_a = 10.5
λ_{max} = 414 nm
(a)
λ_{max} = 367 nm
(b)
HOH_2C
CH_3
pK_a = 8.0
λ_{max} = 419 nm
(c)
λ_{max} = 378 nm
(d)
Enzyme
Z
pK_a = 6.3
λ_{max} = 430 nm
(e)
λ_{max} = 360 nm
(f)

Figure 3

shifts involved in the transaldimination are linked with reversible reorientation of the coenzyme.

The catalytically active form of the pyridoxal phosphate-aspartate aminotransferase complex (PLP-E) at neutral pH has an absorption maximum at 360 nm, while the inactive form at acidic pH has λ_{max} ∿430 nm; the pKa of this transition is 6.3 [4]. By contrast, in free PLP-aldimines, the pKa of this transition (from λ_{max} = 367 nm to 414 nm), attributed to protonation of the phenolate group of pyridoxal, is 10.5 (Fig. 3a,b)[5]. In the proposed mechanism of catalysis, the phenolic group is considered to be ionized in the active form of PLP-E with λ_{max} = 360 nm (Fig. 2a), and the large decrease in pKa, from 10.5 for free PLP-aldimine to the observed 6.3 for the PLP-E, is partially attributed to a postulated hydrogen bonding (or protonation) of the pyridine N atom by a proton-donating group in the enzyme [6]. A positive charge on this atom, however, lowers the pKa only to ∿8.0, as observed in free PLP-aldimine methylated at pyridine N (Figure 3c,d)[7], and further lowering to 6.3 in PLP-E is attributed to the presence of a cationic group (possibly an imidazole group) close to the phenolic group (Fig. 3e,f) [1]. It is this postulated hydrogen bonding (or protonation) of the pyridine nitrogen that can be investigated by ^{15}N chemical-shift measurement of ^{15}N-labeled PLP bound to the enzyme.

On addition of the substrate (Figure 2b), the carboxylate group presumably binds to the same cationic site on the enzyme; neutralization of charge on the carboxylate lowers the basicity of the α-amino group,

allowing the transfer of a proton from the substrate NH_3^+ group to the Schiff-base nitrogen (or phenolate oxygen) of PLP-E (Figure 2c). Now the unionized nucleophilic amino group is ready to attack the highly reactive C=N bond of the protonated Schiff base. However, to form the tetrahedral intermediate (Figure 2d), the pyridine ring of the coenzyme must rotate $\sim 40^{\circ}$ around an axis passing through its $C2'$ and $C5'$, necessitating the disruption of the hydrogen bond between the pyridine N and proton-donating group on the enzyme. On formation of the substrate aldimine (Figure 2e), its α-proton is abstracted, possibly by Lys-ε-NH_2, resulting in the ketimine formation (Figure 2f). On protonation, the $C4'$ atom acquires a tetrahedral configuration, allowing the coenzyme ring to rotate back to the original plane with concomitant reprotonation of the pyridine N by the proton-donating group HZ (Figure 2f-g). On attack of H_2O (or OH^-) at the C_α atom, the α-oxoacid and enzyme-bound pyridoxamine phosphate are formed, completing the first half of the transamination (Figure 2h).

The assignment of absorption maxima to reaction intermediates in Figure 2 is based on the following evidence: (a) Study of transient normal reaction intermediates by the temperature-jump method indicated that intermediates with λ_{max} at 360, 430, 490 and 330 nm are formed [8]; (b) λ_{max} of 430 nm is assigned to substrate aldimine (Figure 2e) because this absorption maximum is also observed on binding of a quasi-substrate, α-methyl aspartate, which forms a stable aldimine with PLP-E and does not undergo further reaction due to the lack of an α-H atom [9];

(c) The PMP-E (Figure 2h) has a pH-independent λ_{max} at 330 nm.

This model, based on kinetic, spectrophotometric and stereochemical evidence to date, is the most favored model proposed so far. Yet, some of the key features of the model remain hypotheses which await experimental verification, viz (1) the hydrogen bonding of pyridine N of the coenzyme with a proton-donating group on the enzyme, which lowers the pKa of the phenolic proton and allows it to abstract a proton from the NH_3^+ group of the substrate, and which then acts as a nucleophile (Figure 2b,c); (2) the breaking of this hydrogen bond on binding of the substrate to the enzyme (Figure 2d,e) to allow the formation of the tetrahedral intermediate.

In the absorption spectra of the phenolate form of free PL-aldimines, the introduction of a positive charge on pyridine N per se causes very little change in λ_{max} (367 nm for pyridine (Figure 3b) vs 378 nm for N-methylpyridinium (Figure 3d) [7]. Therefore, the observed absorption spectra of active PLP-E with λ_{max} at 360 nm provides no evidence for or against protonation or hydrogen bonding at pyridine N. The hydrogen bonding (or protonation) is postulated to explain the large decrease in pKa of the transition from λ_{max} = 430 nm to 360 nm (attributed to phenol ionization) from 10.5 for free PL-aldimine to 6.3 for PLP-E, because the presence of a positive charge at pyridine N was shown to lower the pKa to $\sim$8.0 (Figure 3c,d) [7].

The postulated structure of the PLP-aldimine in aspartate amino-transferase in Figure 2a can be thought of as the dipolar tautomer,

Ib, of PLP-aldimine in Figure 4. For free PLP-aldimine in H_2O, however, recent ^{13}C NMR studies showed that the neutral tautomer, Ic, is predominant at neutral pH, with deprotonation occurring predominantly at pyridine N with pKa ≈ 6.6 [11], as reflected in large ^{13}C shift changes at C-6 and C-2 between pH 4 and 7 [12]. Thus, for the dipolar tautomer to predominate in PLP-E as postulated in the proposed mechanism, the coenzyme-binding site of the enzyme must be a highly polar environment, with a proton-donating group near the pyridine N and a cationic group near the phenol group of the coenzyme. Although crystallization of pig mitochondrial aspartate aminotransferase for X-ray studies has been reported recently [13], the X-ray structure of the active site of the enzyme has not yet been elucidated, and the proximity of these groups remain hypothetical.

^{15}N nuclear magnetic resonance spectroscopy provides a sensitive technique for experimental verification of the postulated hydrogen bonding or protonation of the pyridine nitrogen in PLP-E and its disruption in the PLP-E-substrate complex, because the pyridine nitrogen chemical shift is very sensitive to hydrogen bonding and protonation. [14a,b] R. O. Duthaler and J. D. Roberts [15] showed that, relative to cyclohexane as solvent, the ^{15}N shift of pyridine in H_2O is shielded by 26.6 ppm (Table 1). Compared to the shift in H_2O, a solvent such as trifluoroethanol, capable of stronger hydrogen bonding to the nitrogen unshared pair, causes a further shielding of 11.8 ppm, while protonation at the pyridine N causes a dramatic shielding of 93.9 ppm.

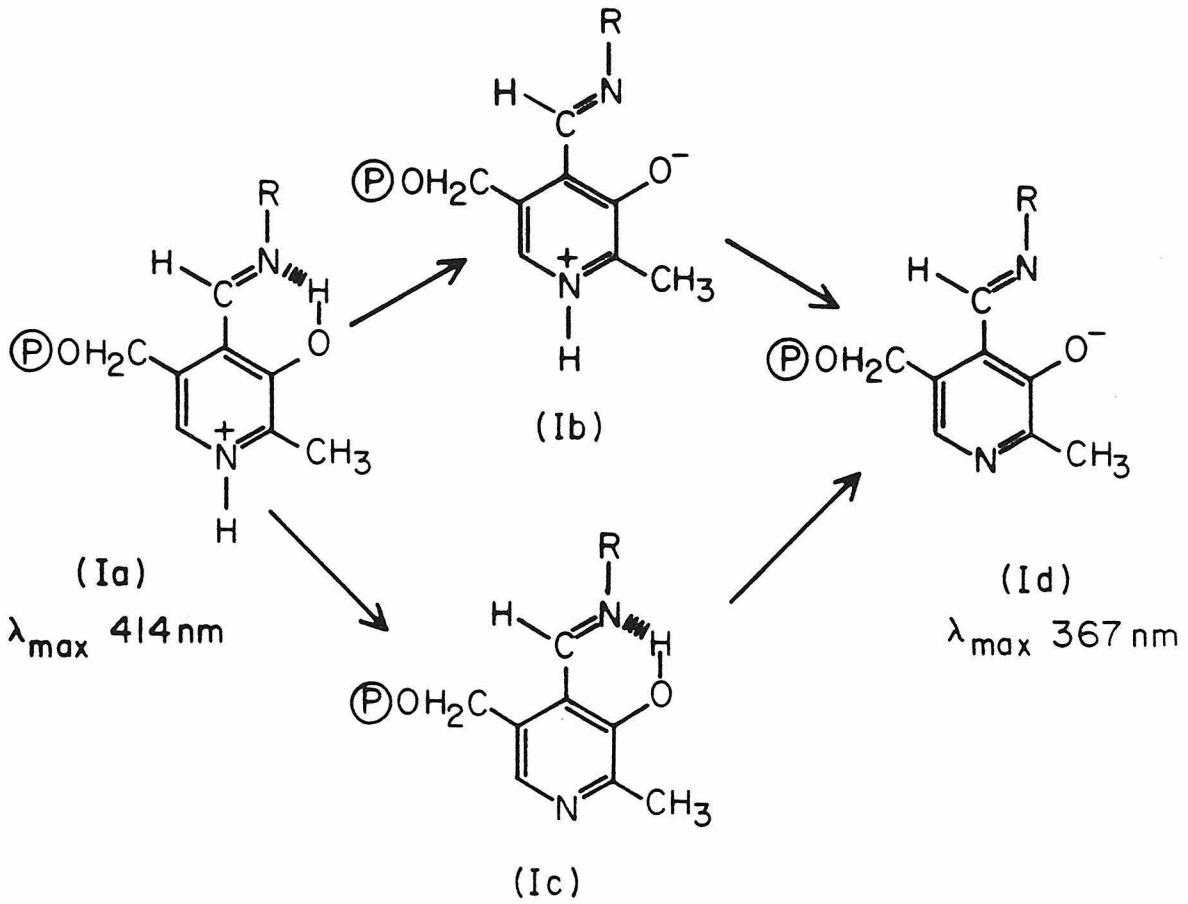

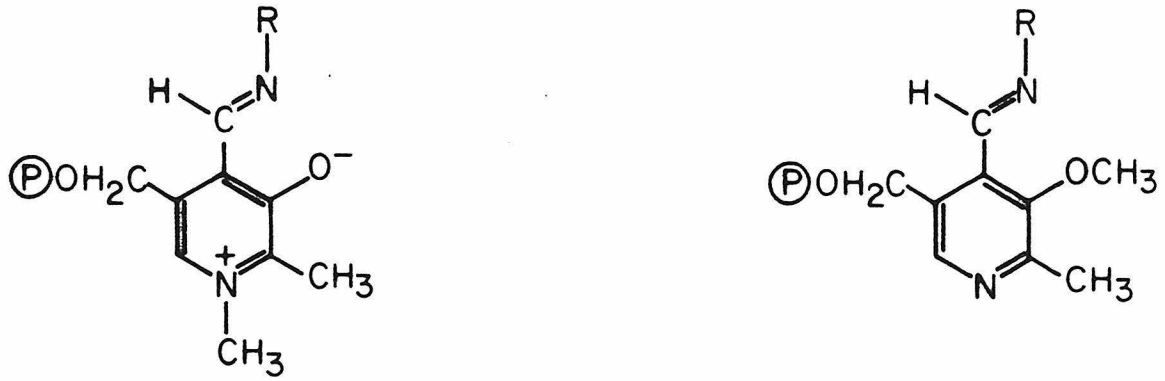

(Ie)

(If)

Figure 4

Table 1

^{15}N Chemical Shifts of Pyridine

Compound	Solvent	δ ^{15}N (ppm from $H^{15}NO_3$)
Pyridine	Cyclohexane	52.9
"	H_2O	79.5
	Trifluoroethanol	91.3
Pyridine hydrochloride	H_2O	173.4
N-methylpyridinium hydrochloride	H_2O	174.5

It is proposed that the postulated hydrogen bonding (or protonation) of the pyridine nitrogen of pyridoxal phosphate to aspartate aminotransferase in the active form, which is an important feature of the proposed mechanism of transamination, be investigated by ^{15}N NMR. The pyridine ^{15}N shift of ^{15}N-enriched PLP-aspartate transaminase can be measured and compared to that of free PLP-aldimine in H_2O at pH 8.5 * to investigate whether any shielding indicative of hydrogen bonding or protonation can be observed in the coenzyme-enzyme complex.

For free PLP-aldimine, absorption and ^{13}C NMR spectra have been obtained in equilibrium mixtures of PLP and amine in H_2O. At a concentration of 0.5 M in each, the formation of aldimine is virtually

---

* This enzyme shows maximum activity over pH 6.3∿9.5.

complete over pH 8.3 ~ 12.05, and ^{15}N spectra of these complexes can be obtained at the natural-abundance level. Because the free PLP-aldimine in H_2O at pH 8.5 can exist as a mixture of tautomers, Ib and Ic, in Figure 4, it is desirable to obtain ^{15}N shifts of methylated derivatives, Ie and If, as models for Ib and Ic, respectively. A comparison of the ^{15}N shift of free PLP-aldimine at pH 8.5 with those of the model compounds, Ie and If, will then indicate the relative contributions of tautomers Ib and Ic in H_2O.

To obtain ^{15}N spectra of the PLP-enzyme complex, it is necessary to synthesize PLP enriched with ^{15}N at the pyridine nitrogen. Among the various methods for chemical synthesis of pyridoxal phosphate, a procedure in which the ^{15}N label is introduced at a relatively late stage in the synthesis is shown in Figure 5; reported yield for each step is shown in parentheses [16,17].

To form the ^{15}N-PLP-E complex, the unlabeled coenzyme in the PLP-E complex(commercially available) can be replaced by ^{15}N-PLP, using the following procedure.

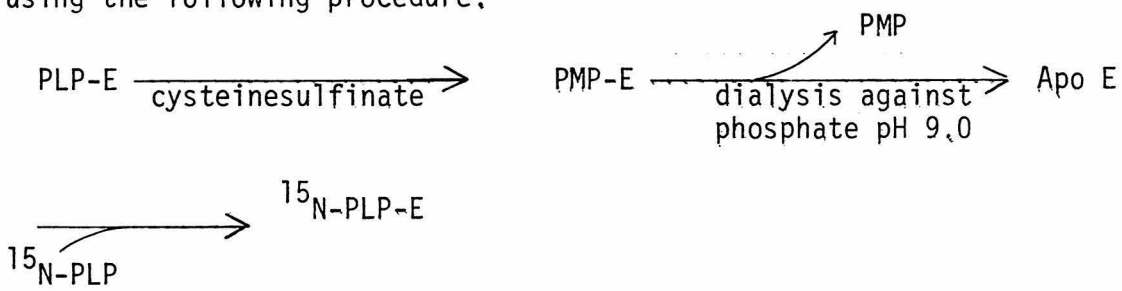

Conversion to PMP-E facilitates dissociation of the coenzyme to form a stable apoenzyme, and addition of equivalent amounts of PLP (two

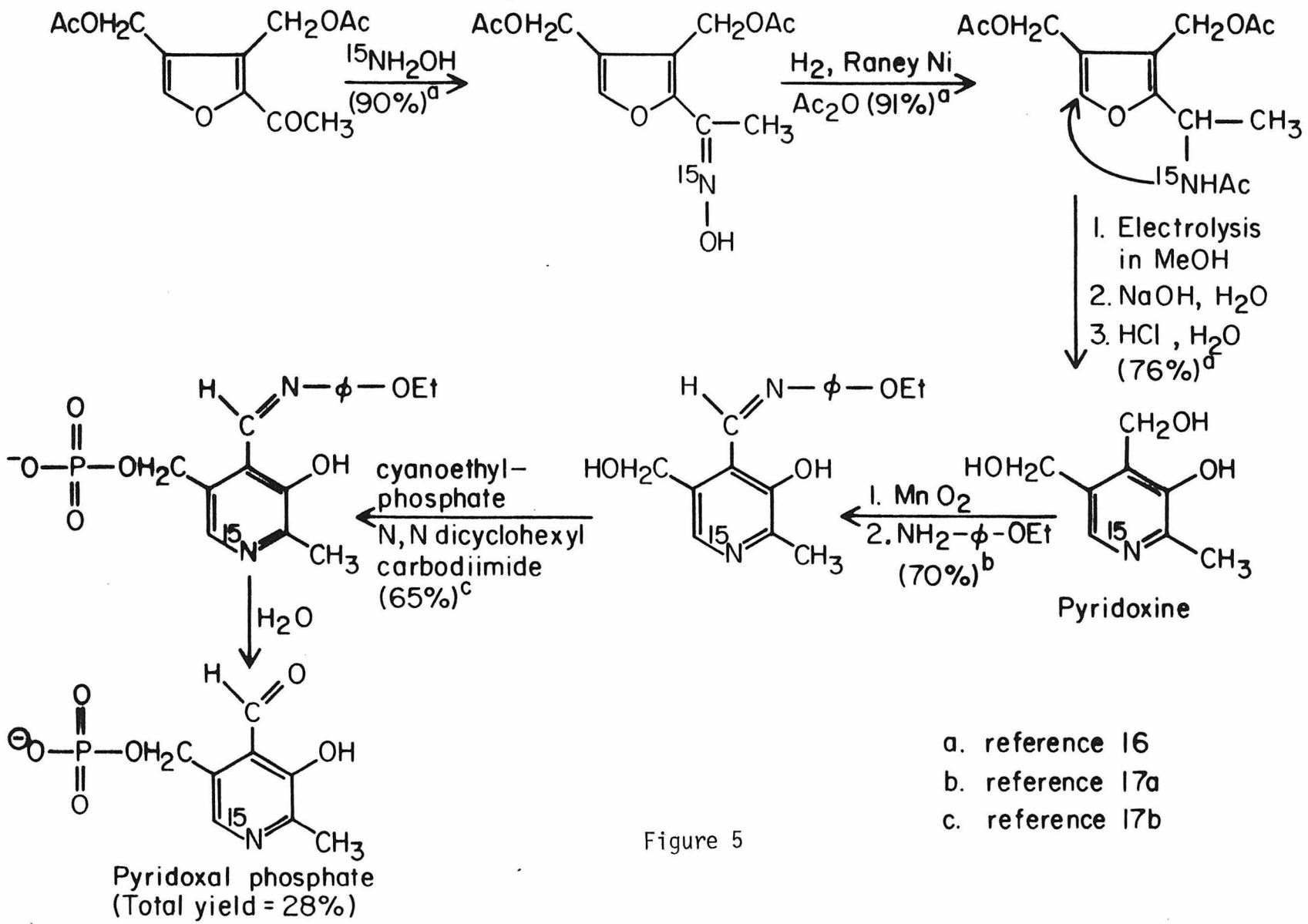

a. reference 16
b. reference 17a
c. reference 17b

Figure 5

moles of PLP per one mole of dimeric apoenzyme) has been shown to result in reconstitution of catalytically active PLP-E [18].

The pyridine ^{15}N shift of PLP-E, when compared with that of free aldimine in H_2O, should be a very sensitive indicator of the postulated hydrogen bonding to (or protonation by) a donor group in the enzyme. On the basis of ^{15}N shifts of pyridine in Table 1, relative to free aldimine in H_2O, we would expect the pyridine N in PLP-E to be shielded by more than 10 ppm for hydrogen bonding to a donor group in the enzyme, and by ~90 ppm for full protonation.

If the ^{15}N-PLP-E experiment proves to be fruitful, a further interesting experiment that can be attempted is the investigation of the postulated disruption of such hydrogen bonding (if it is occurring in PLP-E) on binding of the substrate. A quasi-substrate, α-methyl-L-aspartate, forms a stable aldimine with the enzyme-bound pyridoxal phosphate and, therefore, provides a stabilized analogue of the substrate-enzyme complex (Fig. 2e). By using ^{15}N-labeled α-methylaspartate, which can be synthesized by the procedure [19],

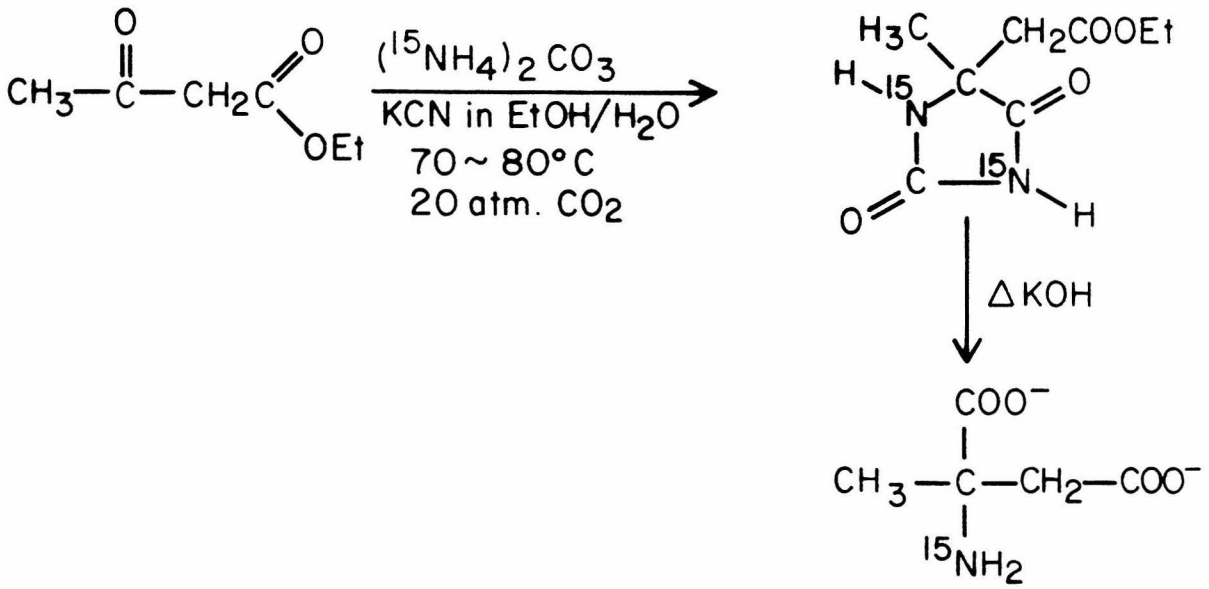

we could obtain a ^{15}N spectrum of the enzyme-quasi-substrate complex ^{15}N-enriched at both pyridine N of the coenzyme and at the substrate aldimine nitrogen. The pyridine ^{15}N shift will indicate whether the postulated disruption of hydrogen bonding or deprotonation actually occurs on substrate binding. In addition, the aldimine ^{15}N shift, which is sensitive to hydrogen bonding and protonation, will indicate whether the protonated aldimine structure for the enzyme-substrate complex (Figure 2e) inferred on the basis of spectrophotometric evidence is borne out by the ^{15}N chemical-shift data.

REFERENCES

1. V. I. Ivanov and M. Ya. Karpeisky, Advan. Enzymol. 32, 21 (1969).
2. A. E. Braunstein in "The Enzymes" ed. P. D. Boyer, vol. IX, p. 379, Academic Press, New York, 1973
3. (a) D. E. Metzler, Advan. Enzymol. 50, 1 (1979);
   (b) J. W. Ledbetter, H. W. Askins and R. S. Hartman, J. Amer. Chem. Soc. 101, 4284 (1979).
4. W. T. Jenkins, D. A. Yphantis and J. W. Sizer, J. Biol. Chem. 234, 51 (1958).
5. D. E. Metzler, J. Amer. Chem. Soc. 79, 485 (1957).
6. I. W. Sizer and W. T. Jenkins in "Chemical & Biological Aspects of Pyridoxal Catalysis", ed. E. E. Snell, et al, p. 123, Pergamon Press, Oxford 1963.
7. C. C. Johnston, H. G. Brooks, J. D. Albert and D. E. Metzler in "Chemical & Biological Aspects of Pyridoxal Catalysis", ed. E. E. Snell, et al, p. 69, Pergamon Press, Oxford 1963.
8. P. Fasella and G. G. Hammes, Biochemistry, 6, 1798 (1967).
9. P. Fasella, A. Giartosio and G. G. Hammes, Biochemistry 5, 197 (1966).
10. W. T. Jenkins, J. Biol. Chem. 236, 1121 (1961).
11. B. H. Jo, V. Nair and L. Davis, J. Amer. Chem. Soc. 99, 4467 (1977).
12. R. C. Harruff and W. T. Jenkins, Org. Mag. Res. 8, 548 (1976).

13. G. Eichele, G. C. Ford, J. N. Jansonius, J. Mol. Biol. 135(2), 513 (1979).

14. (a) R. L. Lichter and J. D. Roberts, J. Am. Chem. Soc. 93, 5218 (1971).

    (b) H. Saito, Y. Tanaka and S. Nagata, J. Am. Chem. Soc. 95, 324 (1973).

15. R. O. Duthaler and J. D. Roberts, J. Am. Chem. Soc. 100, 4969 (1978).

16. N. Elming and N. Clauson-Kaas, Acta Chem. Scan. 9, 23 (1955).

17. (a) V. L. Florentiev, V. J. Ivanov and M. Ya Karpeisky in "Methods in Enzymology", ed. D. B. McCormick and L. D. Wright, vol. XVIII, p. 567, Academic Press, London (1970).

    (b) M. H. O'Leary and J. R. Payne, J. Biol. Chem. 251, 2248 (1976).

18. M. Arrio-Dupont, Biochem. Biophys. Res. Commun. 36, 306 (1969).

19. P. Pfeiffer and E. Heinrich, J. Prakt. Chem. 146, 105 (1936).

PROPOSITION II

A ^{15}N nuclear magnetic resonance study of the binding of the inhibitor sulfanilamide to carbonic anhydrase

Carbonic anhydrase, a zinc metalloenzyme widespread in nature, is a highly efficient catalyst of the reversible hydration of CO_2 in erythrocytes:

$$CO_2 + H_2O \rightleftharpoons HCO_3^- + H^+ \quad .$$

Thus, it serves an important physiological role in facilitating the transport of metabolic CO_2 between the lung and tissues [1]. The activity of carbonic anhydrase around a neutral pH is governed by the ionization of a group with a pK_a near 7. In the generally accepted model of the mechanism of catalysis of this enzyme, this group is thought to be the zinc-bound water molecule which, on ionization to a hydroxide ion, acts as a nucleophile to the substrate CO_2 molecule (Figure 1a) [2]. However, it has also been suggested that the group with pK_a 7 may represent the imidazole moiety of a histidine residue that is involved in a general-base-assisted attack by $ZnOH_2$ on CO_2 (Figure 1b) [3].

The activity of carbonic anhydrase is strongly inhibited by aromatic sulfonamides such as sulfanilamide (1). For this inhibitor,

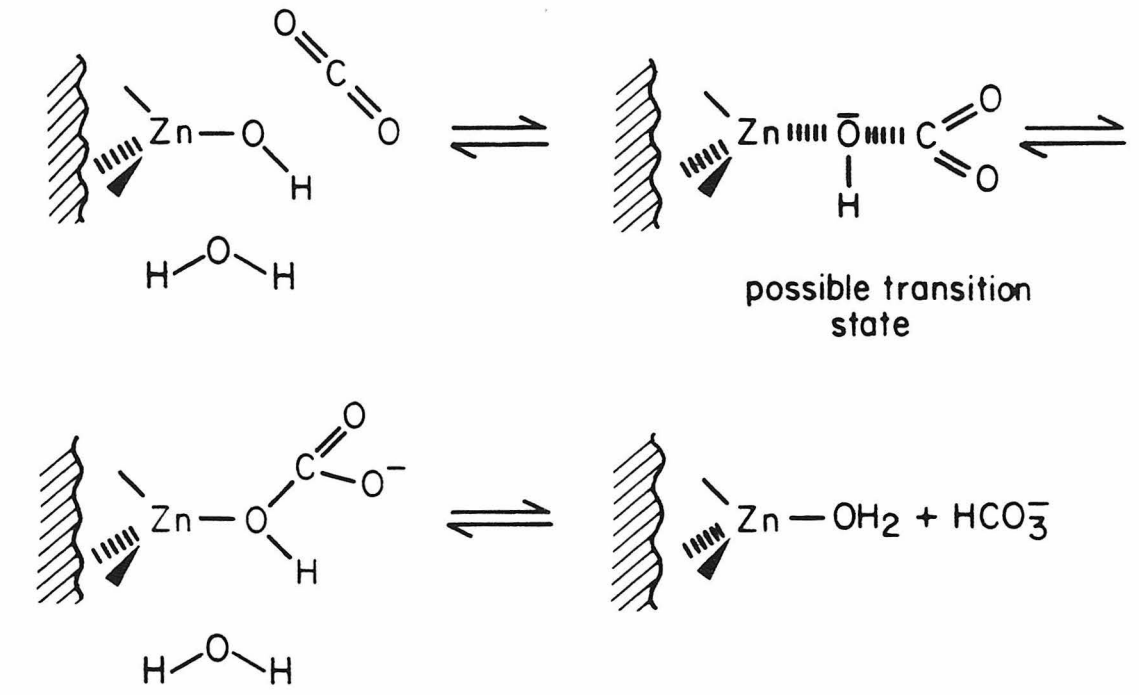

(a)

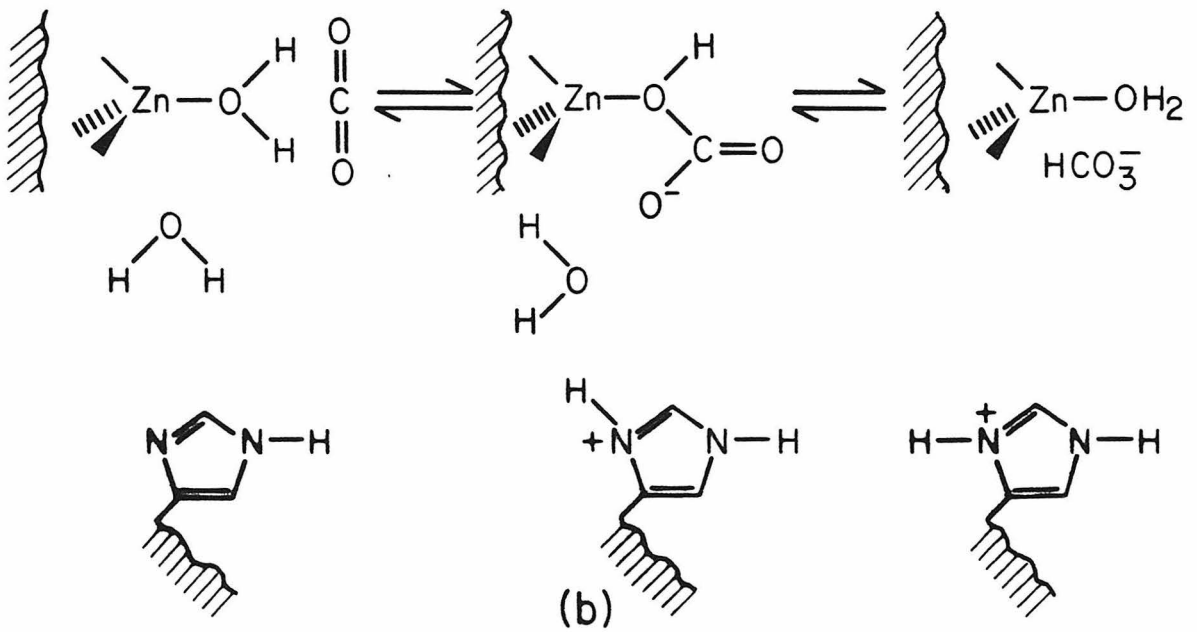

(b)

Figure 1

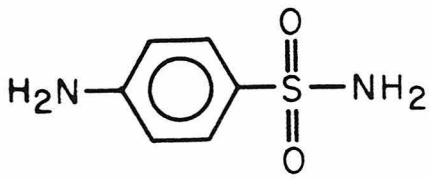

I.

the dissociation constant of the enzyme-inhibitor complex is $K_I = 2.6 \times 10^{-5}$ M [1]. Recent x-ray data show that, in a sulfonamide-carbonic anhydrase complex, the SO_2NH_2 group lies within the primary coordination sphere of the enzyme's single Zn atom [4a-d]. The presence of Zn is required for strong binding of sulfonamides; apocarbonic anhydrase shows only very weak binding [2]. The aromatic ring of the sulfonamide also plays an important part in binding, because aliphatic sulfonamides such as methane-sulfonamides show only weak inhibitory effects [5]. The x-ray structure of the enzyme-inhibitor complex shows that the aromatic part of the inhibitor is in van der Waals contact with a number of side chains, especially those situated on the hydrophobic wall of the active site [4d]. Ultraviolet [6], fluorescence [7] and resonance Raman [8] spectra of the enzyme-inhibitor complexes suggest that the sulfonamide inhibitors are bound as anions

SO_2NH^- . These results suggest the mode of complexation shown in Figure 2.

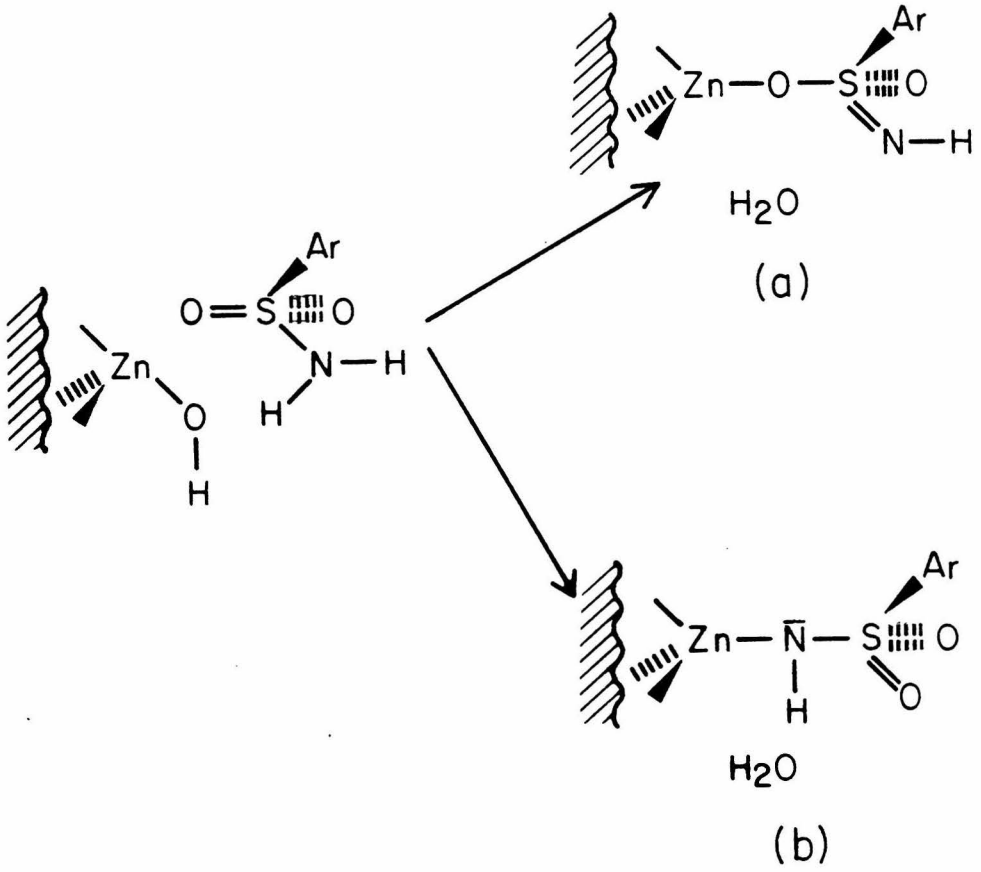

Figure 2

Two possible modes of coordination of the deprotonated sulfanilamide to Zn have been suggested: (1) coordination through one of the oxygen atoms (Figure 2a) [3], and (2) coordination through the nitrogen atom (Figure 2b) [8]. The x-ray structure of a sulfonamide-carbonic anhydrase complex at the resolution obtained to date cannot distinguish

between the two possible modes of binding [4d] and the detailed geometry of coordination remains unknown. N-substituted sulfanilamides such as sulfanilacetamide ($NH_2C_6H_4SO_2NHCOCH_3$) have no inhibitory activity [9]. This provides favorable, but by no means definitive, evidence for coordination through the nitrogen, because if coordination takes place through the oxygen, such substitution is also expected to cause steric hindrance between the N-substituted moiety and the aryl group (Figure 2a) [3].

The precise mode of binding of sulfonamide to the active-site of carbonic anhydrase is of great interest for the following reasons:

1) The binding of sulfonamides to carbonic anhydrase and another zinc enzyme, alkaline phosphatase [10], is highly specific; other well-characterized zinc enzymes such as carboxypeptidase and alcohol dehydrogenase do not bind sulfonamides.

2) Sulfonamides are clinically used as an anticonvulsant and cerebrovasodilator drug because they cause an increase in cerebral blood flow by raising CO_2 levels through inhibition of brain carbonic anhydrase [11].

3) It has been suggested [8] that the sulfonamide in the bound state (Figure 2b) mimics the transition state of the substrate (Figure 1a), and this may account in part for the extremely high affinity of sulfonamides to carbonic anhydrase. Dissociation constants for sulfonamide-carbonic anhydrase complexes vary between 2×10^{-9} M for ethoxzolamide [3] and 2.6×10^{-5} M for sulfanilamide compared to

$10^{-3} \sim 10^{-2}$ M for the CO_2-carbonic anhydrase complex [2].

Stable compounds that are chemically reasonable models for the transition state of the substrate (transition-state analogues) have been shown to be potent inhibitors with affinities three to four orders of magnitude higher than the substrate, for enzymes such as elastase and aldolase [12].

It is proposed that the precise mode of binding of sulfanilamide to the active-site Zn of carbonic anhydrase be investigated by ^{15}N nuclear magnetic resonance spectroscopy. ^{15}N NMR spectroscopy can be a sensitive technique for distinguishing between the two possible modes of binding shown in Figure 2, because the ^{15}N chemical shift of a deprotonated sulfonamide group bound to carbonic anhydrase is expected to be quite different depending on whether it is bound to zinc through the oxygen or the nitrogen atom of the sulfonamide. The ^{15}N chemical shift of N_1 of free sulfanilamide in the neutral form in dimethylsulfoxide is 278.1 ppm upfield of $H^{15}NO_3$ [13]. The ^{15}N shift of free deprotonated sulfanilamide (pKa_1 = 10.4) has not been measured, but is expected to be deshielded by more than 10 ppm relative to that of the neutral form on the basis of shift changes observed in other sulfonamides. On deprotonation of the sulfonamide group, the amide nitrogen shows a downfield shift of 12.8 ppm in p-toluenesulfonamide ($CH_3C_6H_4SO_2NH_2$) in dimethylsulfoxide [14], and of 11.0 ppm in methanesulfonamide ($CH_3SO_2NH_2$) in water [15].

Binding of the deprotonated sulfanilamide through the oxygen atom

to Zn of carbonic anhydrase, as schematized in Figure 2a, is expected to cause a substantial deshielding of the sulfonamide nitrogen chemical shift compared to that of the free deprotonated sulfanilamide due to the increased sulfur-nitrogen double-bond character on binding [16]. By contrast, binding of the deprotonated sulfanilamide through the nitrogen atom to the Zn is expected to cause a substantial shielding of the sulfonamide nitrogen shift compared to that of the free deprotonated sulfanilamide on the basis of previous studies on the effect of metal binding on ^{15}N chemical shifts [17,18].

Sulfanilamide enriched with ^{15}N at N_1 can be synthesized from p-acetamidobenzene sulfonylchloride and ^{15}N-enriched ammonia by the following procedure:

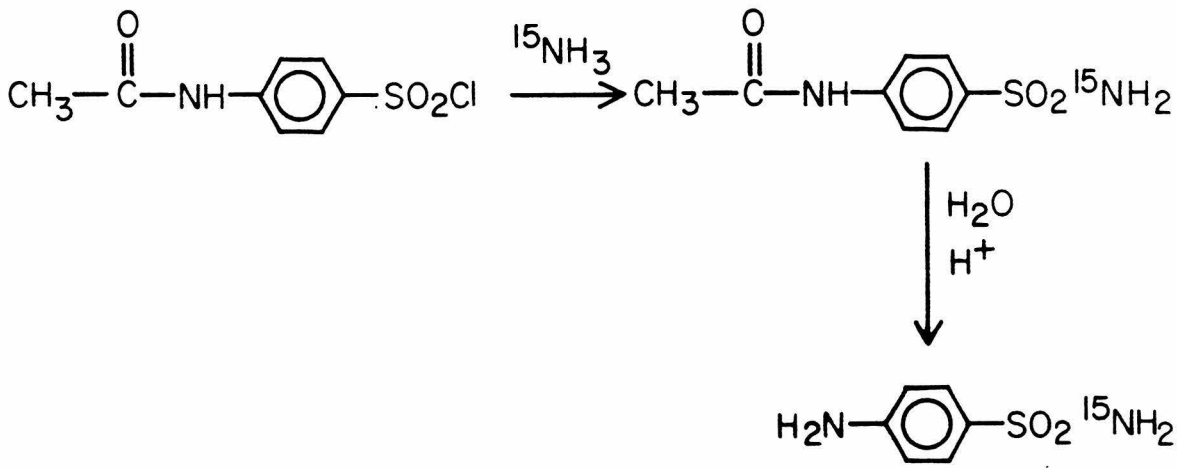

With sulfanilamide 99% enriched in sulfonamide nitrogen, it is quite feasible to obtain ^{15}N spectra of the carbonic anhydrase-sulfanilamide complex. The enzyme is sufficiently soluble ($>1x10^{-3}M$ in CH_3CN:Tris-SO_4 buffer 5:95 v/v[8]), and, because of its relatively small size (MW 29,300 for human carbonic anhydrase B), the molecular correlation time would be within a range where the ^{15}N signal from the bound sulfanilamide can be obtained without excessive linebroadening. Our work on arsanilazotyrosyl 248 carboxypeptidase A (99 % enriched with ^{15}N at both azo nitrogens, MW 34,700) showed that, for 1.5 mM solution of the enzyme, ^{15}N resonances with linewidths of $\sim$100 Hz can be obtained after 8-16 hours of accumulation time [18].

Thus, ^{15}N NMR should be a valuable technique for determining the precise mode of binding of the inhibitor, sulfanilamide, to the active-site zinc of carbonic anhydrase.

REFERENCES

1. T. H. Maren, Physiol. Rev. 47, 595 (1967).

2. S. Lindskog, L. E. Henderson, K. K. Kannan, A. Lilyas, P. O. Nyman, B. Strandberg in "The Enzymes",ed. P. D. Boyer, vol. 5, 585 (1971).

3. Y. Pocker and S. Sarkanen in Adv. in Enzymol., ed. A. Meister 47, 149 (1978).

4. (a) K. Fridborg, K. K. Kannan, A. Lilyas, J. Lundin, B. Strandberg, R. Strandberg, B. Tilander and G. Wirén, J. Mol. Biol. 25 505 (1967).

   (b) P. C. Beystén, I. Vaara, S. Lövgren, A. Liljas, K. K. Kannan and U. Bengtsson in "Oxygen Affinity of Hemoglobin and Red Cell Acid Base Status, Alfred Benzon Symposium IV," M. Rörth, D. Astrup, eds, Munksgaard, Copenhagen, p. 363 (1972).

   (c) I. Vaara "The Molecular Structure of Human Carbonic Anhydrase Form C and Inhibitor Complexes", Inaugural Dissertation, UUIC-B22-2, Uppsala University (1974).

   (d) K. K. Kannan, I. Vaara, B. Natstrand, S. Lovgren, A. Borell, K. Fridborg and M. Petef, in "Proceedings of the Symposium on Drug Action at the Molecular Level", G. C. K. Roberts , ed., MacMillan, London, p. 73, (1977)

5. T. H. Maren and C. E. Wiley, J. Med. Chem. 11, 228 (1968).

6. R. W. King and A. S. V. Burgen, Biochim. Biophys. Acta, 207, 278 (1970).

7. R. F. Chen and J. C. Kernohan, J. Biol. Chem. 242, 5813 (1967).

8. K. Kumar, R. W. King and P. R. Carey, Biochemistry 15, 2195 (1976).

9. T. Mann and D. Keilin, Nature 146, 164 (1940).

10. G. H. Price, Clin. Chim. Acta 94(3) 211 (1979).

11. I. T. Barnish, P. E. Cross, R. P. Dickinson, B. Gadsby, M. J. Parry, M. J. Randall and I. W. Sinclair, J. Med. Chem. 23, 177 (1980).

12. G. E. Lienhard, Science 180, 149 (1973).

13. I. J. Schuster, S. H. Doss and J. D. Roberts, J. Org. Chem. 43, 4693 (1978).

14. C. Casewit, personal communication.

15. H. R. Kricheldorf, Angew Chem. Int., ed Engl. 17, 442 (1978).

16. G. C. Levy and R. L. Lichter, "Nitrogen-15 Nuclear Magnetic Resonance Spectroscopy", Wiley & Sons, New York, 1979.

17. M. Alei, L. O. Morgan, W. E. Wageman, Inorg. Chem. 17, 2289 (1978).

18. The present thesis.

PROPOSITION III

Chromosomal localization of human embryonic ζ globin gene

Proteins are chemical fingerprints of evolutionary history, bearing in their amino-acid sequences records of past mutations. Through investigation of the differences in the amino-acid sequences of a protein in a large number of different species, it becomes possible to estimate the rate of occurrence of mutations and, hence, the rate of evolution of the protein. The rates of evolution of cytochrome C, the globins and fibrinopepetides have been interpreted in terms of the biological roles of the proteins [1]. For hemoglobins, the ubiquitous oxygen carriers in higher organisms, the amino-acid sequences of the component globin chains have provided some intriguing clues to their evolutionary relationships [2].

In human hemoglobin, six different types of globin chains, α, β, γ, δ, ε and ζ , have been identified so far [3]. The globin chain composition of HbA, the predominant adult hemoglobin, is $\alpha_2\beta_2$, while that of HbA_2, a minor adult hemoglobin component of unknown function, is $\alpha_2\delta_2$. HbF, the major fetal hemoglobin with a higher oxygen affinity than HbA, is $\alpha_2\gamma_2$. Embryonic hemoglobins are considered to be of three types: Hb Portland with the well-established composition $\zeta_2\gamma_2$, Hb Gower 2($\alpha_2\varepsilon_2$) and Hb Gower 1 ($\zeta_2\varepsilon_2$ or ε_4) [4]. The types of globin chains synthesized at different stages of human development are summarized in Figure 1 [5].

While adult and fetal hemoglobins have been subjects of extensive study, little is known about the physiological properties of embryonic hemoglobins.

In normal embryos, the embryonic hemoglobins are produced in nucleated erythrocytes derived from the yolk sac in the first 10 weeks of gestation, prior to the appearance of the α and γ chains (Figure 1). In a fetus incapable of α-chain synthesis because of genetic defects, Hb Portland ($\zeta_2\gamma_2$) continues to be produced during fetal life [6,7]. These observations, along with the similarity of the ζ- and α-chains in amino-acid composition (discussed below), suggest that the ζ chain functions as an α-type chain in the early stage of normal embryonic development and is capable of continued activity in an α-deficient fetus. The ζ chain is the only known globin chain that resembles the α-chain in amino acid composition and function and its evolutionary relationship to the α-chain is therefore of great interest.

In their amino acid sequences, the four chains of fetal and adult hemoglobins, α, β, γ and δ, show varying degrees of homology: α and β chains have identical amino acids in 42% of their residues, β and γ chains 71% and β and δ chains 96% [8]. On the basis of these homologies, it is believed that these globin chains evolved from a common ancestral globin gene by gene duplication followed by independent evolution caused by mutations. The evolutionary relationships of the four chains inferred from their homologies are shown in Figure 2.[2]

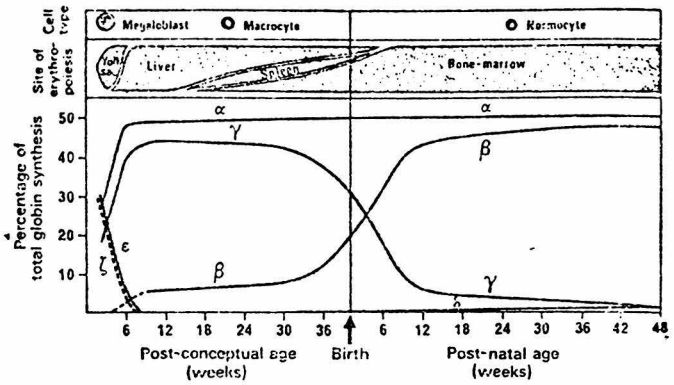

Fig. 1 (After W.G. Wood, Br. Med. Bull. 32, 282 (1976))

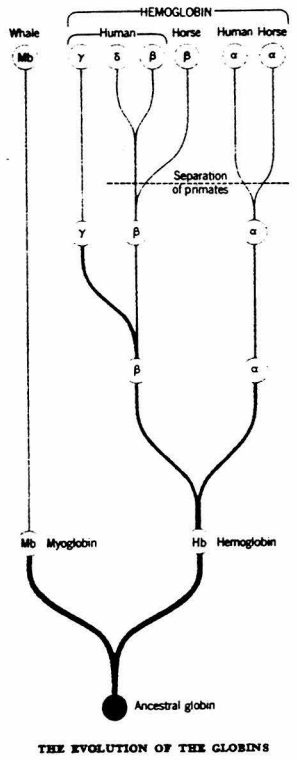

Fig. 2 (After R.E. Dickerson, "The Structure & Action of Proteins" Harper & Row, 1969)

For the ζ chain of embryonic hemoglobin, the complete amino acid sequence has yet to be worked out, but the amino acid sequences of peptide fragments obtained by trypsin and pepsin digestion of the ζ chain are known [9]. When these peptide fragments are aligned so as to maximize homology with the α-chain, the ζ and α-chains have identical amino acids in 61% of the residues. This homology is greater than that of α-β (42%), but less than that of β-γ (71%). This gives rise to a speculation that separation of the ζ-gene from the α-gene occurred prior to the separation of the γ and β genes (Figure 2). Lending support to this speculation is the finding that, while

embryonic hemoglobins are found in a large variety of mammals, including primates, artiodactyls, perissodactyls, carnivores and rodents, fetal hemoglobins are present in primates and artiodactyls only, not in perissodactyls, carnivores and rodents [10].

Within the last few years, molecular hybridization assay using somatic cell hybrids has opened the way to chromosomal localization of human structural genes. The human α-globin gene has been assigned to chromosome 16 and the β and γ globin genes to chromosome 11 [11,12]. The δ globin gene is known to be located next to the β gene on the same chromosome, because globin chains containing segments of both the δ- and β chains as a result of unequal crossing-over between the β and δ gene loci have been found in hemoglobin variants (Hb Leopore and Anti-leopore) [3].

If the α and β globin genes originated from a common ancestral gene, their present loci in separate chromosomes suggest that in the course of evolution, they were formed by one of the following possible processes:

(1) Tandem duplication of the ancestral gene followed by translocation of one of the genes to another chromosome.

(2) Chromosome duplication either of the single chromosome carrying the ancestral globin gene (aneuploidy) or of the total number of chromosomes (polyploidy).

The first process, while possible, is not very likely, because translocation often results in an inviable offspring. More plausible is the assumption that during evolution, nuclear genetic material has

increased by chromosome duplications. In animals, polyploidy would most likely have taken place early in vertebrate evolution, before the chromosomal sex pattern had become firmly established. Subsequent to whatever events may have caused the separation of the α and β globin genes, tandem duplication of the β gene to form the γ gene, and, at a later period, another tandem duplication to form the δ globin gene must have taken place. Such gene duplication is a continuing process; the present-day γ-chain gene is itself duplicated, and the α- gene is duplicated in some populations [3,8].

Where, then, is the ζ globin gene of embryonic hemoglobin located? If this chain separated from the α-chain <u>after</u> the α-β separation, but prior to the β-γ separation, as suggested by the relative homologies of the chains, it is possible that the ζ gene was formed by duplication of the entire chromosome carrying the ancestral α-gene rather than by gene duplication on the same chromosome, as in the formation of the γ from the β gene. It would therefore be interesting to attempt a chromosomal assignment of the human ζ globin gene, to determine whether it is located on chromosome 16, like the α gene, or on a separate chromosome. The fact that individuals totally lacking the α-gene loci can produce Hb Portland ($\zeta_2\gamma_2$) [13] suggests that the α and ζ gene loci are either in separate chromosomes or, at some distance from each other, in the same chromosome.

Chromosomal assignment of the human ζ globin gene can be attempted by the following steps:

(1) Isolation of mixed globin mRNA for ζ, β and γ chains from the erythrocytes of newborns with Bart's hydrops syndrome, which can synthesize only these three chains.

(2) Synthesis of single-stranded [^{3}H]-complementary DNA for ζ, β and γ globin genes by RNA-directed DNA polymerase, using the mixed globin mRNA as templates. Purification of ζ-cDNA by removing $\beta\gamma$-cDNA through hybridization with $\beta\gamma$-mRNA.

(3) Assay the hybridization of the ζ-cDNA with DNA extracted from a series of human-mouse hybrid cell lines, each of which contains only certain ones of human chromosomes. If the ζ-cDNA hybridizes only with the DNA fragments extracted from the hybrid cell lines that contain i^{th} human chromosome, evidence will be provided that the ζ gene is located on the i^{th} chromosome. The feasibility of each step is discussed below.

1. Isolation of Mixed Globin mRNA for ζ, β and γ Chains

For unambiguous chromosomal assignment of the ζ gene, it is essential to obtain globin mRNA which contains ζ-mRNA and is uncontaminated by α-mRNA. In a normal fetus, synthesis of the ζ globin chain is mostly limited to the first 10 weeks of gestation (Figure 1), with only a trace amount (up to 0.2%) of Hb Portland ($\zeta_2\gamma_2$) found in cord blood at birth [6]. However, newborns with Hb Bart's hydrops syndrome, which is often lethal, totally lack the α-gene loci [7]; their erythrocytes contain no α-chain, 10 $\sim$ 15% of Hb Portland ($\zeta_2\gamma_2$), 80% of Hb Bart (γ_4), and a small percentage of HbH (β_4) [13].

Therefore their erythrocytes will yield globin mRNA for the ζ, β and γ chains only. Globin mRNA can be obtained from reticulocytes by cell lysis, phenol extraction of protein to obtain crude RNA followed by sucrose gradient centrifugation, oligo (dT) cellulose column chromatography and gel electrophoresis [14,15].

2. Synthesis of [^{3}H] cDNA for the ζ Globin Gene

The mixed globin ζβγ-mRNA can be incubated with [^{3}H] deoxyribonucleotides and RNA-directed DNA polymerase (reverse transcriptase) to synthesize [^{3}H]-complementary DNA for ζ, β and γ globin genes [11,15]. To separate the ζ-cDNA from βγ-cDNA, the latter can be annealed to globin αβγ-mRNA from normal newborns and the resulting duplex (βγ-cDNA-βγ-mRNA) separated from single-stranded ζ-cDNA by passage over a column of hydroxylapatite [16].

3. Hybridization of ζ-cDNA with DNA from Human-mouse Hybrid Cells

When human-mouse hybrid cells are formed by fusion of human and mouse somatic cells, the nuclei of the hybrid cells contain the chromosomes of both parent cells. In subsequent cell divisions, there is a progressive and preferential loss of human chromosomes from the hybrid cells; the resulting clones of hybrid cells have only certain chromosomes of the original parent cell [17]. For the hybridization assay, a series of about 20 cell lines can be chosen on the basis of complementarity of the overlapping subsets of human chromosomes that they contain. The human and mouse chromosomes can be distinguished, and the human chromosomes present in each hybrid clone can be identified

by a variety of differential staining and banding techniques [11].

Single-stranded DNA extracted by standard procedure from the hybrid cell lines of various human chromosomal compositions can be tested for hybridization with the [^{3}H]-ζ-cDNA. The formation of the [^{3}H]-ζ-cDNA-DNA hybrid can be monitored by measuring the radioactivity of the hybrid, after removal of unhybridized [^{3}H]cDNA by digestion with single-stranded specific S_1 nuclease, and comparing the radioactivity to that of the total [^{3}H]-cDNA initially added [18]. If the [^{3}H] -cDNA for ζ gene is found to hybridize only with those DNA fragments extracted from the cell lines that contain i^{th} human chromosome, it would provide evidence that the ζ gene is located in the i^{th} chromosome.

REFERENCES

1. R. E. Dickerson, J. Mol. Evol. 1, 26 (1971).
2. R. E. Dickerson, "The Structure and Action of Proteins", Harper & Row, New York, 1969
3. W. P. Winter, S. M. Hanash and D. L. Rucknagel, Adv. in Human Genetics 9, 229 (1979).
4. E. R. Huehns and A. M. Farooqui, Nature 254, 335 (1975).
5. W. G. Wood, Br. Med. Bull. 32, 282 (1976).
6. F. Hecht, R. T. Jones and R. D. Koler, Ann. Hum. Genet. (London) 31, 215 (1967).
7. J. M. Taylor, A. Dozy, Y. W. Kan, H. E. Varmus, L. E. Lie-Inyo, J. Ganesau and D. Todd, Nature 251, 392 (1974).
8. H. Lehmann and R. G. Huntsman, "Man's Hemoglobins including the Hemoglobinopathies and their Investigation", 2nd ed., J. B. Lippincott, Philadelphia, 1974.
9. H. Kamuzora and H. Lehmann, Nature 256, 511 (1975).
10. H. Kitchen and I. Brett, Ann. N. Y. Acad. Science 241, 653 (1974).
11. A. Deisseroth, A. Nienhuis, P. Turner, R. Veles, W. F. Anderson, F. Ruddle, J. Lawrence, R. Greagan, and R. Kucherlapati, Cell 12, 205 (1977).
12. A. Deisseroth, A. Nienhuis, J. Lawrence, R. Giles, P. Turner and F. H. Ruddle, Proc. Natl. Acad. Sci. USA 75, 1456 (1978).
13. D. J. Weatherall, J. B. Glegg and W. H. Boon, Br. J. of Haematol. 18, 357 (1970).

14. A. W. Nienhuis, A. K. Falvey and W. F. Anderson in "Methods in Enzymology", ed. S. P. Colowick and N. O. Kaplan, vol. 30, p. 621 (1974).

15. J. T. Wilson, B. G. Forget, L. B. Wilson and S. M. Weissman, Science 196, 200 (1977).

16. A. W. Nienhuis, P. Turner and E. J. Benz, Proc. Natl. Acad. Sci. USA 94, 3960 (1977).

17. V. A. McKusick and F. H. Ruddle, Science 196, 390 (1977).

18. E. J. Benz, C. E. Geist, A. W. Steggles, J. E. Barker and A. W. Nienhuis, J. Biol. Chem. 252, 1908 (1977).

PROPOSITION IV

A study of an alcohol dehydrogenase-substrate complex by resonance Raman spectroscopy

Within the last decade, resonance Raman spectroscopy has become a valuable technique for observing selectively the vibrational spectra of a chromophoric group in a biomolecule; it has been used extensively for the study of hemeproteins [1], visual pigments [2] and, more recently, flavoproteins [3]. An advantage of Raman over infrared spectroscopy for the study of biomolecules is that water, a poor solvent for the infrared, is an excellent solvent for Raman spectroscopy. For the study of a chromophoric group in a macromolecule, the resonance Raman effect is especially useful. Excitation of the molecule with a laser having a frequency close to the absorption frequencies of the chromophore causes an enormous enhancement of the Raman lines due to the chromophore vibrations which can then be observed at a low concentration, unobscured by vibrational features of the nonchromophoric part of the macromolecule.

A new promising area of application for this technique is the study of interaction of a chromophoric natural substrate with an enzyme, because resonance Raman spectra are expected to be sensitive to changes such as bond distortion and electron polarization that are induced in the substrate on binding to the active site, and are postulated to be crucial steps in the mechanism of enzyme catalysis [4].

Recently, Carey and co-workers [5] studied the resonance Raman spectra of a chromophoric substrate for the enzyme papain, 4-dimethylamino-3-nitro-α-benzamido-cinnamic acid methyl ester (1). In the process of esterolysis, this substrate forms an acyl-enzyme intermediate, 4-dimethylamino-3-nitro-α-benzamido-cinnamoylpapain, in which the cinnamoyl group is covalently bound at the S atom of the cysteine-25 residue of the enzyme. The acyl-enzyme intermediate,

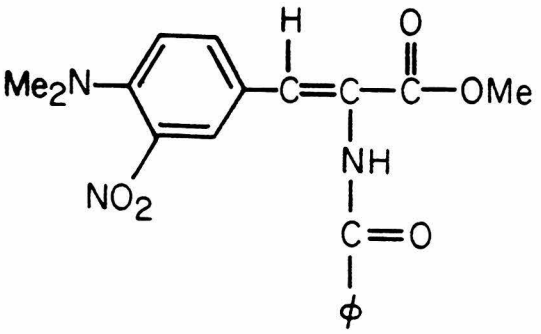

1.

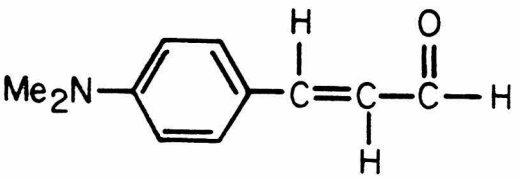

2.

which remains stable when maintained at pH3 and 4°C, shows spectral features quite distinct from that of the substrate. In the absorption spectrum, λ_{max} shifts from 350 nm for the substrate to 412 nm for the intermediate, and in the resonance Raman spectrum, the frequency of the ethylenic stretching vibration, $\nu_{C=C}$, shifts from 1642 cm^{-1} for the substrate to an intense peak at 1570 cm^{-1} in the intermediate. The

spectral properties of the acyl enzyme are attributed not to the formation of the acyl-cysteine 25 linkage per se (since neither the denatured acyl-enzyme nor thioethyl ester of the substrate show these properties) but to interaction of the acyl moiety with the intact active site. The absorption and resonance Raman properties of the acyl enzyme closely resemble those of 4-dimethylaminocinnamoylimidazole, which are characterized by a very strong electron-attracting group (imidazole) at the carbonyl end and an electron-donating group (e.g., dimethyl-amino) at the other extremity of the molecule. Thus these residues, acting through chemical bonds, set up a highly polarized π-electron system. Carey and co-workers proposed that a similar polarization of π electrons is produced in the acyl group by papain's active site, either by strong hydrogen bonding of a neighboring group to the carbonyl group of the substrate, or by proximity of a cation such as the imidazolium ion of His 159.

The implication of their study is that the electron polarization induced in the cinnamoyl substrate by interaction of its carbonyl group with the active site of the enzyme can be detected by a marked decrease in the frequency of the ethylenic stretching mode in the resonance Raman spectrum. If this proves to be true, resonance Raman spectroscopy can be a sensitive and useful technique for detecting such electron polarization in a suitable substrate or quasi-substrate-enzyme complex where such polarization is postulated to be a crucial step in catalysis.

An interesting enzyme to which the resonance Raman technique can be applied is horse liver alcohol dehydrogenase (LADH), a NADH-dependent zinc metalloenzyme which catalyzes the transfer of a hydride from the reduced nicotinamide adenine dinucleotide (NADH) to the carbonyl carbon of an aldehyde:

$$R\text{-}\overset{O}{\overset{\|}{C}}\text{-}H + NADH + H^+ \rightleftharpoons RCH_2OH + NAD^+ \quad .$$

In the proposed mechanism of catalysis, it is postulated that the catalytic zinc of the enzyme coordinates to the carbonyl oxygen of the substrate, thereby polarizing the carbonyl carbon and making it more susceptible to attack by the hydride ion. The chromophoric compound, 4-dimethylaminocinnamaldehyde (2) (λ_{max} 398 nm)*, is a natural substrate for alcohol dehydrogenase and has been found to react rapidly with the LADH-NADH complex to form a transient chemical intermediate (λ_{max} 464 nm) which has been detected by a combined stopped-flow temperature-jump rapid kinetic technique [6]. In a model study, the λ_{max} of this compound (367 nm)** shifts to 431 nm on addition of excess $ZnCl_2$ [7]. It was proposed that the magnitude of the red shift in the chromophore spectrum, the pH independence of the intermediate formation between pH 6 and 9, and the absence of a deuterium isotope rate effect on substituting NADD for NADH are consistent only with a structure for the intermediate that involves a coordination bond between the catalytic zinc and the carbonyl oxygen [8]. In a recent X-ray study of the alcohol dehydrogenase-H_2NADH-dimethylaminocinna-
8

* in water
** in diethyl ether

maldehyde complex at 3.7 Å resolution, the carbonyl oxygen of the substrate appears to be displacing the water molecule coordinated to Zn of the enzyme [9].

Because the chromophoric substrate, 4-dimethylaminocinnamaldehyde, shows an intense resonance Raman band for $\nu_{C=C}$ at 1591 cm^{-1}, [5], the LADH-NADH-4-dimethylaminocinnamaldehyde intermediate (which can be stabilized at pH > 9 and 4°C when the enzyme concentration is high)[6] is well suited for study by resonance Raman spectroscopy.

It is proposed that the model system, a 4-dimethylaminocinnamaldehyde-$ZnCl_2$ mixture, and the enzyme-substrate complex, LADH-NADH-4-dimethylaminocinnamaldehyde intermediate, be studied by resonance Raman spectroscopy to investigate whether the proposed coordination of the carbonyl oxygen of the substrate to the Zn^{2+} in the model system and to the catalytic zinc in the enzyme can be detected by a decrease in the frequency of the ethylenic stretching vibration. Because the substrate chromophore in the LADH-NADH-substrate complex has $\lambda_{max} \sim 464$ nm, laser excitation at, for example, 458 nm, is expected to enhance only the Raman lines that are due to the substrate and not those due to the NADH chromophore which has λ_{max} at 325 nm. If a significant decrease in the frequency of the ethylenic vibration is observed in both the model system and the LADH-NADH-4-dimethylaminocinnamaldehyde intermediate, it will provide strong evidence that π electrons in the substrate are polarized on binding to the enzyme active site, due to the interaction of the carbonyl oxygen of the substrate with the catalytic zinc of the enzyme.

REFERENCES

1. T. G. Spiro, Biochem. Biophys. Acta 416, 169 (1975).

2. R. Callender and B. Honig, Ann. Rev. Biophys. Bioeng. 6, 33 (1977).

3. (a) P. K. Delta, J. R. Nestor and T. G. Spiro, Proc. Natl. Acad. Sci. USA 74, 4146 (1977).

   (b) Y. Nishina, T. Kilagawa, K. Shiga, K. Horiike, Y. Matsumura, H. Watan and T. Yamano, J. Biochem. 84, 925 (1978).

   (c) T. Kitagawa, Y. Nishina, K. Shiga, H. Watain, Y. Matsumura and T. Yamam, J. Amer. Chem. Soc. 101, 3376 (1979).

   (d) M. Benechy, T. Y. Li, J. Schmidt, F. Freeman, K. L. Walters Biochemistry 18, 3471 (1979).

4. P. R. Carey and H. Schneider, Acc. of Chem. Res. 11, 122 (1978).

5. P. R. Carey, R. G. Caniere, D. J. Phelps and H. Schneider, Biochemistry 17, 1081 (1978).

6. M. F. Dunn and J. S. Hutchison, Biochemistry 12, 4882 (1973).

7. C. T. Angelis, M. F. Dunn, D. C. Muchmore and R. M. Wong, Biochemistry 16, 2922 (1977).

8. R. G. Morris, G. Saliman and M. F. Dunn, Biochemistry 19, 725 (1980).

9. C. I. Brändén, H. Eklund, J. P. Samana and L. Wallen, 11th International Congress of Biochemistry, Toronto, Canada, July 8-13, 1979 Abstr. No. 03-4-S95, p. 194.

PROPOSITION V

Mechanism of Action of an Anticancer Drug

The nitrosoureas are an important class of antitumor agents with a broad spectrum of activity in human cancer [1]. However, all the clinically available agents, with the exception of streptozotocin, produce bone marrow depression that limits the clinical usefulness of these agents [2].

Streptozotocin, an antibiotic produced by Streptomyces achromogenes, is a 2-deoxy-D-glucose derivative of N-methyl N-nitrosourea (Figure 1)

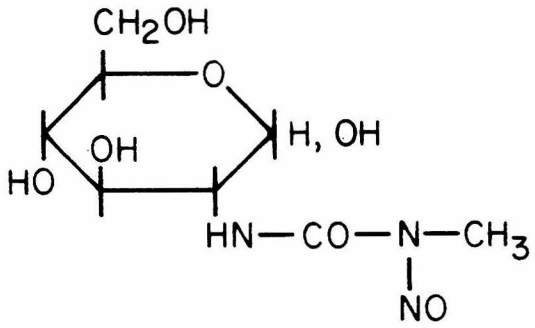

Figure 1. Structure of Streptozotocin

It is an anticancer agent currently being used clinically, which is particularly effective in the treatment of malignant islet cell cancer of the pancreas, gastrinomas and Hodgkin's disease [3].

While the clinical and therapeutic aspects of this drug have been extensively studied, there have been relatively few studies on its mechanism of action. F. Reusser [4] found that streptozotocin induces rapid degradation of deoxyribonucleic acid (DNA) in actively dividing or resting Bacillus subtilis cells. H. S. Rosenkranz and coworkers [5] observed a similar degradation of cellular DNA in E. Coli cells treated

with streptozotocin; the drug was also found to inhibit the incorporation of (^{3}H)-labeled precursors into DNA. B. K. Bhuyan [6] studied the action of streptozotocin on mammalian cells and found that streptozotocin inhibits the incorporation of precursors into DNA more than into RNA or protein. It also inhibits the progress of cells into mitosis and cell replication. However, enzymes involved in DNA synthesis, such as DNA polymerase, deoxycytidine kinase, thymidine kinase and thymidylate synthetase, were not significantly inhibited at a concentration of streptozotocin much higher than that needed for a complete inhibition of DNA synthesis. These studies suggest that the inhibition of DNA synthesis, possibly through degradation of template DNA, and the resulting inhibition of cell replication, are the basis for the carcinostatic activity of streptozotocin. However, the precise mechanism by which streptozotocin causes inhibition of DNA synthesis and cell replication is not presently understood.

Because N-methyl-N-nitrosourea (MNU) is known to alkylate DNA, it has been speculated that streptozotocin, its 2-deoxy-D-glucose derivative, acts as an alkylating agent. However, no direct evidence of alkylation, such as the isolation of alkylated bases from the DNA of cells treated with streptozotocin, has yet been obtained. Moreover, MNU possesses mutagenic and carcinogenic activities, whereas streptozotocin is primarily carcinostatic. This raises an interesting possibility that the glucose moiety may endow streptozotocin with a mechanism of action which is basically different from that of MNU. Alternatively, strepto-

zotocin may alkylate DNA, but the effect of DNA alkylation may be potentially mutagenic or potentially template-inactivating, depending on the site and extent of alkylation.

To gain some insight into these problems, it is proposed that possible alkylation of DNA in mammalian cells by streptozotocin be studied by the following steps: (1) administration of (methyl-^{14} C) streptozotocin to mouse leukemia L1210 cells; (2) extraction of DNA followed by mild acid hydrolysis, and (3) separation, identification and determination of the relative abundance of (methyl-^{14} C) bases by radiochromatography.

(Methyl-^{14} C) streptozotocin can be synthesized from tetra-O-acetyl glucosamine and (methyl-^{14} C) methyl isocyanate by the method of Herr and coworkers [7] (Figure 2).

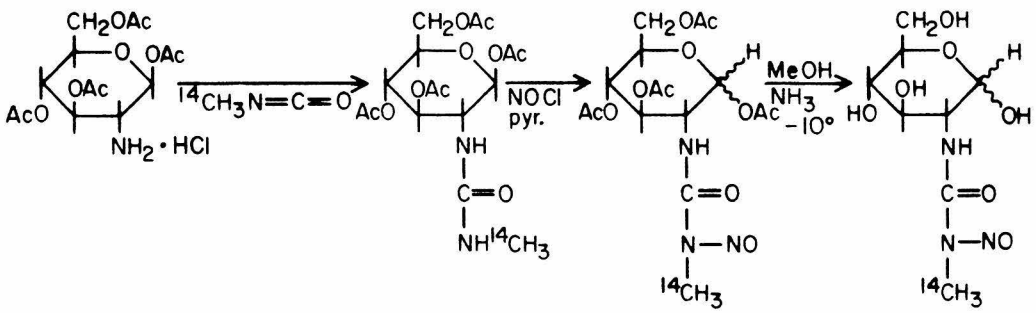

Figure 2. Synthesis of Streptozotocin

(Methyl-^{14} C)-streptozotocin can be administered to a culture of mouse leukemia L1210 cells at a concentration high enough to inhibit DNA synthesis. After a suitable incubation period, the cells can be lysed by sonication, and DNA extracted by standard procedures. DNA can be hydrolyzed in mild acid, and, after the addition of authentic methylated bases as nonradioactive markers, the bases can be separated, on an ion-exchange column such as Dowex 50. The chromatographic positions of methylated bases can be identified by analysis of the respective UV absorption spectra. By measuring the radioactivity of the chromatographic fractions containing each methylated base, we can determine the relative abundance of methylated bases, if any, produced by treatment with (methyl-^{14} C) streptozotocin. If detectable quantities of (methyl-^{14} C) bases are recovered from DNA by this method, they would provide direct evidence that streptozotocin alkylates DNA in mammalian cells. In addition, it would be interesting to compare the relative abundance of methylated bases produced by streptozotocin with that produced by other alkylating agents such as methylmethane sulfonate and MNU; treatment with these drugs yields 7-methylguanine as the major product and 3-methyladenine, 1-methyladenine and O^6-methylguanine as minor products [8].

Alkylation of DNA can lead to (a) anomalous base pairing in DNA replication, which is potentially mutagenic, or (b) depurination and cleavage of DNA strands at the site of alkylation, which can inactivate the template DNA. Anomalous base pairing involving O^6-methylguanine

has been observed by L. L. Gerchman and coworkers [9]; the presence of O^6-methylguanine in the template for polynucleotide synthesis has been shown to cause misincorporation of UMP or AMP into the complementary strand. Moreover, the inability of an organ to remove O^6-methylguanine from its DNA has been shown to correlate with the organ-specific carcinogenic action of alkylating agents [10]. Such evidence suggests that O^6-methylguanine plays an important role in the mutagenic and carcinogenic activities of alkylating agents. Particularly important is the finding that, in fibroblasts from individuals with a hereditary skin disease, xeroderma pigmentosum, which is associated with defects in DNA repair mechanisms, removal of O^6-methylguanine from DNA is significantly slower than in normal individuals [11], and the incidence of cancer in such individuals is significantly higher [12].

Another possible effect of DNA alkylation is the depurination and breakage of DNA strand(s) at the site of alkylation. Depurination of the methylated base can occur enzymatically or by spontaneous hydrolysis. P. D. Lawley and coworkers [13] showed that alkylation of guanine at the N7 position labilizes the N-glycosidic bond and leads to spontaneous depurination of the base at neutral pH. On the other hand, removal of 3-methyladenine, which is lost more rapidly from DNA than expected from spontaneous hydrolysis, and of O^6-methylguanine, which is chemically stable at neutral pH, is considered to be enzyme-catalyzed. Endonuclease II which recognizes the alkylated site on DNA has been isolated from

E. Coli [14a] and DNA *N*-glycosidase, which removes 3-methyladenine from DNA by cleavage of *N*-glycosidic bond, has been purified from *M. Luteus* [14b]. Depurination can lead to enzymatic cleavage of DNA at apurinic sites; bacterial and mammalian endonucleases which cleave DNA at apurinic sites have also been isolated [15].

These considerations suggest that, if streptozotocin acts as an alkylating agent, depurination and cleavage of template DNA at the site of alkylation is a possible cause of the inhibition of DNA synthesis observed in streptozotocin-treated cells. To test whether streptozotocin induces single-strand breaks in DNA of mammalian cells, it is proposed that DNA of L1210 cells prelabeled with (methyl-^{3}H) thymidine and exposed to an appropriate dose of streptozotocin be studied by centrifugation in alkaline sucrose density gradients to detect single-strand breaks. When the normal, heavy DNA chains are cleaved by single-strand breaks into lighter chains, a change in the sedimentation pattern, as monitored by radioactivity, is observed; the radioactive peak shifts from the heavy to the lighter side of the gradients.

If streptozotocin is found to induce single-strand breaks in DNA, it would be interesting to measure the extent of these breaks, and the extent of the inhibition of incorporation of (^{3}H)-labeled precursors into DNA at various concentrations of streptozotocin. Finding that incorporation of (methyl-^{3}H) thymidine into DNA is increasingly inhibited with increasing incidence of single-strand breaks in DNA

would lend support to the hypothesis that streptozotocin inhibits DNA synthesis by inducing single-strand breaks in the template DNA.

Alkylated DNA can be repaired by the excision-repair process. Excision of alkylated purine and incision of the phosphodiester chain at the apurinic site by the enzymes described above is followed by removal of the defective sugar phosphate by an exonuclease, formation of the correct nucleotide by DNA polymerase and, finally, by joining of the repaired chain segment to the intact chain by DNA ligase [16]. Partial repair of depurinated DNA *in vitro* by incubation for 1 hour with nuclease and DNA polymerase from a human lymphoblastoid line and DNA ligase from T-4-infected *E. Coli* has been reported [17]. Such excision-repair process, occurring *in vivo* would remove at least some of the alkylated purines and single-strand breaks in DNA induced by treatment with streptozotocin. It would be interesting, therefore, to vary the incubation period after streptozotocin treatment in the experiments described above to permit varying periods for repair, and to look for variations in the amounts of methylated bases or the single-strand breaks in DNA relevant to the period allowed for *in vivo* excision-repair process.

If those studies on L1210 cells prove to be fruitful, they can be extended to *in vivo* studies in rats. A particularly intriguing study would be a comparison of the site of alkylation and the extent of DNA cleavage induced by equimolar concentration of MNU and streptozotocin in the brain and pancreas of rats. MNU induces malignant tumors in rat brain while streptozotocin is carcinostatic in rat pancreas.

Any significant differences found in the site of alkylation or in the extent of DNA cleavage between DNA from the pancreas of streptozotocin-treated rats and the DNA from the brain of MNU-treated rats, may provide valuable clues to the different effects, carcinostatic vs carcinogenic, of the two alkalating agents.

REFERENCES

1. S. K. Carter, Cancer Chemotherapy Rep. Part 3, 4 35 (1973).
2. L. C. Panasci, P. A. Fox, and P. S. Schein, Cancer Res. 37, 3321 (1977).
3. (a) R. W. DuPriest, M. C. Huntington, W. H. Massey, A. J. Weiss, W. L. Wilson and W. S. Hetcher, Cancer 35, 358 (1975)
   (b) P. S. Schein, M. J. O'Connell, J. Blom, S. Hubbard, I. T. Magrath, P. Bergevin, P. H. Wiernik, J. L. Ziegler and V. T. DeVita, Cancer 34, 993 (1974).
   (c) P. Lins and E. Suad, Diabetes 28, 190 (1979).
   (d) J. A. Van Heerden, A. J. Edis and F. J. Service, Ann. Surg. 189, 677 (1979).
   (e) F. Stadil, G. Stage, J. F. Rehfeld, F. Efsen and K. Fischerman, N. Engl. J. Med. 294, 1440 (1976)
4. F. Reusser, J. Bacteriology 105, 580 (1971).
5. H. S. Rosenkranz and H. S. Carr, Cancer Res. 30, 112 (1970).
6. B. K. Bhuyan, Cancer Res. 30, 2017 (1970).
7. (a) R. R. Herr and H. K. Jahnke, J. Amer. Chem. Soc, 89, 4808 (1967).
   (b) P. F. Wiley, R. R. Herr, H. K. Jahnke, C. G. Chidester, S. A. Mizsak, L. B. Spaulding and A. D. Argoudelis, J. Org. Chem. 44, 9 (1979).
8. D. M. Kirtikar and D. A. Goldthwait, Proc. Natl. Acad. Sci. U.S.A. 71, 2022 (1974).

9. L. L. Gerchman and D. B. Ludlum, Biochem. Biophys. Acta 308, 310 (1973).

10. (a) J. W. Nicoll, P. F. Swann and A. E. Pegg, Nature 254, 261 (1975).

(b) P. Kleihues and G. P. Margison, J. Natl. Cancer Inst. 53, 1839 (1974).

(c) R. Goth and M. F. Rajewsky, Proc. Natl. Acad. Sci. U.S.A. 71, 639 (1974).

11. R. Goth-Goldstein, Nature 267, 81 (1977).

12. R. B. Setlow, Nature 271, 713 (1978).

13. P. D. Lawley and P. Brookes, Biochem. J. 89, 127 (1963).

14. (a) D. M. Kirtikar, G. R. Cathcart and D. A. Goldthwait, Proc. Natl. Acad. Sci. U.S.A. 73, 4324 (1976).

(b) J. Laval, Nature 269, 829 (1977).

15. (a) S. Ljungquist and T. Lindahl, J. Biol. Chem. 249, 1536 (1974).

(b) S. Ljungquist, J. Biol. Chem. 252, 2808 (1977).

(c) V. Bibor and W. G. Verley, J. Biol. Chem. 850 (1978).

16. J. Laval, Biochimie 60, 1123 (1978).

17. K. Bose, P. Karran and B. Strauss, Proc. Natl. Acad. Sci. U.S.A. 75, 794 (1978).